Targeted transduction of T cell subsets for immunotherapy of cancer and infectious disease

D i s s e r t a t i o n

zur Erlangung des akademischen Grades

d o c t o r r e r u m n a t u r a l i u m

(Dr. rer. nat.)

im Fachbereich Biologie

eingereicht an der

Lebenswissenschaftlichen Fakultät

der Humboldt-Universität zu Berlin

von

Diplom-Biologe Inan Edes

Präsident der Humboldt-Universität zu Berlin

Prof. Dr. Jan-Hendrik Olbertz

Dekan der Lebenswissenschaftlichen Fakultät

Prof. Dr. Richard Lucius

Gutachter/innen:
1. Prof. Dr. Wolfgang Uckert
2. Prof. Dr. Antonio Pezzutto
3. Prof. Dr. Christian Buchholz

Tag der mündlichen Prüfung: 09. September 2016

To Setareh & Allegra

Zusammenfassung

Immunotherapien mit T-Zellen, die mit tumor-reaktiven Rezeptoren ausgestattet wurden, werden in Zukunft herkömmliche Krebstherapien komplementieren. Solide Tumore bestehen aus Krebszellen, die Moleküle der Haupthistokompatibilitätskomplexe (MHC, *engl*. major histocompatibility complex) der Klasse I (MHC I) exprimieren und umgebendem Stromagewebe, welches MHC I und II Moleküle exprimiert. Die Unfähigkeit aktueller Therapien solide Tumore abzustoßen könnte durch den gleichzeitigen Einsatz MHC I-restringierter $CD8^+$ (*engl*. cluster of differentiation) und MHC II-restringierter $CD4^+$ T-Zellen überwunden werden. Geeignete Werkzeuge zur simultanen Erzeugung $CD8^+$ und $CD4^+$ T-Zellen mit unterschiedlich restringierten tumor-reaktiven T-Zell-Rezeptoren (TZR) fehlen bisher. Das Ziel der vorliegenden Arbeit bestand darin, ein Vektorsystem zu entwickeln, das den simultanen Transfer verschiedener Transgene in $CD8^+$ und $CD4^+$ T-Zellen und dadurch die Herstellung eines immunotherapeutischen T-Zell-Produkts ermöglicht, welches aus zwei unterschiedlich modifizierten T-Zell-Subtypen besteht.

Im ersten Teil der Arbeit wurde die auf der Masern-Virus-Hülle (MV) basierende Targeting-Technologie von lentiviralen (LV) auf γ-retrovirale (gRV) Vektoren übertragen. Durch die Optimierung des Herstellungsprotokolls der Vektoren und den Einsatz spezifischer Varianten der MV-Glykoproteine konnte der Titer um das ca. 400-fache erhöht werden.

Der zweite Teil dieser Arbeit beschreibt die Herstellung von Targeting-Vektoren, die spezifisch für murines CD4 (MVm4) oder CD8 (MVm8) sind. Deren Spezifität wurde zum einen durch die exklusive Expression des grün-fluoreszierenden Proteins (GFP) in $CD4^+$ oder $CD8^+$ Reporterzellen und zum anderen durch den Dosis-abhängigen Verlust des GFP-Signals nach Inkubation der $CD4^+$ oder $CD8^+$ Reporterzellen mit CD4- und CD8-blockierenden Antikörpern nachgewiesen.

Im dritten Teil der Arbeit wird gezeigt, dass MVm8 aber nicht MVm4 T-Zellen aus C57BL/6 (B6)-Mäusen transduzieren kann. Jedoch sind beide Targeting-Vektoren in der Lage, T-Zellen aus BALB/c-Mäusen zu transduzieren. MVm8-vermittelter Transfer des Ovalbumin (OVA)-reaktiven TZRs OT-I hatte zur Folge, dass von B6-Mäusen stammende T-Zellen OVA^+ Tumor-Zelllinien erkannten und Interferon-γ sezernierten.

Der vierte Teil dieser Arbeit beschäftigt sich mit der *in vivo* Transduktion primärer T-Zellen mithilfe von MVm8, welches den OT-I-TZR und eine Luciferase transferiert (MVm8/OT-I-

luc). Zu diesem Zweck wurden Rag2-defiziente (*engl*. recombination-activating gene) B6-Mäuse entweder mit polyklonalen (B6) oder monoklonalen T-Zellen, aus P14-TCR-transgenen Mäusen (P14), repopuliert. Durch systemische Applikation von MVm8/OT-I-luc wurden die transferierten T-Zellen *in vivo* transduziert. Bildgebende Verfahren wiesen eine erfolgreiche *in-vivo*-Transduktion nach. Die stärksten luc-Signale wurden in Mäusen gemessen, die mit P14-T-Zellen repopuliert wurden. Durch Immunisierungen konnten antigen-spezifisches Homing, Expansion und Kontraktion *in vivo* transduzierter T-Zellen gezeigt werden. Mäuse mit starker OT-I-luc-Expression waren gegenüber einer Infektion durch OVA-transgene *listeria monocytogenes* (LM-OVA) geschützt.

Zusammenfassend lässt sich sagen, dass das in dieser Arbeit entwickelte Vektorsystem in der Lage ist zwischen Subtypen von T-Zellen zu unterscheiden und sie simultan mit unterschiedlichen Transgenen auszustatten. Für MVm8 konnte gezeigt werden, dass es T-Zellen direkt *in vivo* transduzieren kann, was möglicherweise zur Entwicklung neuer Therapieoptionen im Kampf gegen Krebs und pathogenen Infektionen führen kann.

Summary

Immunotherapies using T cells modified with tumor-reactive receptors will in future complement current tumor treatments. Solid tumors consist of cancer cells, expressing major histocompatibility complex class I (MHC I) molecules and surrounding stromal tissue, expressing both MHC I and II. The inability of current treatments to reject solid tumors might be overcome with the simultaneous use of MHC I-restricted $CD8^+$ (CD: *cluster of differentiation*) and MHC II-restricted $CD4^+$ T cells, although tools for the generation of mixed cultures of $CD8^+$ and $CD4^+$ T cells, expressing differently restricted TCRs, are lacking. The aim of this thesis was to generate a vector system that allows the simultaneous transfer of different transgenes into $CD8^+$ and $CD4^+$ T cells, allowing the generation of a immunotherapeutic T cell product comprised of two differently engineered T cell subsets.

The first part of the thesis describes the transfer of the measles virus (MV) envelope-based targeting technology from lentiviral (LV) to γ-retroviral (gRV) vectors. By optimizing the vector production protocol and using specific tail variant combinations of MV glycoproteins the titer could be enhanced approximately 400-fold.

The second part reports the generation of two targeting vectors specific for murine CD4 (MVm4) or CD8 (MVm8). The exclusive specificity of MVm4 and MVm8 was proven (i) by expression of green fluorescent protein (GFP) in $CD4^+$ and $CD8^+$ reporter cells, respectively, but not in $CD4^-CD8^-$ cells after transduction, and (ii) by a dose-dependent loss of GFP signal after incubation of reporter cells with CD4 or CD8 blocking antibodies before transduction. Finally, MVm4 and MVm8 transferred different genes simultaneously in their respective target cells in mixed T cell cultures without loss of specificity.

The third part shows that MVm8 but not MVm4 transduced primary C57BL/6 (B6)-derived T cells. Both targeting vectors were able to transduce primary BALB/c-derived T cells. MVm8-mediated transfer of the ovalbumin (OVA)-reactive TCR OT-I resulted in B6-derived T cells secreting interferon-γ (IFNγ) upon recognition of OVA^+ tumor cell lines.

The final part of this thesis describes the *in vivo* transduction of primary T cells using MVm8 transferring OT-I and a luciferase (MVm8/OT-I-luc). To this end, B6 mice deficient for the recombination-activating gene *2* (Rag2) have been repopulated with either polyclonal (B6) or monoclonal T cells derived from P14-TCR transgenic mice (P14). One day later the transferred T cells were transduced *in vivo* by systemic application of MVm8/OT-I-luc. Live

imaging of mice showed successful *in vivo* transduction with strong luciferase signals from P14-repopulated mice. Upon immunization *in vivo*-transduced T cells homed, expanded and contracted repeatedly in an antigen-dependent manner. Finally, mice exhibiting strong luc-signals showed improved protection against infections by OVA-transgenic *listeria monocytogenes* (LM-OVA).

In conclusion, the viral vector system developed within this thesis is able to discriminate between the two main T cell subsets and to equip them with distinct transgenes simultaneously. Beyond that, MVm8 can transduce T cells directly *in vivo*, opening new options for immunotherapy of cancer and infectious disease, which were so far not accessible.

1 Introduction

1.1 T cell-mediated immunity

Immunity is a protective mechanism of an individual's body in order to maintain its integrity. Shaped by co-evolution with pathogens, higher organisms have developed an eminent and complex apparatus of cells and organs, which in its entirety is called the immune system.[1] Of particular interest is the adaptive immune system of vertebrates equipping the host with lymphocytes expressing a highly diverse repertoire of antigen receptors, generated by somatic recombination during the development of B and T cells. Especially T cells have been thoroughly investigated regarding their clinical potential in treating cancer and infectious disease because of their ability to recognize and destroy malignant and infected cells.[2]

1.1.1 Individual T cell receptors are generated by somatic recombination

Unlike cells of the innate immunity, which recognize fixed pathogen-associated molecular patterns (PAMPs), T cell receptors (TCRs) can potentially recognize all chemical and biological structures. The nearly unlimited flexibility of the T cell repertoire is given by the modular organization of TCR loci and a somatic recombination process mainly driven by the recombination-activating genes 1 and 2 (Rag1 and 2), which are the key enzymes of the VDJ recombinase complex. Lack of Rag1 or Rag2 in mice blocks development of mature lymphocytes completely.[3,4]

Functional TCRs consist of one α and one β chain, which are slightly different in structure. During development the β chain locus is rearranged first. One D segment is randomly fused to one of the six J segments of the first DJC cluster. Next, one out of 52 V segments is fused to the DJ segment to generate the variable region of the TCR. The recombined VDJ segment is finally fused to the constant segment of the first cluster yielding a fully recombined β chain (VDJC). This β chain pairs with an invariant pre-α chain to form a pre-TCR expressed on the cell surface, triggering recombination at the α chain locus. The α chain locus lacks D segments and recombination starts with the fusion of one of the 61 J segments to one of up to 80 V segments. The recombined VJ segment is then fused to the only constant segment of the α chain locus, giving rise to a fully recombined α chain (VJC). Fusion of the different segments involves double-strand breaks of the genomic DNA. During this process the nucleotide-sequence is altered by addition of P- and N-nucleotides leading to additional junctional diversity.[5,6]

The complex process of somatic recombination inherently harbors the possibility of generating non-functional TCR chains, e.g. by frame-shift mutation. If β chain rearrangement fails, a second round of recombination is initiated by combining D and J segments of the second cluster, which in turn are fused to a V segment upstream of the V segment in the first round. If rearrangement leads again to a non-functional β chain, the second allele is activated and again two rounds of recombination start. Only when both alleles fail to generate a productive rearrangement in the β chain loci, the thymocyte is entering the γ:δ T cell lineage. If the β chain is successfully rearranged the α loci undergo the same procedure until a functional α:β TCR is expressed. Expression of a TCR is necessarily accompanied by co-expression of cluster of differentiation (CD) protein 3 (CD3). The CD3 complex is composed of four distinct chains ($\gamma\delta\varepsilon_2\zeta$) and is required for T cell activation.[5,6]

1.1.2 T cell education in the thymus shapes the peripheral TCR repertoire

Although the same genetic processes lead to the development of B cell and T cell receptors, they differ substantially. B cell receptors recognize linear and non-linear three-dimensional surface structures of intact molecules independent of any other protein-interaction. TCRs on the other hand can only recognize linear epitopes derived from degraded proteins and presented on molecules of the major histocompatibility complex (MHC).[7–9] MHC-restriction is imposed on T cells during development in the thymus and accounts to which subset T cells belong.[10–12] The main T cell subsets are cytotoxic T cells (Tc), defined by expression of CD8 and T helper cells (Th), defined by expression of CD4.

Lymphoid progenitors lacking expression of TCR, CD4 and CD8 (double negative) enter the thymus at the cortico-medullary junction. After rearrangement of the β and α loci these thymocytes express a α:β TCR, CD4 and CD8 and are termed double positive (DP). DP thymocytes interact with cortical thymic epithelial cells capable of presenting any self-peptide on both MHC class I as well as MHC class II. T cells recognizing self-peptides on MHC I are committed to the CD8-lineage, whereas T cells recognizing self-peptides on MHC II are committed to the CD4-lineage, both subsequently becoming single positive. CD4 and CD8 are co-receptors of the TCR and enhance its overall avidity to peptide-MHC (pMHC) complexes by binding to MHC II and MHC I, respectively. T cells unable to interact with any pMHC complex are deprived of survival signals and undergo apoptosis (“death by neglect”). Single positive T cells interact with medullary thymic epithelial cells as well as dendritic cells (DCs) upon migration into the medulla. Positive selection occurs if T cells interact with pMHC complexes at an intermediate level. T cells with avidities above a certain threshold for self-pMHC are mostly negatively selected to avoid autoimmunity as part of central tolerance.[13] Few high-avidity T cells can become committed to a regulatory T cell (Treg)

phenotype and counteract autoimmunity in the periphery as part of peripheral tolerance.[14,15] Positively selected single positive clonal T cells, now capable of recognizing any foreign (and mutated self) antigen, enter the bloodstream to populate the periphery of the organism as naïve T cells.[5,6,16]

However, this is a simplified view of the educational process of T cells in the thymus. Analyses in mice and humans have shown, that T cells reactive against self-pMHC complexes are a natural part of the peripheral repertoire.[17,18] Usually self-reactive T cells are suppressed by peripheral tolerance mechanisms.[19] Failure of these mechanisms may lead to autoimmune disease. Recent studies argue that self-reactive T cells are an important part of the peripheral TCR repertoire and that lack of these cells, by e.g. a strict negative selection process, would open up "holes" in adaptive immunity, which could be readily exploited by pathogens.[20]

1.1.3 Course of an adaptive immune response

Any infection that is not cleared by the innate immune response generates a threshold dose of antigen that in turn activates the adaptive immune system. Naïve T cells recirculate between the bloodstream, secondary lymphoid organs and the lymphatic vessels back into the bloodstream until they encounter their specific antigen. Upon infection tissue-derived DCs are activated, take up antigen and migrate to draining lymph nodes as mature DCs, where they present pMHC complexes to T cells. DCs are the most powerful professional antigen presenting cells (APCs).[21] Macrophages and B cells are also able to present pMHC complexes to T cells and activate them. Circulating naïve T cells regularly scan APCs in peripheral lymphoid organs for the presence of their specific pMHC complex. If T cells encounter their respective pMHC complex on a mature DC they get activated and start proliferating at site. A hallmark of mature DCs is the expression of costimulatory molecules, especially the B7 proteins (CD80, CD86), necessary to fully initiate a T cell response. T cells are fully activated and become effector T cells if their TCR-CD3 complex transmits a first signal after pMHC binding and CD28 a second signal after binding to B7 molecules on APCs. If a T cell receives signal one without signal two it either undergoes apoptosis or becomes anergic.[22] The need for signal one and signal two to fully activate a T cell is part of the peripheral tolerance to self-antigen. Proliferation of effector T cells is mainly driven by expression of interleukin-2 (IL-2) and CD25, which together with CD122 and CD32 form the high-affinity IL-2 receptor. After proliferation and phenotypic changes effector T cells leave the secondary lymphoid organs and home to the site of infection where they exert their effector functions and clear the infection. The cytotoxic T-lymphocyte-associated protein 4 (CTLA-4, CD152) is expressed shortly after activation of T cells. CTLA-4 also binds to B7 molecules, but, in contrast to CD28, inhibits intracellular signaling.[23] Thus, the activation of T cells is controlled by a

negative feedback loop. During clearance of the infection, the level of antigen drops steadily and effector T cells get deprived of antigen and cytokine stimulation, which drives the majority of T cells into apoptosis. Surviving effector T cells are driven into a memory phenotype able to respond to an identical infection with faster kinetics.[5,6]

1.1.4 T cell subsets

During the course of an infection T cell subsets exert different effector functions. $CD8^+$ Tc cells recognize their respective pMHC I complex, presenting cytosolic antigens directly on infected or transformed cells. Subsequent killing is achieved by directed release of cytotoxic effector proteins perforin and granzymes.[24,25] Perforin creates pores in the target cells membrane through which granzymes enter the cytoplasm and induce apoptosis. This mode of killing is restricted to $CD8^+$ Tc cells and strictly calcium-dependent.[26] Studies of calcium-deprived $CD8^+$ Tc cells revealed a mode of calcium-independent killing, which can also be exerted by some $CD4^+$ Th cells. This second mode involves binding of Fas ligand, expressed by effector T cells, to Fas, expressed on target cells.[27–29] Upon binding of Fas, caspases are activated leading to apoptosis of the Fas^+ target cell. $CD8^+$ Tc cells also produce several cytokines upon activation including Interferon γ (IFNγ) and tumor necrosis factor α and β (TNFα, TNFβ).[30–32] IFNγ is the central effector cytokine of $CD8^+$ effector T cells and can also be produced by certain $CD4^+$ T cell subsets.[33] Release of IFNγ inhibits viral replication and increases expression of MHC I molecules as well as other components of the peptide generating and loading machinery.[34]

$CD4^+$ Th cells recognize their respective pMHC II complex on APCs, presenting exogenously taken up antigen. While MHC I is expressed on all nucleated cells, MHC II expression is restricted to APCs. The $CD4^+$ T cell subset is central to the immune system, as highlighted by the acquired immune deficiency syndrome (AIDS) caused by the human immunodeficiency virus (HIV). HIV^+ individuals developing AIDS die of usually "harmless" pathogens due to the inability of the immune system to clear the infection without the $CD4^+$ T cell subset.[35] The main function of $CD4^+$ Th cells is to provide help, largely in form of cytokines acting on other types of cells. The $CD4^+$ Th cell subset is more diverse than the $CD8^+$ compartment. Depending on the type of pathogen encountered by the innate immune system DCs create a cytokine milieu within secondary lymphoid organs dictating the fate of differentiation of $CD4^+$ Th cells. The variety of $CD4^+$ T cell subsets includes Th1, Th2, Th9, Th17, Th22, follicular helper T (Tfh) and Treg cells, all of them expressing their characteristic cytokine profile and transcription factors.[33] The classical subsets are Th1 and Th2 cells producing IFNγ and IL-4, respectively, and thereby supporting $CD8^+$ Tc cell-dependent and B cell-dependent immune responses.[36,37] In addition to these classical subsets,

Th17 cells are a well characterized third subset, which play a role in fighting extracellular bacteria and fungi.[38] Tfh cells reside in lymph nodes where they provide help to B cells.[39–41] Th9 and Th22 cells are newly discovered and less well characterized subsets, which seem to play a role in mucosal and epithelial immunity.[42,43] Although expressing CD4, Treg cells are not helper T cells. Nevertheless, regarding their ability to shut off immune reactions to foreign and self-antigens, they play a central role in the course of immune reactions and autoimmunity, emphasizing the critical role of $CD4^+$ T cell subsets.

Many immunotherapeutic approaches have focused on $CD8^+$ Tc cells since they can directly attack infected as well as transformed cells. In recent years several studies emphasized the importance of including $CD4^+$ T cells into immunotherapeutic regimens, either as cytotoxic cells themselves or as helper cells boosting the cytotoxic effects of $CD8^+$ T cells.[44–52]

1.2 Cancer immunotherapies

The term "immunotherapy" comprises any treatment of disease by inducing, enhancing or suppressing an immune response. This includes cytokine and antibody treatments as well as cellular therapeutics as e.g. DCs or T cells.

Immunotherapy has a long history usually being regarded to have started with the first cancer vaccine ("Coley´s toxin") being developed in 1893.[53] Early immunological insights gained by scientists around 1900 led to the notion that not only infectious but also malignant diseases might be curable by new immunological techniques.[54–56] Already in 1905 efforts were undertaken to immunize mice against tumors. Mice, spontaneously rejecting implanted tumors, became resistant against subsequent challenges with tumors of identical origin.[57] These experiments were performed with outbred mice and immunological reactions were most probably directed against foreign pMHC complexes. This is highlighted by the fact that recipient mice also rejected healthy tissue. With the upcoming technology of inbred mice in the 1940´s these tumor-unspecific effects could be eliminated and perceived tumor regressions led to the identification of tumor antigens able to elicit antibody- and cell-mediated immunity, which in turn gave rise to the field of cancer immunotherapies in the upcoming decades.[58,59] To date immunotherapy has entered the clinic with the first cytokine (TNFα) being approved in 1986 and the first monoclonal antibody (mAb) being approved by the US food and drug administration (FDA) in 1997.[60] Until the end of 2015 more than a dozen mAbs and four cytokines have been approved to treat certain types of cancer.[61] Further, the discovery of checkpoint inhibitors in 1990s by Allison *et al.* led to three such molecules being approved for cancer therapy.[60,62] Finally, one cell-based anti-tumor vaccine has been approved in 2010.[60] Examples of these immunotherapies will be discussed in the following sections.

1.2.1 Antigen-independent therapies

First cancer immunotherapies started with using antigen-independent cytokine therapies including IL-2, IFNα and IFNβ. Clinical studies showed response rates of 20-40% on average, with peak responses of up to 80-90% in the setting of hairy cell leukemia.[63–65] However, the pleiotropic effects of cytokines are not restricted to anti-tumor immunity but also give rise to autoimmunity in treated patients.

The same holds true for immune checkpoint inhibitors. Immune checkpoint molecules like CTLA-4 or programmed death protein 1 (PD-1) dampen an ongoing immune response, ultimately leading to its shut off, by interacting with their respective ligands on APCs or tumor cells.[66] Antibodies that block these protein-protein interactions have proven highly valuable in tumor treatment in clinical trials.[67–70] To date, three checkpoint inhibitors are available, ipilimumab (CTLA-4 blocker), nivolumab and pembrolizumab (PD-1 blocker). The most advanced is ipilimumab, which led to an increase in overall survival of two months (11.2 vs. 9.1) in a clinical phase III study including 502 patients, being treated with ipilimumab plus chemotherapy compared to the group of patients that received chemotherapy alone. Beyond that ipilimumab-treated patients were superior in one-, two- and three-year survival rates with 21% survival compared to 12% after three years. Although no statistical difference in tumor-shrinkage was observed, there was a 24% improvement in progression-free survival. At the same time, there was a two-fold increase in high-grade adverse events in patients receiving ipilimumab compared to chemotherapy alone.[68]

Thus, antigen-specific approaches, activating the immune system more specifically and leading to fewer side effects, are favorable.

1.2.2 Antigen-specific therapies

Antigen-specific cancer immune therapies include therapeutic antibodies, cancer treatment and preventive vaccines as well as adoptive T cell therapies, the latter being discussed separately in the following paragraph. The theoretical reduction of side effects is dependent on how tumor-specific the targeted epitope is. Antibody or T cell therapies targeting antigens exclusively expressed by tumor cells should not elicit autoimmunity, whereas it can occur in varying severities if the target is shared between tumor and healthy tissues.[71]

Therapeutic antibodies appear in various forms. They can either be applied as monoclonal antibodies or as antibody-drug conjugates (ADC), for example. Trastuzumab, a HER2-specific monoclonal antibody, is available for treatment of HER2-overexpressing breast cancer since 1998.[72] Since 2013 an ADC combining Trastuzumab with DM1 (a cytotoxic agent) is approved for metastatic breast cancer.[73] Rituximab, a CD20-specific monoclonal

antibody, is another success story in cancer immunotherapy and has become a mainstay in the treatment of some B cell lymphomas and B cell chronic lymphocytic leukemia.[74,75] Rituximab leads to destruction of both malignant and healthy B cells. Since CD20 is absent on terminally differentiated plasma cells, the loss of healthy B cells is well tolerated. Rituximab is a good example for a non-tumor- but antigen-specific treatment. The effector functions of monoclonal antibodies leading to the death of their target cells can be (i) induction of apoptosis, (ii) complement- or (iii) antibody-dependent cell-mediated cytotoxicity. In case of rituximab all three mechanisms have been detected in patients.

Cancer treatment vaccines are cell-based vaccination approaches to strengthen an anti-tumor immune response. In 2010 Sipuleucel-T has been approved for treatment of some forms of prostatic cancer.[76,77] So far, it is the only approved immunotherapy for advanced prostate cancer. Treatment includes the isolation of autologous DCs and loading them with the tumor antigen prostatic acid phosphatase (PAP), which is present in >95% of prostate cancer cells. After maturation of the antigen-loaded DCs, they are re-infused into the patient in order to activate PAP-specific T cells, which in turn home to the prostate and kill tumor cells. Sipuleucel-T exhibits only moderate side effects.

Preventive vaccines aim at preventing infection of the host with tumorigenic pathogens as e.g. human papillomaviruses (HPV). These vaccines are considered tumor vaccines because of the high tumorigenic potential of the targeted pathogens. In case of HPV, type 16 and 18 account for 70% of all cervix carcinomas.[78] Currently, there are three highly effective vaccines for different HPV serotypes available: Gardasil (since 2006), Cervarix (since 2007) and Gardasil 9 (since 2014).[79] Worldwide, Chronic hepatitis B virus (HBV) infection causes 80% of all liver cancer. Two FDA-approved vaccines (Engerix-B, Recombivax HB) protect against HBV only, whereas several others protect against infection by HBV as well as other viruses (Twinrix, Pediarix). The FDA approved the original HBV vaccine Heptavax already in 1981, making it the first anti-cancer vaccine.

1.2.3 Adoptive T cell therapies

Most of aforementioned therapeutic strategies aim at activating or inducing tumor-reactive T cell populations pre-existing in a given individual. However, the adoptive transfer of T cells offers the advantage of being able to directly interfere with the final therapeutic cell type, either by enlarging the number of autologous tumor-reactive T cells (non-modified T cells) or by introducing otherwise absent or anergic tumor reactivity (TCR- or chimeric antigen receptor (CAR)-engineered T cells). Evidence for tumor-reactivity of adoptively transferred T

cells exists since mid-1960´s, but it was the discovery and utilization of IL-2 that paved the way for *ex vivo* culture and therapeutic use of T cells.[80–82] Since then T cells can be expanded *in vitro* to large numbers and kept in culture long-term. Strategies have been developed to give rise to autologous T cell populations with defined tumor reactivities or to introduce such reactivities by means of genetic engineering.[83,84] Thus, it is now possible to generate high-avidity T cells in therapeutic numbers. Another advantage is, that the host can be preconditioned prior to adoptive cell transfer. It has been shown, that a nonmyeloablative chemotherapy regimen given immediately before adoptive cell transfer led to increased cancer regression and facilitated engraftment of transferred T cells.[85] Besides the removal of "cytokine sinks", the ablation of the peripheral immunity also eliminates immune cells with a suppressor phenotype (Tregs or myeloid-derived suppressor cells).

Today adoptive T cell therapy is divided into two main categories, (i) the transfer of non-modified T cells and (ii) the transfer of antigen receptor-engineered T cells.

Transfer of non-modified T cells has been pioneered by the group of Steve Rosenberg.[86] The general procedure is to isolate tumor-infiltrating lymphocytes (TILs) from tumor biopsies. For this purpose, resected tumor material is chopped into small fragments containing tumor cells as well as TILs. These fragments are then cultured with high doses of IL-2 for two to three weeks until the TILs have proliferated and destroyed all tumor cells. A pure lymphocyte culture is generated. The individual fragment-derived TILs are then tested for tumor reactivity in coculture assays and expanded to therapeutical numbers before reinfusion into the patient.[87] The therapeutic product that is generated this way is usually a highly undefined mixture of T cells with unknown specificities. Lately, a more sophisticated strategy has been proposed, which is able to isolate neoantigen-specific T cells from the tumor as well as from peripheral blood lymphocytes.[83] This strategy could overcome one of the biggest drawbacks of TIL therapy, which is its restriction to melanomas and allow a more widespread use of autologous tumor-reactive T cells with a defined specificity.[88] Another drawback is the long *ex vivo* culture periods needed to reach therapeutical numbers, which may negatively affect the *in vivo* functionality of transferred TILs.[89]

Transfer of antigen receptor-modified T cells results in a much better defined therapeutic product compared to bulk TIL therapy.[90,91] The introduced antigen receptor, either a TCR or a CAR, has a defined specificity. Characteristics of the receptors are well known and thoroughly studied in preclinical experiments. This allows the widespread use of T cell therapy, even in patients that have failed to generate effective TILs. In some cases TILs could

be isolated from primary tumor tissue, but the T cells were not able to lyse their target tumor cells and means to break the unresponsiveness remained unsuccessful. Since the specificity of a T cell is solely determined by its TCR, the transfer of TCR-coding sequences into other T cells redirects these cells towards the introduced specificity.[92] By identifying the TCR coding sequences it becomes possible to treat patients having unresponsive or no TILs at all, and, further, to "choose" the best T cell phenotype with the highest lytic capacity for example. To date, central memory or naïve T cells seem to be the optimal T cell subset for adoptive T cell therapy because of their high self-renewal and lytic capacity.[93–95] Based on these principles a therapeutic approach, using TCR gene-modified T cells, has been developed, which starts with the isolation of a patients peripheral T cells. Activated T cells are then TCR- or CAR-engineered and propagated. Finally, a therapeutic number of gene modified T cells is re-infused into the patient and the clinical course is observed (Fig.1).[71,87]

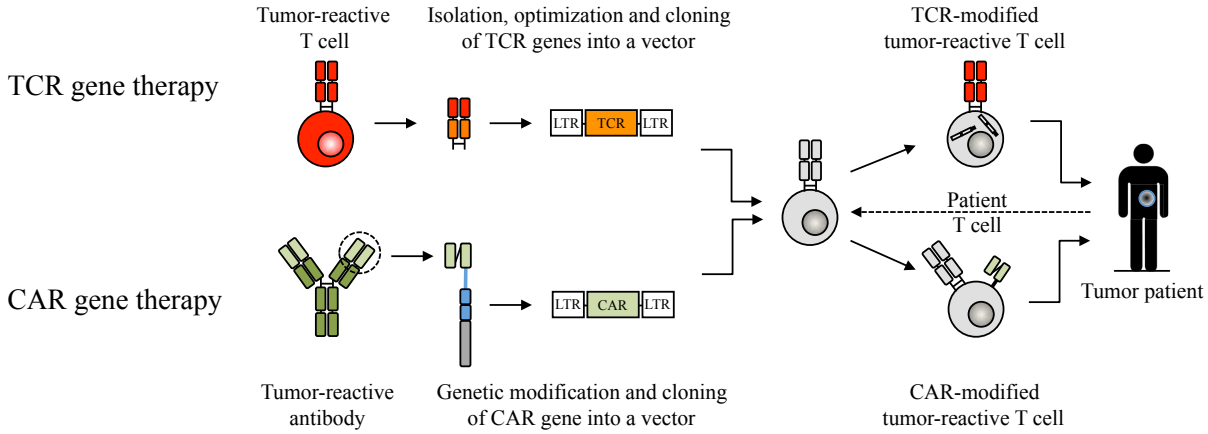

Fig.1 Course of TCR and CAR gene therapy
The schematic drawing depicts the general course of adoptive T cell therapy using TCR- or CAR-engineered T cells. TCR-encoding genes are isolated from a tumor-reactive T cell clone. CARs are constructed by fusing the variable regions of a tumor-reactive antibody to T cell specific intracellular signaling domains. By employing viral vectors the TCR- or CAR-encoding genes are transferred into stimulated T cells derived from a tumor-bearing patient. Ideally the exogenous tumor-reactive TCR (red) replaces the endogenous TCRs (gray). The CAR (green) is not competing for surface expression and does not mispair with endogenous TCRs. The engineered T cells are then rapidly expanded and re-infused into the patient. LTR: long terminal repeat

Using this approach many clinical trials with TCR-engineered T cells mainly targeting tumor-associated antigens have been performed treating melanoma and synovial sarcoma.[96–100] Exchanging the TCR by a CAR extends adoptive T cell therapy to a broader patient pool, because, unlike TCRs, CARs are not MHC-restricted.[2,101] Nevertheless, CARs can only target surface molecules, whereas TCRs can target epitopes derived from intracellular as well as surface antigens. Furthermore, CARs are useful when tumor cells downregulate MHC molecules or fail to process a T cell epitope. CD19-specific CARs show the best results in clinical trials using engineered T cells, so far. They have been used to treat B cell lymphoma,

chronic lymphatic leukemia and, most spectacular, acute lymphoblastic leukemia, with 90% complete remission among 30 patients.[101–103] These overwhelming results led the FDA to grant CD19-CAR therapy breakthrough therapy designation in 2014. However, treating solid tumors using CAR-engineered T cells failed so far, with one exception. A GD2-specific CAR achieved complete remission in three out of eleven neuroblastoma patients.[104] All other attempts to treat solid tumors using CAR-engineered T cells were disappointing.[105–107]

1.2.4 Drawbacks of *ex vivo* engineered T cells

The main aim of adoptive T cell transfer is to break the immune systems tolerance towards cancer. In case of T cell engineering two factors are pivotal for treatment success.

First, the antigen has to be chosen very carefully and an antigen receptor has to be identified. Antigen choice is crucial for success of adoptive cell therapy using engineered T cells. Deciding which antigen to target and retrieval of associated antigen receptors are the bottlenecks of T cell gene therapy. One quality of the perfect rejection antigen is its exclusive expression on tumor cells. These can be either cellular epitopes harboring somatic mutations or foreign (e.g. virus-derived) epitopes for which the natural repertoire of T cells is not negatively selected against in the thymus. Further, the antigen should be involved in cancer formation and transformation and thus be indispensable for all tumor cells. This way no antigen escape variants of the tumor can be formed.[108] To date, no such epitope has been targeted in clinical trials of adoptive T cell therapy. The complex matter of antigen choice and methods to detect and retrieve TCRs or CARs goes beyond the scope of this thesis and is described elsewhere.[108–113]

Second, the engineered T cells need to be fully functional in terms of proliferation, homing and tumoricidal effector functions. Removing T cells from their natural environment and culturing them for long periods of time *in vitro* counteracts these requirements.[89] TCR- or CAR-engineered T cells are generated in a two-step process. First, retroviral (RV) vector particles encoding for the therapeutic antigen receptor are generated, and second, T cells are isolated from the patients peripheral blood, engineered using the RV particles, expanded to sufficient numbers and then reinfused into the lymphodepleted patient (Fig.2).[114] The time needed for expansion is critical for a positive outcome of therapy. It has been shown, that effector functions of T cells are negatively correlated with the length of *in vitro* culture.[89] Beyond that, this production process is technically demanding and laborious, requiring highly specialized and well trained staff as well as a high-tech facility able to perform all steps in good manufacturing practice (GMP). This increases the costs thereby limiting the availability and widespread of adoptive T cell therapy using engineered T cells.

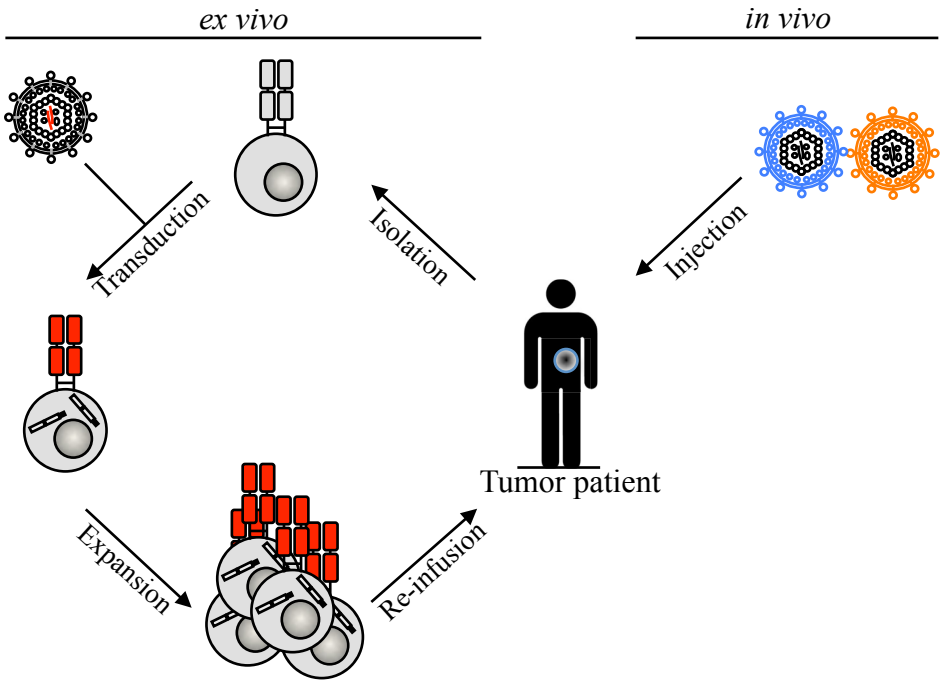

Fig.2 Genetic engineering of T cells *ex vivo* and *in vivo*
The advantage of *in vivo* T cell engineering is graphically illustrated. *Ex vivo* engineering using non-specific vectors requires the isolation, transduction and expansion of patient-derived T cells, which is laborious and cost-intensive (left panel). Extended *ex vivo* cultures also harbor the risk of loss of *in vivo* functionality of engineered T cells. The use of targeting vectors reduces the complexity of T cell engineering by allowing transduction of T cells directly *in vivo* by systemic administration of vector particles (right panel). The application of targeting vectors with different specificities (indicated by the different colors) allows the simultaneous *in vivo* engineering of distinct cell types with identical or different transgenes.

Transducing T cells directly *in vivo* would make any *ex vivo* culture obsolete and also reduce the costs of T cell gene therapy dramatically. The generation of RV vector particles would be sufficient (Fig.2). One key prerequisite of *in vivo* transduction is the specific delivery of transgenes to the target cell type. This can either be achieved by transcriptional (e.g. by means of cell-specific promoters) or phenotypic targeting (e.g. by exclusive expression of a cell surface molecule). Phenotypic targeting enables the design of vectors specific for T cells by targeting CD3 for example. As mentioned above, the two main subsets of T cells, $CD4^+$ Th and $CD8^+$ Tc, use TCRs with different MHC-restriction. The generation of two independent vectors, one specific for CD4 and the other specific for CD8, would allow the simultaneous delivery of two different, e.g. tumor-reactive, TCRs into the respective T cell subsets (Fig.3).

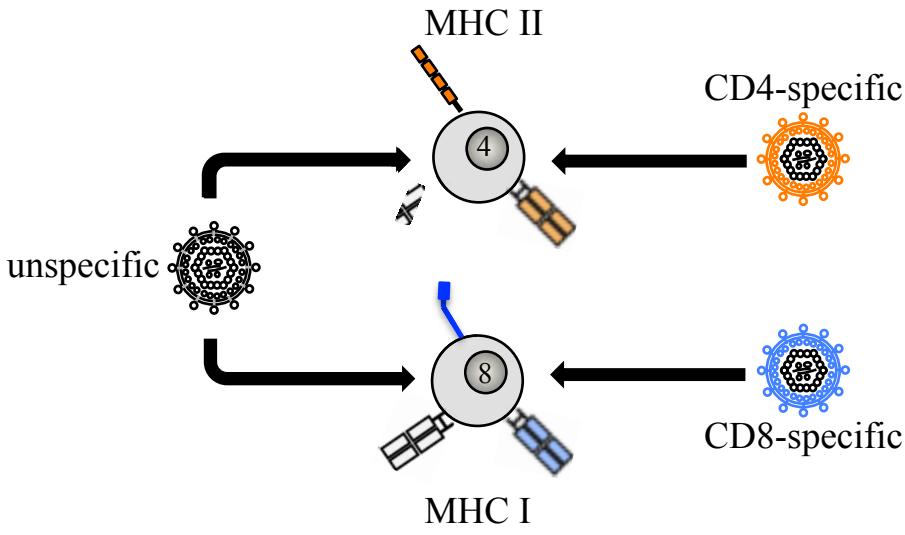

Fig.3 Simultaneous delivery of two different TCRs by specific targeting vectors
Unspecific vector particles (gray) equip both $CD4^+$ and $CD8^+$ T cell with identical TCRs (gray). By using two independent vectors, one specific for $CD4^+$ T cells (orange) and one specific for $CD8^+$ T cells (blue) it is possible to simultaneously engineer both subsets with an MHC II- (orange) or an MHC I-restricted (blue) TCR, respectively. Depicted are also the CD4- (orange) and the CD8α-molecule (blue) on the respective T cells.

1.3 Cell type-specific transgene delivery

The discovery that viruses are introducing their own genome into host cells in 1952 and the subsequent development of viral vectors in 1980´s and 1990´s merged into the broad spectrum of viral gene transfer systems available today, fulfilling nobel prize laureate E.L. Tatum´s anticipation from 1966, that „[…] *viruses will be effectively used for man´s benefit* [...] *in genetic therapy*“.[115–119]

RV vectors are among the most commonly used viral vectors in gene therapy due to their ability to mediate efficient and stable transgene expression in almost all human and murine cell types.[120] While this broad tropism made RV vectors a useful tool for *ex vivo* gene therapy, it is the major obstacle for *in vivo* transduction. *Ex vivo* it is possible to pre-select or enrich the desired cell type, whereas *in vivo* it is not. The major prerequisite for successful *in vivo* gene therapy is the specific and exclusive delivery of transgenes to a given cell type. Usage of such targeting vectors increases *in vivo* transduction efficiency dramatically by decreasing unspecific uptake of vector particles by irrelevant cells, which is also a matter of safety, since a transgene can be therapeutic in one cell type but potentially harmful in another. On the other hand, there are viruses with more restricted tropism, such as HIV, which transduces mostly human $CD4^+$ cells. The tropism of a virus is dictated by its envelope glycoprotein. By combining the envelope glycoprotein of a given virus with a RV transfer vector it is possible to change the tropism of vector particles.[121–123] This process is called pseudotyping. Nonetheless, naturally occurring cell type-specific viruses are limited. Thus,

efforts were undertaken to redirect vector particles by means of engineered virus glycoproteins. This approach, first attempted 23 years ago, involves detargeting of the envelope glycoprotein from its natural receptors and retargeting it to a new cell surface molecule by introducing a new specificity using single-chain variable region antibody fragments (scFv).[124,125] Using this strategy, retargeting of pseudotyped vector particles was achieved but membrane fusion was impaired. Hence, following studies focused on two-component envelopes, in which receptor binding and membrane fusion is separately mediated by two distinct glycoproteins. Sindbis virus-derived envelope glycoproteins are the first example of such a two-component system being successfully retargeted while maintaining membrane fusion function[126,127] The pH-dependent Sindbis-derived envelope requires uptake of vector particles by the target cell, possibly limiting their applicability, while Measles Virus (MV)-derived envelopes mediate pH-independent fusion directly at the cell membrane.[125] Two years later MV-derived envelope glycoproteins hemagglutinin (H) and fusion (F) were introduced to retarget RV vectors to specific cell types.[128]

1.3.1 Measles virus biology

MV, a major human pathogen, belongs to the *Morbillivirus* genus within the *Paramyxovirus* family. All paramyxoviruses are structurally related, containing a single-stranded, negative-sense RNA genome, which is encapsulated by nucleocapsid proteins. Between core and the host cell-derived lipid bilayer matrix proteins are residing. All paramyxoviruses harbor two integral membrane proteins, H and F. Functionally, H mediates binding of the virus to its cellular receptors and F the fusion of the viral envelope with the membrane of the host cell. H, a type II transmembrane glycoprotein, forms disulfide-linked homodimers that associate to form tetramers. It has a 34 amino acid cytoplasmic tail, followed by a hydrophobic transmembrane domain and a large C-terminal ectodomain. F, a type I transmembrane glycoprotein, is synthesized as an inactive precursor (F_0) and cleaved into an F_1 and F_2 subunit by furin. F_1 and F_2 are linked via a disulfide-bond to yield the fusion-competent trimerized F protein. F has a 33 amino acid cytoplasmic tail, a hydrophobic transmembrane and a large N-terminal ectodomain, harboring a highly conserved stretch of hydrophobic aminoacids (113-145) probably mediating membrane fusion. Mechanistically, binding of H to one of its cellular receptors triggers engagement of F, which initiates the fusion of both membranes by a series of irreversible conformational changes.[129–132]

Wild type MV enters and probably exits the host via Nectin-4, expressed in the epithelium and spreads within the host by infecting $CD150^+$ (aka SLAM, signaling lymphocyte activation molecule) lymphocytes.[133,134] MV is the first virus shown to have an immunosuppressive effect.[135] Enders and Peebles were the first to propagate MV in cultures

of human kidney cells.[136] The virus was derived from blood of David Edmonston, a child infected with measles. This virus strain (MV_{vc}) was attenuated and used for the generation of a highly effective vaccine.[137,138] During the many years of *in vitro* culture MV_{ED} gained the ability to also infect cells via CD46, an almost ubiquitously expressed complement inhibitory molecule, although affinity to CD150 is higher than to CD46.[139,140]

1.3.2 De- and retargeting of the measles virus envelope

As mentioned above, initial attempts to redirect viral vectors based on envelopes consisting of a single glycoprotein. Modifications of these glycoproteins negatively affected the cell entry process, since both functions, binding and fusion, are mediated by the same molecule. Instead, the MV cell entry system relies on two interacting proteins, decreasing the likelihood of negative effects on membrane fusion and increasing the chances of a functionally redirected vector.

Targeting MV to new specificities is a two-step process. First, H has to be detargeted from its natural receptors and second, a protein binding domain introducing a new specificity, has to be added.[141] Detargeting is achieved by insertion of four distinct point mutations into the H ectodomain (Y418A, R533A, S548L, and F549S).[142] The first successfully retargeted MV particles have been employed as oncolytic agents targeting CD38, epidermal growth factor receptor (EGFR) or its mutant EGFRvIII.[143,144] Funke *et al.* first described MV-pseudotyping of a RV transfer vector, in this case derived from HIV-1 lentivirus (LV), being retargeted to CD20.[141] To accomplish LV pseudotyping truncated tail variants of H and F had to be employed.[141,145] Subsequently, this system has been extended to many other target cells and proven to be an efficient and highly flexible tool for delivery of transgenes stably into desired cell types *in vitro* and *in vivo*.[146] Mostly, scFv have been used as targeting domain, but also other protein binding domains can be utilized, such as DARPins (designed ankyrin repeat proteins), as in case of targeting human $CD4^+$ T cells.[147] Accordingly, a human CD8-specific targeting vector has been developed.[148] Both retargeted vectors were able to selectively transduce their respective target cells *in vitro* and *in vivo*. Nevertheless, to study potential benefits of human *in vivo* gene transfer technologies in the context of TCR- or CAR-engineered T cells for immunotherapy of cancer and infectious disease, preclinical testing is mandatory.

2 Aims of Thesis

The aim of this thesis was to develop a vector system that allows the simultaneous delivery of MHC I- and MHC II-restricted TCRs into $CD8^+$ Tc and $CD4^+$ Th cells, respectively, both *in vitro* and *in vivo*.

The project started with the transfer of the targeting technology from LV to gRV vectors, to overcome the insusceptibility of primary murine T cells for LV-mediated transduction:

- Can MV glycoproteins pseudotype gRV vectors?
- Which H and F tail variants yield the highest titers when pseudotyping gRV vectors?

Second, the H protein had to be engineered to be specific for murine CD4 or CD8:

- Isolation and identification of sequences encoding for CD4- and CD8-specific antibodies from hybridomas.
- Generation of single chain antibody fragments as targeting domains.
- Cloning of both targeting domains on individual MV H proteins.
- Establishment of a cellular test system for both targeting vectors.
- Can target cell lines be transduced simultaneously with different transgenes?

The third part of the thesis deals with the transduction of primary splenocytes and their functional characterization:

- Can the targeting vectors transduce primary murine T cells?
- Can they both be applied simultaneously on primary cells?
- Are primary cells, transduced by the targeting vectors as functional in *in vitro* assays, as primary cells transduced with conventional non-targeting vectors?

Finally, the ability of the targeting vectors to transduce primary murine T cells *in vivo* had to be analyzed:

- Can the targeting vectors transduce primary T cells *in vivo*?
- Are *in vivo*-transduced T cells functional in terms of homing, proliferation and introduced antigen-specificity?
- Can *in vivo*-transduced T cells built up a functional immunity against tumors or pathogens?

3 Results

3.1 Adapting targeting technology to γ-retroviral vector systems

LV vector systems are able to efficiently transduce a broad variety of different cell types originating from different species within Mammalia, including e.g. human T cells and murine fibroblasts. However, transduction efficiency drops dramatically using T cells of murine origin as target cells. While murine T cells are nearly refractory to LV-mediated transduction, they can be easily transduced by gRV vector systems.[47] Initially, the MV envelope-based targeting technology had been developed and optimized for LV vectors[128]. Therefore, in the first part of the project, the targeting technology was transferred from LV to gRV vector systems.

3.1.1 Pseudotyping γ-retroviral vectors with measles virus glycoproteins leads to low titers

The segregation of viral genes to distinct plasmids, as part of developing a vector system, allows exchanging the gene(s) encoding for the envelope of a given virus by envelope gene(s) derived from a different virus. This process is named pseudotyping. The success and efficiency of pseudotyping strongly depends on interactions between group-specific antigen-(gag)-encoded matrix proteins and the intracellular part of envelope glycoproteins. In case of LV vectors pseudotyped with MV glycoproteins the optimal length of the intracellular domains has been determined previously. Highest titers were obtained by combining the H-protein with an 18 amino acid N-terminal truncation (HΔ18) and the F-protein with a 30 amino acid C-terminal truncation (FΔ30)[128]. Thus, we initially employed the HΔ18-FΔ30 combination for pseudotyping gRV vectors.

Three different types of transfer vectors were compared: a self-inactivating LV vector (SIN-LV), a self-inactivating gRV vector (SIN-gRV) and a gRV vector with an intact 3´-LTR. All 3 vectors use the same variant of a mouse proliferative sarcoma virus-derived (MPSV) promoter (MP71) to regulate transgene expression.[149] The SIN vectors harbor an inactive 3´-LTR and thus drive transgene expression from an internal promoter position, whereas gRV expression is LTR-driven (Fig.4A). To illustrate differences between the types of transfer vectors it was important to use identical genetic elements, like promoter or posttranscriptional regulatory element (PRE). Additional features of the 3 vector types are summarized in table 1.

Table 1 • Characteristics of transfer vectors applied in this study

	gRV	SIN-gRV	SIN-LV
designation	pMP71	pSERS11	pRRL
backbone & LTR	MPSV	RSV	RSV
Promoter position	LTR	internal	internal
packaging plasmid	pcDNA3.2	pcDNA3.2	psPAX2
max. cargo-size	8 kb	8 kb	18 kb
transduction of			
human T cell	yes	yes	yes
murine T cell	yes	yes	no
reference	Engels *et al.*[149]	Schambach *et al.*[150]	Zhou *et al.*[148]

Gray shaded boxes indicate identical features. MPSV: mouse proliferative sarcoma virus, RSV: Rous-sarcoma-virus

In order to compare the titer of the three vector supernatants a $CD150^+$ (aka SLAM) Jurkat 76 T cell line was generated (J76S8). J76S8 was also engineered to express CD8 to analyze a human CD8-specific targeting vector and to enable functional assays after TCR-transduction, which is not part of this study. From bulk-transduced J76 cells a clone with high and stable expression of both transgenes was chosen (Fig.4B).

In parallel generated vector supernatants titered on J76S8 cells showed that the MVvc HΔ18-FΔ30 combination is an inept pseudotype for both gRV and SIN-gRV (Fig.4C). SIN-LV performed best, with reaching titers of up to $1x10^5$ transducing units per ml (TU/ml).

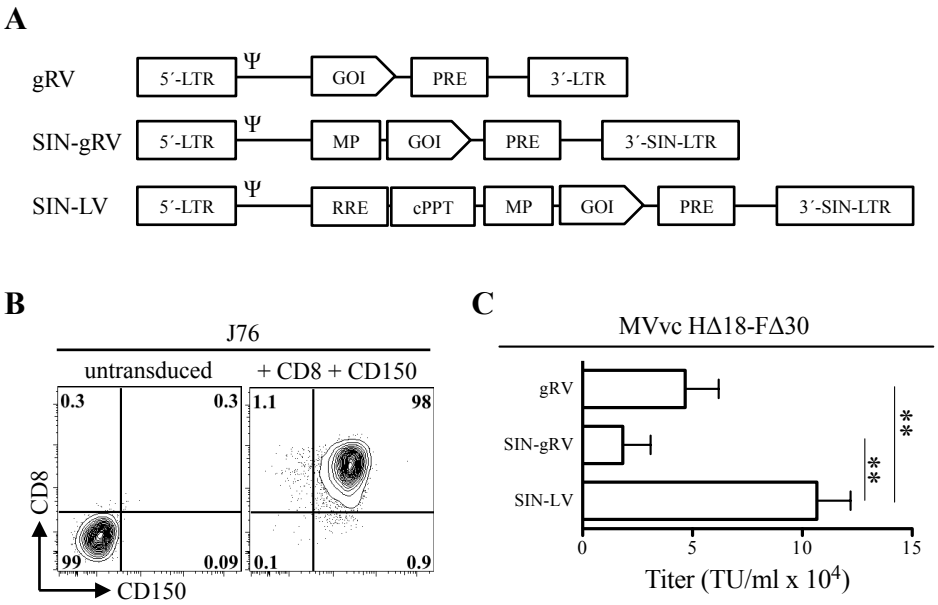

Fig.4 Inefficient pseudotyping of gRV vectors by MVvc HΔ18-FΔ30
(A) Graphic illustrations of transfer vectors applied in this study. LTR: long terminal repeat, Ψ: packaging signal, GOI: gene of interest, PRE: posttranscriptional regulatory element, MP: MP71-promoter, RRE: rev-responsive element, cPPT: central polypurine tract. (B) Surface expression of human CD8 and CD150 on transduced J76 cells. Untransduced J76 cells served as control. The percentage of gated cells is indicated. (C) Titers of MVvc HΔ18-FΔ30-pseudotyped transfer vectors are shown. Bar diagrams depict pooled data of three independent experiments. Asterisks indicate a p value < 0.01.

In each repetition the same hierarchy of titers was observed (SIN-LV > gRV > SIN-gRV). Although statistically not significant, gRV outperformed SIN-gRV each time by approximately a 2-fold higher titer (p=0.07).

3.1.2 Optimization of vector production protocol

In general pseudotyping RV vectors with MV envelope glycoproteins is inefficient and yields low titers. Therefore, vector production had to be performed large scale, including the increase of number of packaging cells per production cycle as well as concentrating the vector supernatant via ultracentrifugation, which led to detectable numbers of vector particles using identical volumes for titration (Fig.5A).

For establishment of the large-scale vector production protocol, the SIN-LV transfer vector pseudotyped by MVvc HΔ18-FΔ30 encoding for the green fluorescent protein (SIN-LV/GFP) has been used. In all analyzed timelines the titer peaked at the earliest time point of harvesting the supernatant (48 hrs after transfection, Fig.5B). Among those, changing the medium 36 hrs after transfection decreased the titer substantially (compare II-1 with I-1 and III-1). Repeatedly, the highest titer was obtained when medium was changed 24 hrs after transfection and the supernatant was harvested additional 24 hrs later (Fig.5C). All large-scale vector productions were thus performed accordingly.

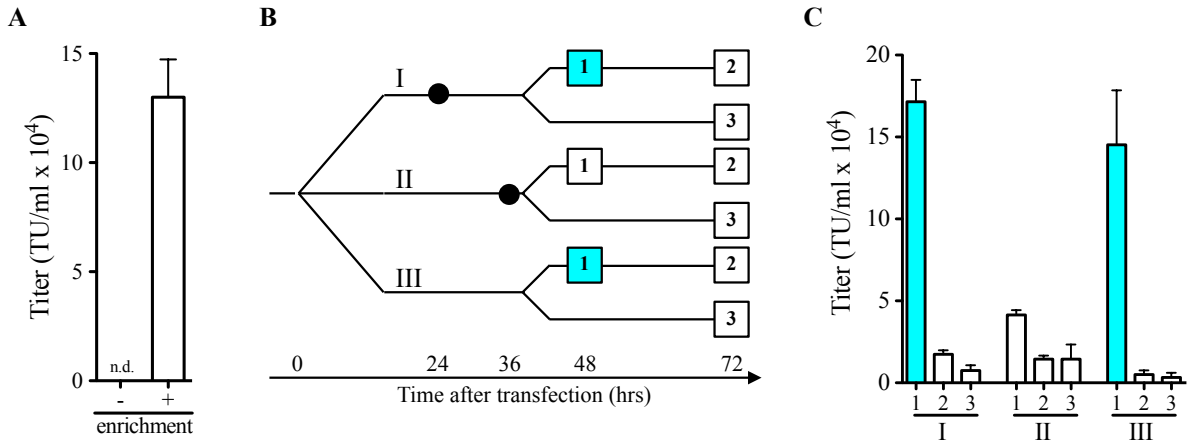

Fig.5 Increasing viral titer by optimization of production procedure
SIN-LV/GFP pseudotyped by MVvc HΔ18-FΔ30 was used to generate presented data. (A) Titer before (-) and after (+) ultracentrifugation (n=3). n.d.: not detectable. (B) Timeline of all vector production protocols performed. I, II and III were all started in parallel. Black filled circles indicate time points of medium change. Boxed numbers indicate time point of harvesting the supernatant. (C) Bar diagrams depicting the differences in titer caused by the different vector production protocols (n=2). Titration was performed by transducing J76S8 cells with serial dilutions of concentrated supernatant. Colored boxes and bars belong together.

3.1.3 Screening of measles virus glycoprotein tail variants

Large-scale virus production is one mean to increase viral titers to a sufficient amount. Improving the compatibility of the different parts of the vector system is a second one. Thus, in parallel to the optimization of the vector production protocol different tail variants have been analyzed for their ability to pseudotype gRV vectors. The structures of MV H and F proteins as well as available tail variants are depicted in Fig.6A (see also section 1.3.1). Including the full-length proteins there are 16 H and three F tail variants, leading to 48 possible combinations of MV envelopes. To determine the best-suited combination, gRV vectors encoding for GFP (gRV/GFP) were pseudotyped with all 48 MV envelopes. Successful transfection of 293T cells was determined by expression of GFP and functional expression of MV H and F proteins was indicated by formation of syncytia (Fig.6B).

J76S8 cells were transduced in parallel by all 48 vector supernatants using identical volumes. Eight vector supernatants surpassed the MV HΔ18-FΔ30 by an at least ten-fold higher transduction rate (Fig.6C). Next, those supernatants were titrated in parallel on J76S8 cells, revealing a peak in titer when gRV/GFP was pseudotyped with MV HΔ21A-FΔ24 (Fig.6D). However, it was not possible to produce all 48 vector supernatants in parallel. To rule out external factors being responsible for the peak in titer, the five best supernatants were produced again in parallel under identical conditions and titrated. Again, MV HΔ21A-FΔ24 performed best, achieving an approximately 400-fold higher titer than MV HΔ18-FΔ30 (Fig.6E).

Fig.6F illustrates all results obtained from this analysis. None of the combinations using full-length MV H and F proteins was able to efficiently pseudotype gRV vectors. Interestingly, seven out of eight vector supernatants that reached an at least ten-fold higher transduction rate than MV HΔ18-FΔ30 made use of FΔ24 (Fig.6C-F). Only one of those utilized FΔ30, however, in combination with HΔ21A. Hence, all supernatants yielding high titers were composed either of HΔ21A or FΔ24. Considering this pattern it is not a surprise that MV HΔ21A-FΔ24 is the best-suited pseudotype for gRV vectors.

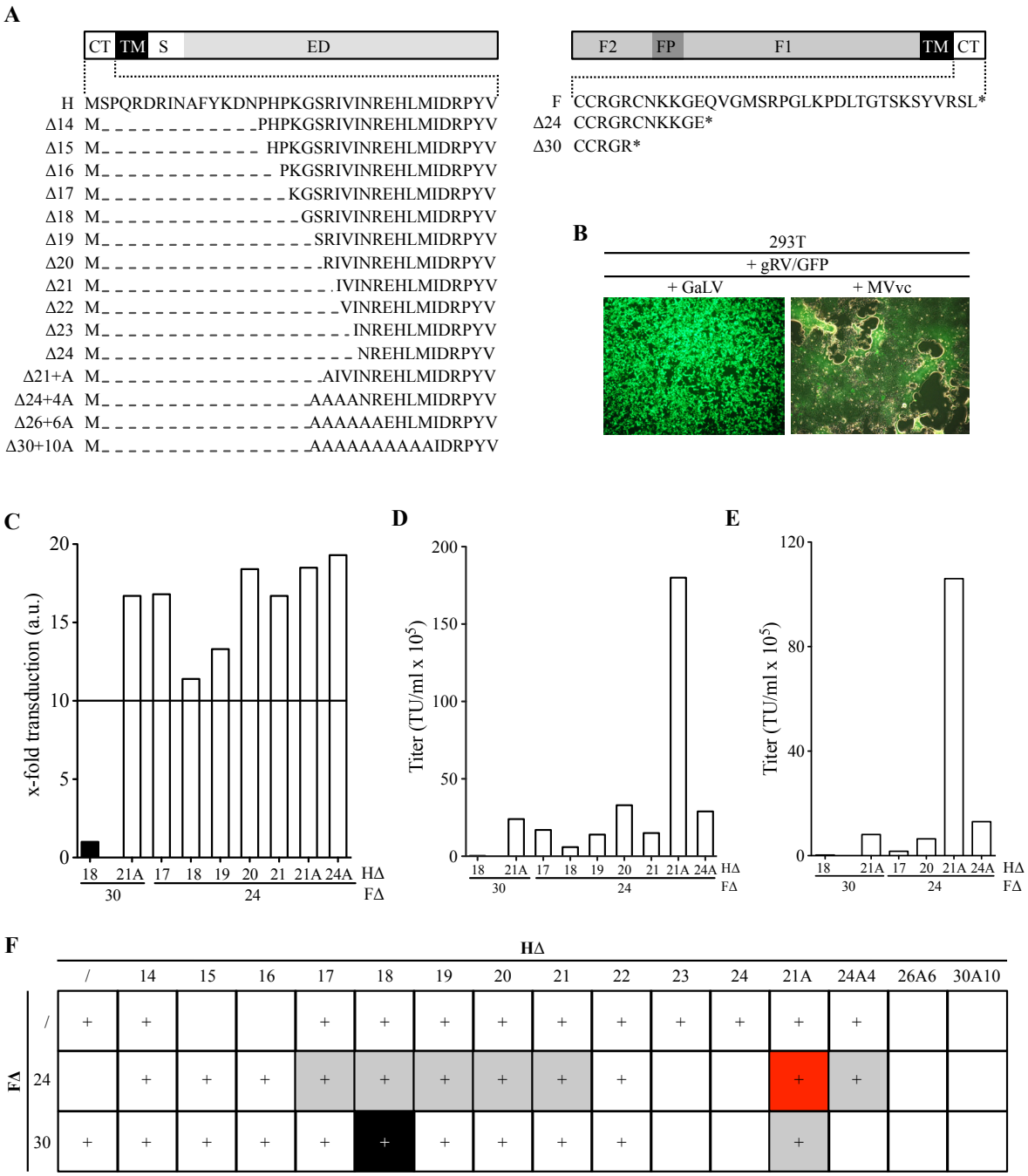

Fig.6 MV HΔ21A-FΔ24 is the best suited pseudotype for gRV vectors
(A) Graphical illustration of MV H and F proteins. The amino acid truncations leading to different tail variants of H and F are depicted. CT: cytoplasmic tail, TM: transmembrane domain, ED: ectodomain, F1: fusion domain 1, F2: fusion domain 2, FP: fusion protein, S: stalk region. (B) GFP expression and syncytia formation in MV-pseudotyped gRV/GFP-transfected 293T cells analyzed by fluorescence microscopy. Gibbon ape leukemia virus (GaLV)-pseudotyped gRV/GFP vectors served as control. One exemplary picture is shown. 40-fold magnification. (C) GFP expression in J76S8 cells transduced with differently pseudpotyped gRV vector particles (white bars) normalized to MV HΔ18-FΔ30 (black bar). Horizontal line indicates threshold for inclusion of MV tail variants to further analysis. a.u.: arbitrary units (D, E) Titer of tail variants selected in (C) determined by serial dilution of vector supernatant on J76S8 cells. (F) Graphical overview of all 48 MV envelopes used in this screening. Each box represents one H and F combination. All combinations were compared to MV HΔ18-FΔ30 (black box). White boxes indicate combinations that yielded less than ten-fold higher transduction rates than MV HΔ18-FΔ30. Gray boxes indicate combinations that yielded an at least ten-fold higher transduction rate than MV HΔ18-FΔ30. The combination yielding the highest titer is filled in red. Syncytia forming combinations are marked (+).

3.2 Generation of targeting-vectors specific for murine CD4 and CD8

In parallel to the transfer of the targeting technology to gRV transfer vectors, described in 3.1, targeting vectors specific for murine CD4 (mCD4) and CD8 (mCD8) were generated.

3.2.1 Generation of targeting-domains specific for murine CD4 and CD8

The hybridomas GK1.5 and 2.43 express monoclonal antibodies specific for mCD4 (L3T4) and mCD8 (Lyt-2.2), respectively. After isolation of total RNA from the GK1.5 and 2.43 hybridoma, cDNAs were generated using primers specific for the heavy and light chain variable regions (VH, VL). A poly-C-tail was added to the cDNA molecules and a second PCR using again gene-specific reverse primers and a forward primer with an eleven-guanosin-overhang was performed. The resulting amplicons were analyzed by gel electrophoresis and appeared at approximately 700 bp for VH and 750 bp for VL, as expected (Fig.7A). After identifying the sequences of the amplicons, scFvs were designed *in silico* by linking the respective VH and VL with a glycine-serine-sequence ($(G_4S)_3$). Subsequently, both scFvs were compared with corresponding deposit amino acid sequences from IMGT. In case of the GK1.5-derived scFv 8 amino acids were exchanged in VH, and 2 amino acids were exchanged and one was added to VL (Fig.7B). Exchanging rare amino acids by most commonly used amino acids is supposed to increases the stability of the expressed proteins. The 2.43-derived scFv sequences were not altered.

The targeting domain of the MV human CD8-targeting HΔ18 (Hh8-Δ18) was exchanged by either CD4-specific or CD8-specific scFv resulting in Hm4-Δ18 and Hm8-Δ18, respectively (Fig.7C). Next, 293T cells were transfected with identical amounts of DNA for each construct in order to analyze expression levels of Hm4-Δ18 and Hm8-Δ18. Both were expressed superior compared to Hh8-Δ18 (MFI: 3353 and 3133 vs. 1685; Fig.7D). Expression levels of Hh8-Δ18 were sufficient to generate functional and high-titered LV vector stocks, as described elsewhere.[148] Hm4-Δ18 and Hm8-Δ18 expression-levels on transfected 293T cells were, thus, considered sufficient. However, as described in 3.1, HΔ18 is not able to pseudotype gRV vectors sufficiently. Therefore we generated HΔ21A-variants by PCR using Hm4-Δ18 and Hm8-Δ18 as templates.

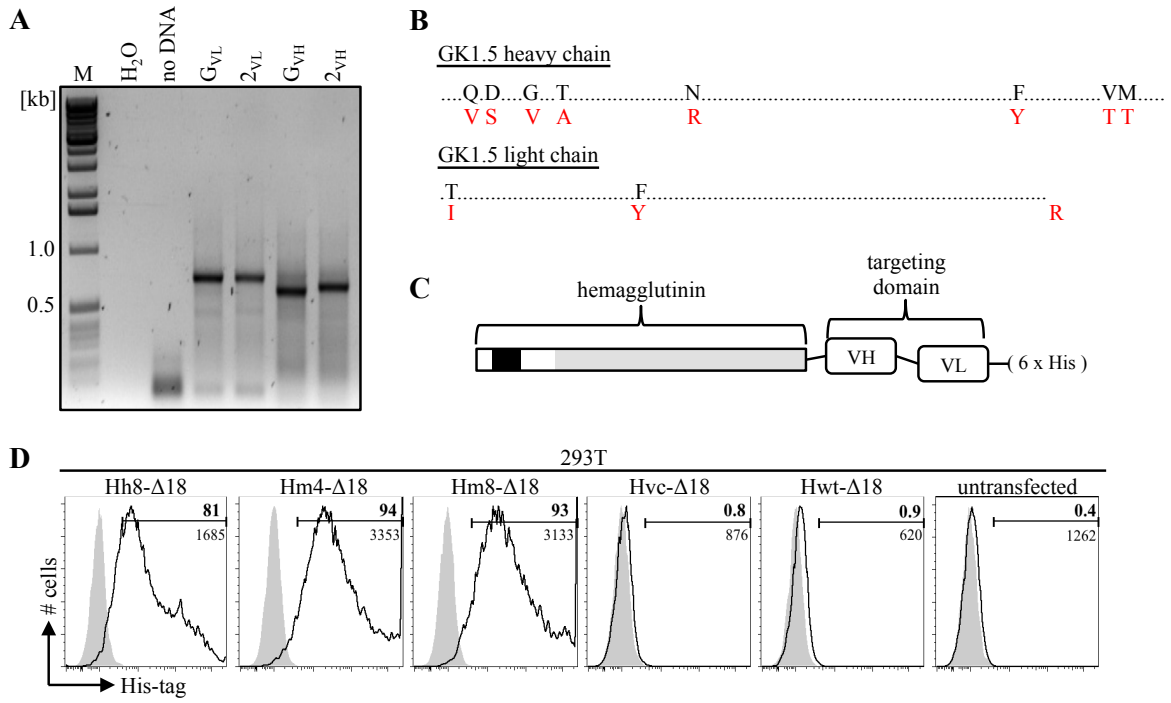

Fig.7 Hm4-Δ18 and Hm8-Δ18 are expressed on transfected 293T cells
(A) Amplicons of GK1.5- and 2.43-derived heavy- and light chains used for sequencing, visualized by ethidium bromide staining. (B) Schematic view of GK1.5-derived sequences. Original (black) and replacement amino acids (red) are shown. Dots represent unmodified sequence. (C) Graphical illustration of H protein fused to an scFv targeting-domain followed by a histidin-tag. (D) Surface expression of different HΔ18 proteins on transfected 293T cells determined by staining with a histidin-tag specific antibody by flow cytometry. Gating was set according to untransfected 293T cells. Bold numbers indicate the percentage of $H\Delta18^+$ cells. Lower numbers indicate the mean fluorescence intensity (MFI) of $H\Delta18^+$ cells. Gray curves are unstained 293T cells of identical origin for each construct. Hvc and Hwt are not fused to a histidin-tag and serve as staining control.

3.2.2 Specific transduction of target cells by MVm4- and MVm8-pseudotyped vectors

58 T cell is a TCR^- derivative of BW5147 thymoma and expresses neither CD4 nor CD8.[151] It was used to generate $CD4^+CD8^-$ (58m4) and $CD4^-CD8^+$ (58m8) daughter cell lines to allow testing the specificity of MVm4- and MVm8-pseudotyped vectors. Transduced bulk 58 cells were single cell sorted into 96-well-plates and selected for high expression of CD4 or CD8. The clones with the highest and most stable expression of the transgenes were selected for all further experiments (Fig.8A).

Supernatants harboring gRV/GFP vectors pseudotyped with MVm4 (HΔ18-FΔ30), MVm8 (HΔ18FΔ30), MVm4 (HΔ21AFΔ24) or MVm8 (HΔ21AFΔ24) were generated by transient transfection of 293 T cells. Those supernatants were then titrated on 58m4 and 58m8 cells, respectively. MVvc-pseudotyped gRV/GFP vectors were titrated on J76S8 cells and reached average titers of $2.2x10^4$ TU/ml. MVm4- and MVm8-pseudotyped gRV/GFP vectors employing the same tail variants as MVvc (HΔ18-FΔ30) reached average titers of $8.5x10^5$ and $2.8x10^5$ TU/ml, respectively (Fig.8B). That is an approximately 39-fold and 13-fold increase in titer, respectively, by addition of one of the targeting domains to MV HΔ18. Using

MVm4 and MVm8 in the HΔ21A-FΔ24-configuration (from now on referred to as MVm4 and MVm8) further increased average titers 8.5-fold ($72x10^5$ TU/ml) and 15-fold ($43x10^5$ TU/ml), respectively (Fig.8B).

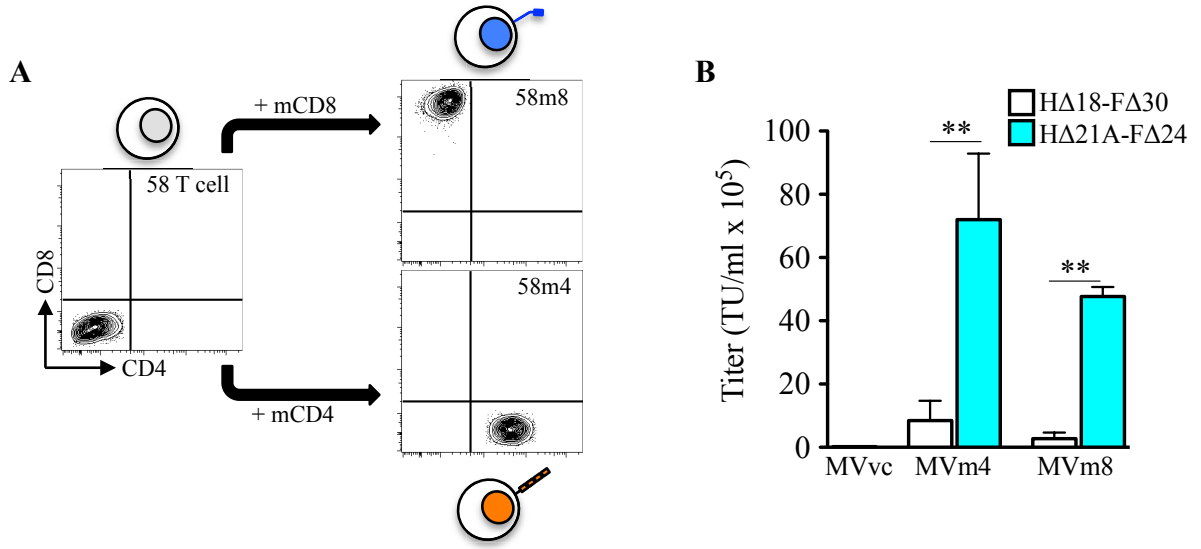

Fig.8 Titration of MVm4 and MVm8 on 58m4 and 58m8 cells
(A) Surface expression of mCD4 and mCD8 on 58, 58m4 and 58m8 cells analyzed by flow cytometry. 58m4 and 58m8 were transduced by MP71-mCD4 and MP71-mCD8, respectively, and single-cell cloned. The final clone for each cell line is shown. (B) Titers of MVvc-, MVm4- and MVm8-pseudotyped gRV/GFP vectors are shown, as analyzed by serial dilutions of concentrated supernatant on J76S8, 58m4 and 58m8, respectively. Bar diagrams depict pooled data of three to eight independent vector productions. Asterisks indicate p values < 0.01.

Next, the specificity of MVm4 and MVm8 was addressed. Therefore, 58 T cells were mixed in a 1:1-ratio with either 58m4 or 58m8 cells. Application of gRV/GFP vectors pseudotyped with the glycoprotein of the vesicular stomatitis virus (VSV) proved the general transducability of all cells in the mixed culture. Application of MVm8- (Fig.9A) or MVm4- (Fig.9B) pseudotyped gRV/GFP vectors resulted in a selective expression of GFP in $CD8^+$ or $CD4^+$ cells, respectively.

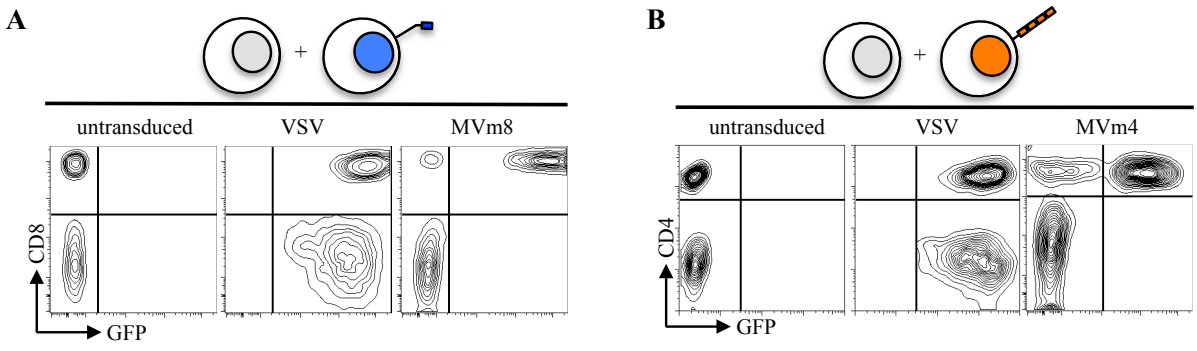

Fig.9 Targeted transduction of 58m8 and 58m4 cells by MVm8 or Mvm4, respectively
Flow cytometric analysis of GFP expression in a mixed culture of 58 and 58m8 or 58m4 cells transduced either by VSV, MVm8- or MVm4-pseudotyped gRV/GFP vectors. One representative data set of two is shown.

The transducability of 58m4 and 58m8 cells by MVm4 or MVm8, respectively, was almost abolished if cells were pretreated with high amounts of CD4- or CD8 blocking antibodies (80 µg/ml). Using decreasing concentrations of blocking antibodies revealed a dose-dependent

transduction of the target cells by MVm4 and MVm8 pseudotyped gRV/GFP vectors (Fig.10A,B). However, if an ecotropic (Eco) gRV/GFP vector was applied to the pretreated cells, they were readily transduced despite the presence of CD4- or CD8 blocking antibodies. Application of CD4 blocking antibodies to 58m8 cells or CD8 blocking antibodies to 58m4 cells had no effect on general transducability by the targeting vectors, even in high concentrations. The same is true for the application of isotype controls (IgG2b) to both cell lines.

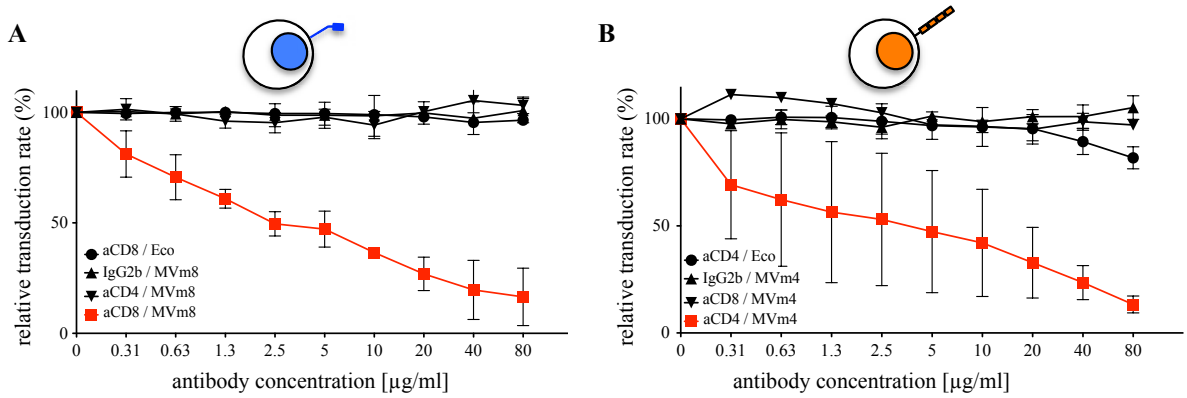

Fig.10 Dose-dependent effects of blocking antibodies on MVm8 and MVm4
Target cells, pretreated either with a CD8- or a CD4 blocking-antibody or an isotype control, were transduced by either MVm4-, MVm8- or Eco-pseudotyped vector particles. 48 hrs later GFP expression of all samples was analyzed by flow cytometry. Data was normalized to individual samples without antibody. Each datapoint represents pooled data of duplicates from two independent experiments.

Taken together, the results from Fig.9 and Fig.10 prove the exclusive specificities of both targeting vector envelopes. However, a major question was if MVm4 and MVm8 will be able to simultaneously deliver different transgenes into mixed cultures of target cells without losing specificity. To answer this question, 58m4 and 58m8 cells were mixed in a 1:1-ratio (Fig.11A). MVm8 gRV/GFP and MVm4 gRV/mCherry vectors were thawed and mixed as well before being applied to the target cells. Subsequent flow cytometric analysis revealed no decrease in specificity. MVm8 delivered GFP exclusively into 58m8 cells, whereas MVm4 delivered mCherry exclusively into 58m4 cells (Fig.11B). To our knowledge, it has been shown for the first time that targeting vectors can be used in parallel to deliver different transgenes into different cells in a mixed culture.

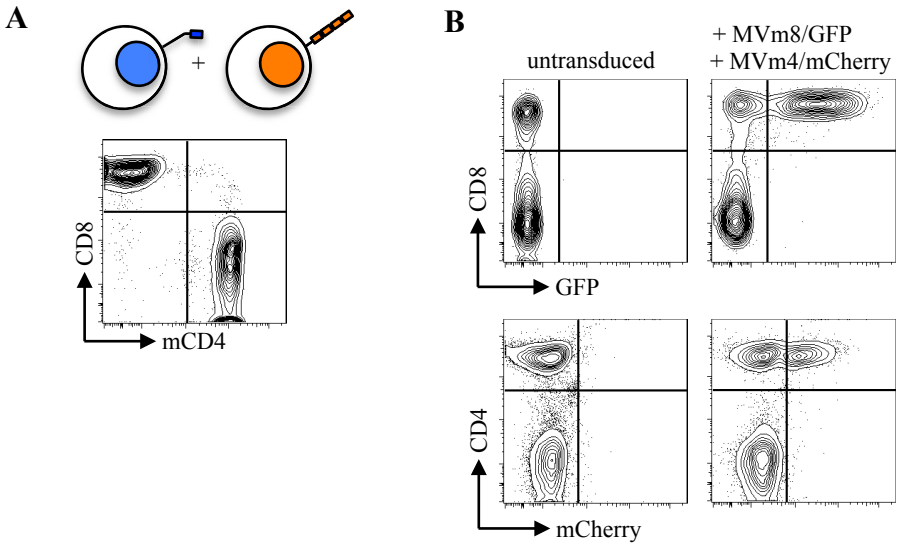

Fig.11 MVm4 and MVm8 deliver distinct transgenes simultaneously and exclusively to their target cells (A) CD4 and CD8 expression in a 1:1-mixture of 58m4 and 58m8 cells analyzed by flow cytometry. (B) The tropism of simultaneously added MVm4 gRV/mCherry and MVm8 gRV/GFP vectors was analyzed by flow cytometry. One representative experiment out of two is shown.

3.3 Transduction of primary T cells using MVm4 and MVm8

3.3.1 Transduction of B6-derived T cells by MVm8

Initial experiments on primary cells were performed using B6-derived T cells. Splenocytes activated by aCD3- and aCD28-simulation were transduced with MVm8 gRV/GFP or SIN-LV/GFP. The expression of GFP was analyzed on day two, five, nine and 14 after transduction. Both vector supernatants exhibited an exclusive expression of GFP in primary $CD8^+$ T cells (Fig.12A). MVm8 gRV/GFP achieved a transduction rate of 32% $CD8^+GFP^+$ cells of total cells, whereas MVm8 SIN-LV/GFP transduced 47% of all cells. As expected primary murine T cells were not stably transduced by SIN-LV/GFP, instead there was a steady decrease of GFP^+ cells over time. Starting from 47% the transduction rate dropped down to 3% on day 14. However, MVm8 gRV/GFP was able to efficiently mediate stable expression of GFP in primary B6-derived $CD8^+$ T cells over a period of two weeks (Fig.12B).

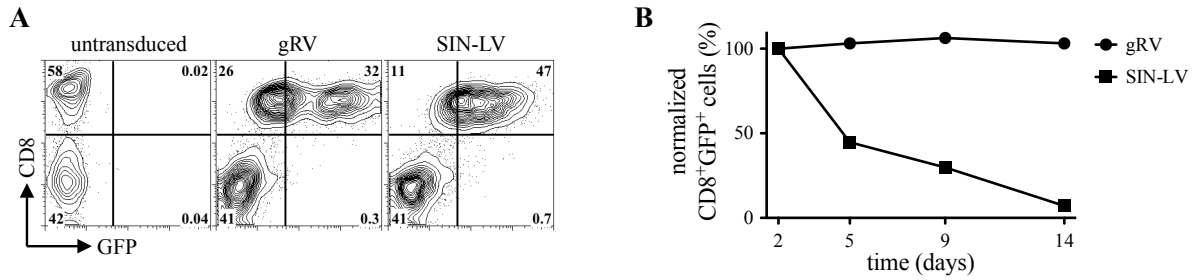

Fig.12 MVm8-pseudotyped gRV/GFP vector transduces B6-derived T cells stably and exclusively
(A) GFP expression in primary B6-derived $CD8^+$ T cells analyzed by flow cytometry two days after transduction by gRV or SIN-LV vectors is shown. Gating was set according to untransduced control. Numbers indicate percentages of cellular events within the gates. (B) GFP expression analyzed by flow cytometry for a time period of 14 days is depicted as line chart. Data was normalized to $CD8^+GFP^+$ cell fraction on day two.

Transduction of B6-derived T cells was repeated using MVm8- or Eco-pseudotyped gRV vectors encoding for the OT-I TCR, which is an MHC I-restricted ($H2k^b$) TCR recognizing the SIINFEKL epitope of ovalbumin (OVA). Comparing the pattern of TCR expression in MVm8- and Eco-transduced samples showed that MVm8 exclusively transduced the $CD8^+$ T cells whereas Eco transduced both $CD8^+$ and $CD4^+$ T cells. Although Eco showed an overall higher transduction rate than MVm8 (36% vs. 19% OT-I TCR^+CD3^+), it also transferred 2/3 of the MHC I-restricted OT-I TCR into $CD4^+$ T cells (69% OT-I TCR^+CD4^+) and only 1/3 into $CD8^+$ T cells (27% OT-I TCR^+CD8^+) (Fig.13A). In conclusion, MVm8-mediated TCR gene-transfer generated more OVA-reactive $CD8^+$ T cells compared to Eco-mediated gene-transfer, which preferentially transduced $CD4^+$ T cells. The preferential transduction of $CD4^+$ T cells in mixed cultures mediated by the non-targeting envelope Eco was seen in repeatedly and could also be observed using other non-targeting envelopes like VSV (Fig.13B).

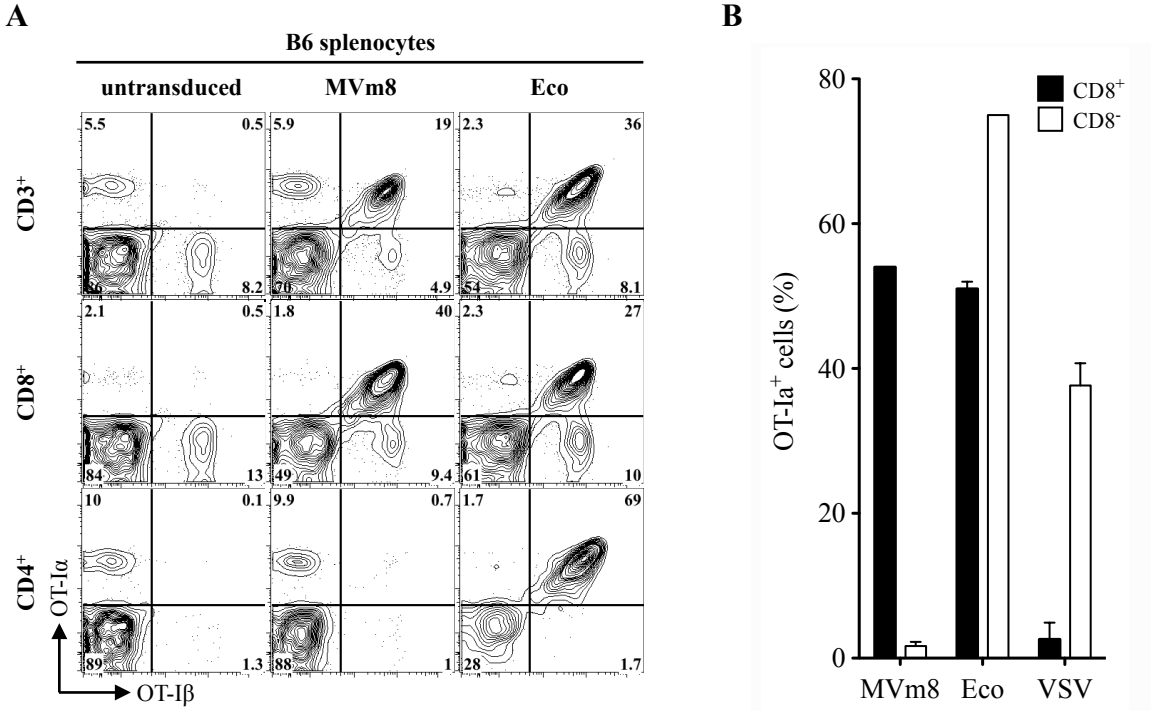

Fig.13 MVm8-mediated gene transfer is restricted to primary CD8$^+$ T cells
(A) OT-Iα and β chain, as well as, CD3, CD4 or CD8 surface expression analyzed by flow cytometry. Numbers indicate percentages of positive cells. (B) Percentage of OT-Iα chain surface expression amongst either CD8$^+$ or CD8$^-$ cells is depicted as bar diagrams. Pooled data from two experiments.

Next, T cells were cocultured with H2k^{b+}OVA$^+$ tumor cell lines for 24 hrs. T cells transduced by MVm8 or Eco exhibited an antigen-specific release of IFNγ, showing that MVM8-mediated transduction generates functional CD8$^+$ T cells. Untransduced T cells produced background levels of IFNγ only. Although more OT-I TCR$^+$CD8$^+$ T cells were present in MVm8-transduced samples there was no difference in IFNγ release compared to Eco-transduced samples (Fig.14).

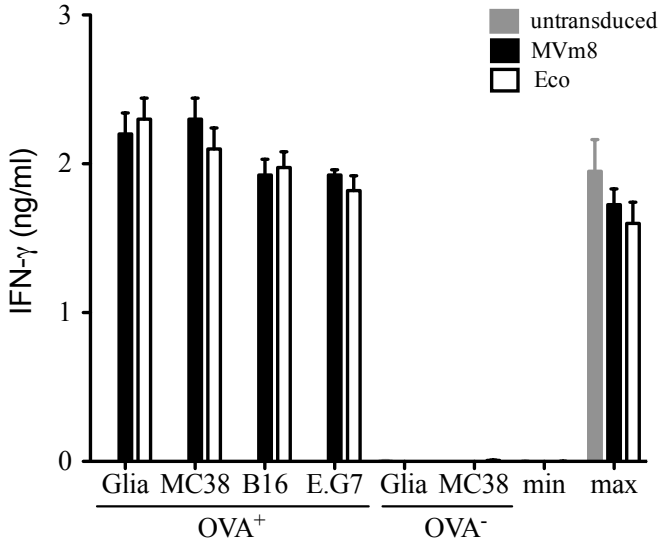

Fig.14 MVm8- and Eco-transduced primary T cells are equally functional
Untransduced and transduced T cells from Fig.13 were cocultured with (OVA$^+$) or without (OVA$^-$) ovalbumin- and H2k^b-expressing tumor cell lines (duplicates). T cells were incubated with medium alone (min) or ionomycin and PMA for TCR-independent simulation (max). Each bar depicts the mean and standard deviation of two independent experiments. IFNγ concentration was determined by ELISA.

3.3.2 Transduction of B6-derived T cells by MVm4

Next, the ability of MVm4 to transduce primary B6-derived T cells was tested using the identical procedure described in the previous section. Initial flow cytometric analysis on day two showed a slight expression of GFP (16%) mediated by MVm4 SIN-LV/GFP. Although not that pronounced, GFP expression was also detectable in cells transduced by MVm4 gRV/GFP (1,7%). Nevertheless, on day five, in both samples the amount of GFP$^+$ cells was reduced by approximately 90% (Fig.15A).

Disaggregation of the nuclear envelope during the cell cycle is essential for stable transduction by gRV vectors. Thus, target cells have to be activated. This is achieved by the culture conditions including aCD3- and aCD28-antibodies as described above. Additionally,

the culture is supplemented with cytokines like IL-2 and IL-15 leading to an outgrowth of $CD8^+$ over $CD4^+$ T cells (Fig.15A, compare D2 and D5). To analyze if the presence of $CD8^+$ T cells and the culture conditions led to the low transducability of $CD4^+$ cells by MVm4, we negatively isolated them using magnetic beads, reaching purities above 90%. Since IL-15 is mostly beneficial for $CD8^+$ T cells we supplemented with IL-2 only. General transducability of the cells was proven by application of Eco- and VSV-pseudotyped gRV/GFP reaching high transduction rates (Fig.15B). Nevertheless, transduction by MVm4 failed again and resulted in an initial shift of the $CD4^+$ population towards GFP expression and a subsequent reduction of GFP^+ cells until day five (Fig.15C).

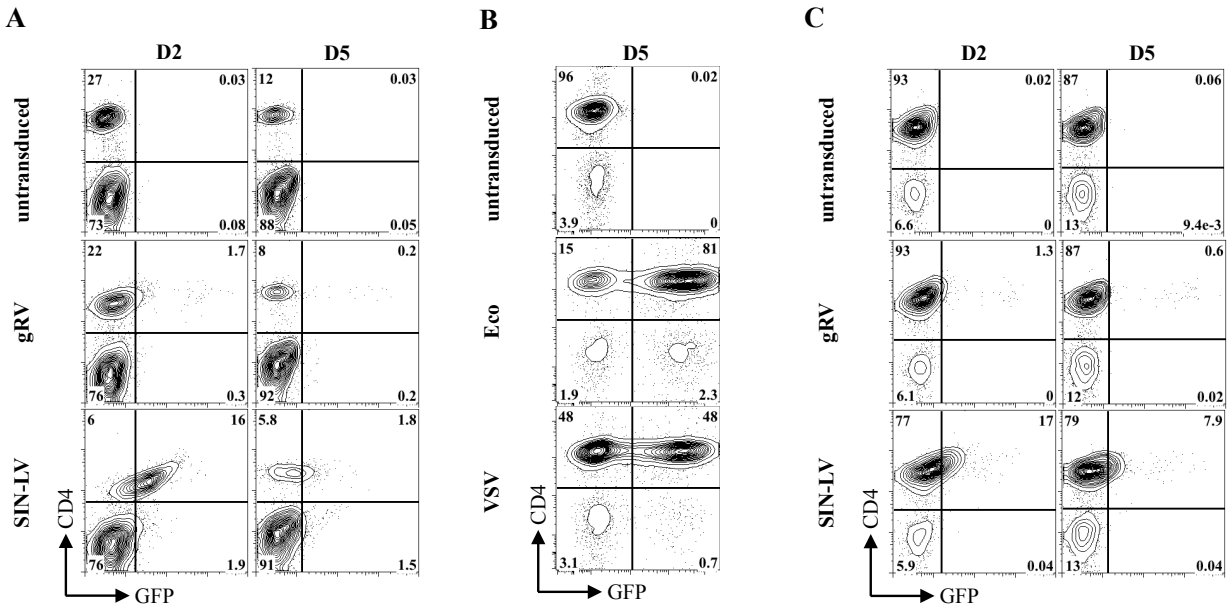

Fig.15 MVm4-mediated transduction of primary B6-derived T cells is inefficient
(A) GFP and CD4 expression of unsorted B6-derived T cells by MVm4 gRV/GFP or SIN-LV/GFP. (B) GFP- and CD4 expression of CD4-enriched B6-derived T cells by two non-targeting vectors (Eco & VSV) harboring a gRV transfer vector and (C) by MVm4 gRV/GFP or SIN-LV/GFP. Numbers indicate percentages of cellular events within the gates. Analysis was performed by flow cytometry.

As described in section 3.2.1, MVm4 harbors a targeting domain derived from the GK1.5 hybridoma. To test whether the failure to transduce primary T cells is caused by this targeting domain, three new hybridomas were selected for generation of CD4-specific targeting domains. First, binding properties of the antibodies produced by the hybridomas were tested. To do so, concentrated supernatant from YTS.177.9.6.1 (177), YTS.191.1.1.2 (191) and YTA.3.1.2 (YTA) was used to stain primary CD4-sorted B6-derived splenocytes. A secondary fluorescein isothiocyanate (FITC) labeled antibody was used to visualize successful binding of primary CD4-specific antibodies to their target. All three new antibodies, as well as GK1.5, were able to stain primary B6-derived splenocytes compared to isotype controls. The 177-derived supernatant showed the lowest efficiency, while all others performed equally well (Fig.16A).

Subsequently, all three antibodies, derived from 177, 191 and YTA, were configured as scFvs and cloned onto the MV HΔ21A protein. To test whether the newly generated CD4-specific targeting envelopes are efficiently packaging gRV/GFP, vector particles were generated and titrated on 58m4 cells. The newly generated targeting domains, 177, 191 and YTA, packaged gRV transfer vectors less efficiently and generated lower titers than GK1.5-pseudotyped vector particles (Fig.16B).

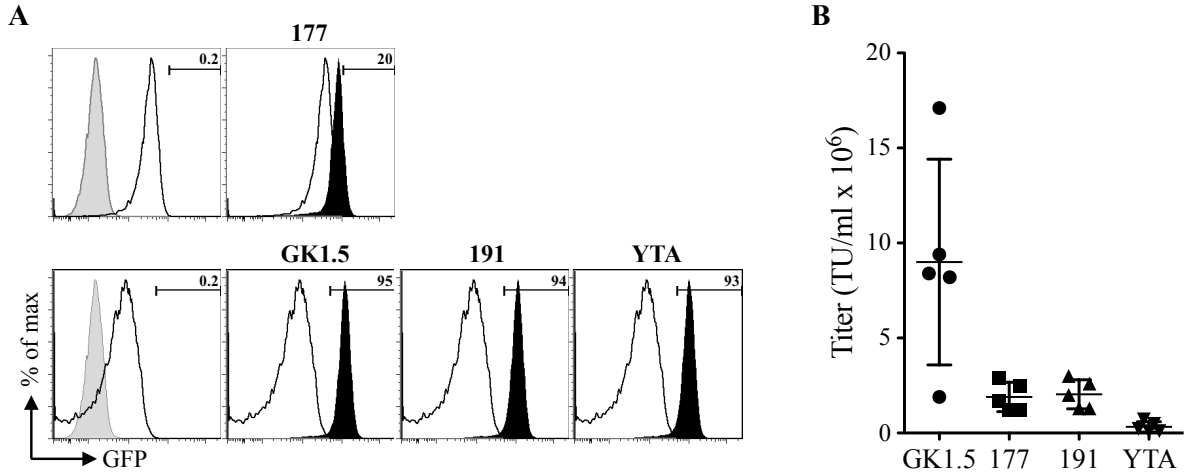

Fig.16 Newly generated mCD4-specific MV envelopes exhibit decreased viral titers
(A) Histograms show primary B6-derived T cells stained by supernatant derived from the four different hybridomas (GK1.5, 177, 191, YTA). Primary cells were activated and staining was performed at the time point usually used for transduction. Gray curve: unstained cells. Black curve: Isotype control and secondary FITC-conjugated antibody. Black filled curves: hybridoma supernatant and secondary FITC-conjugated antibody. Numbers indicate percentage of positive cells. Gating was set according to isotype control staining. (B) Titer of the gRV/GFP pseudotyped with one of the four mCD4-targeting envelopes was analyzed by titration of concentrated supernatant on 58m4 cells. (n=5)

Nevertheless, when transducing mixed cultures of 58 T cells and 58m4 cells, with identical or similar multiplicity of infection (MOI=1), the 177- and the 191-pseudotyped vector particles performed as well as GK1.5-pseudotyped gRV/GFP, whereas YTA-pseudotyped gRV/GFP were less efficient (MOI=0.5). Low vector titers of YTA-pseudotyped vectors excluded the usage of MOIs higher than 0.5. Exclusive transduction of 58m4 cells showed that the specificity of all three newly generated CD4-specific targeting vectors was successfully redirected (Fig.17A).

However, 177, 191 and YTA were also not able to transduce primary B6-derived splenocytes efficiently. GK1.5- and 177-pseudotyped vector particles reached around 5% stable transduction rate using an MOI of 1, which was never exceeded in repetitions of this experiment (Fig.17A).

Using increasing MOIs of the different CD4-targeting vectors did not result in higher transduction rates but revealed a dose-dependent reduction in CD4 expression (Fig.17B). Compared to untransduced cells a reduction of CD4 expression was already visible at MOIs

of 0.5. The strongest decrease was seen when using 191-pseudotyped vectors. Downregulation of CD4 was not an effect of transduction or culture conditions per se, since application of CD4-unspecific vectors to the same cells did not result in lower expression levels of CD4 (Fig.17C).

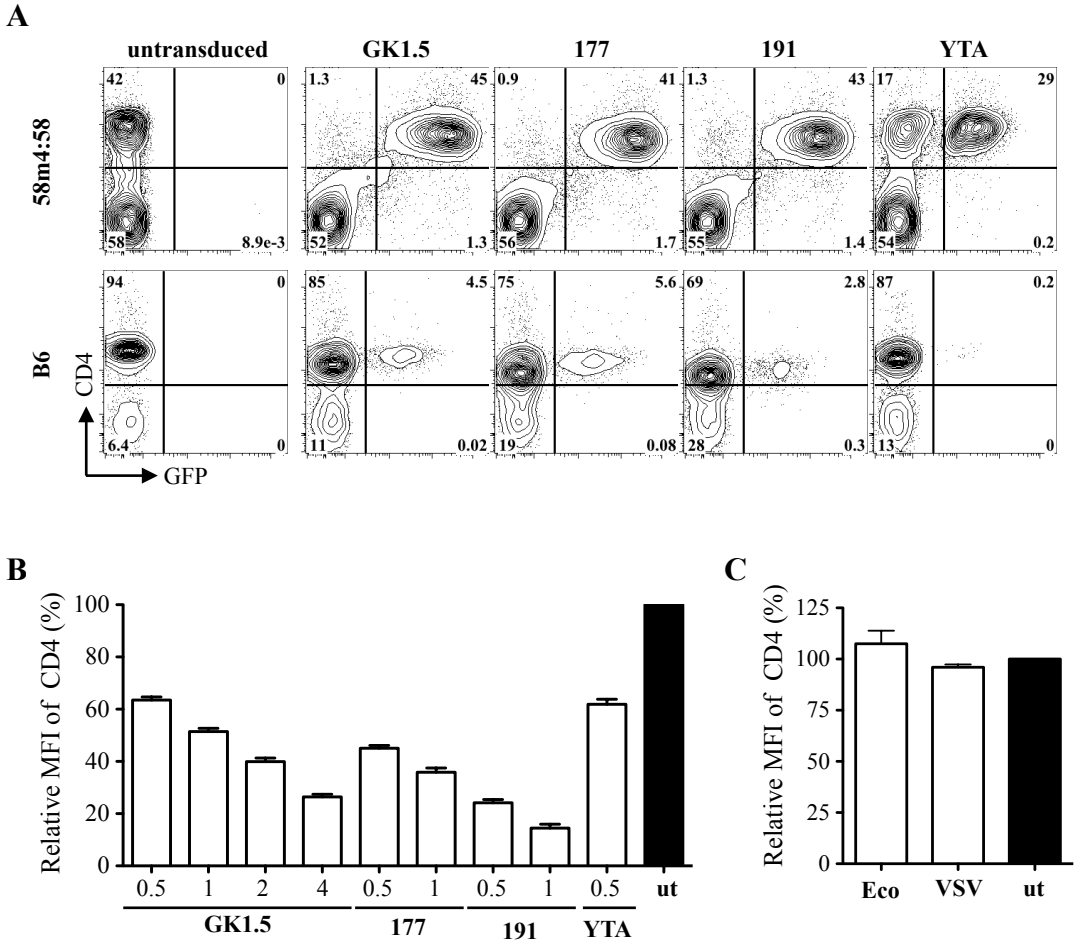

Fig.17 B6-derived CD4$^+$ T cells are refractory to MVm4-mediated high level transduction
(A) 1:1 ratio of 58 and 58m4 cells (upper row) or CD4-sorted primary B6-splenocytes (lower row) were analyzed for expression of CD4 and GFP by flow cytometry on day five after transduction. Gates were set accroding to untransduced controls. Numbers indicate percentage of positive cells. (B,C) Transduced B6-derived CD4$^+$ T cells were analyzed for expression-levels of CD4 by flow cytometry on day two after transduction. Bar diagarms depict mean data and standard deviation of two independent experiments. All datapoints were normalized to untransduced cells. (B) Indicated below is the MOI of respective viruses used for transduction.

Taken together these results indicate, that MVm4 binds to CD4 on primary cells, but either does not initiate the fusion of the viral and the cell membrane or is not able to integrate into the host genome after cell entry. The latter possibility is highly unlikely, since gRV vectors, unlike LV vectors, delivered by other pseudotypes are able to stably integrate into primary B6-derived T cells (Fig.17C). Therefore, it is assumed, that upon binding of the MVm4 to CD4 the fusion process of the viral and cellular membrane is impaired.

To test this hypothesis, B6-derived splenocytes were transduced again with MVm4-(GK1.5) and Eco-pseudotyped gRV/GFP vectors. Stable and efficient transduction was obtained using Eco- but not MVm4 gRV/GFP. MVm4-transduced cells displayed a shift

towards GFP expression, which was lost after one week in culture, similar to previous observations (Fig.18A). In parallel to flow cytometry, confocal microscopy was performed. Eco-transduced cell exhibited an evenly distributed expression of GFP throughout the cell, indicating that GFP is located in the cytosol, whereas, GFP signal from MVm4-transduced cells was only detectable at the rim of the cells indicating that GFP is located at the cell membrane (Fig.18B). GFP is a cytosolic protein and is neither transported to the membrane nor secreted. From this, it is assumed that the GFP signal detected in MVm4-transduced samples represents viral particles harboring GFP molecules, expressed and packaged in transfected 293T cells. This phenomenon, named pseudotransduction, also explains the initial shift of the MVm4-transduced cells towards GFP expression as well as the loss of expression after a certain time of culture. This assumption is in line with the dose-dependent "down-regulation" of CD4 after transduction described above. MVm4 particles bound to CD4 on the cell surface block staining by aCD4 antibodies. In conclusion, we were able to show that MVm4 is able to bind to its target but not to initiate the fusion of the viral and cellular membrane.

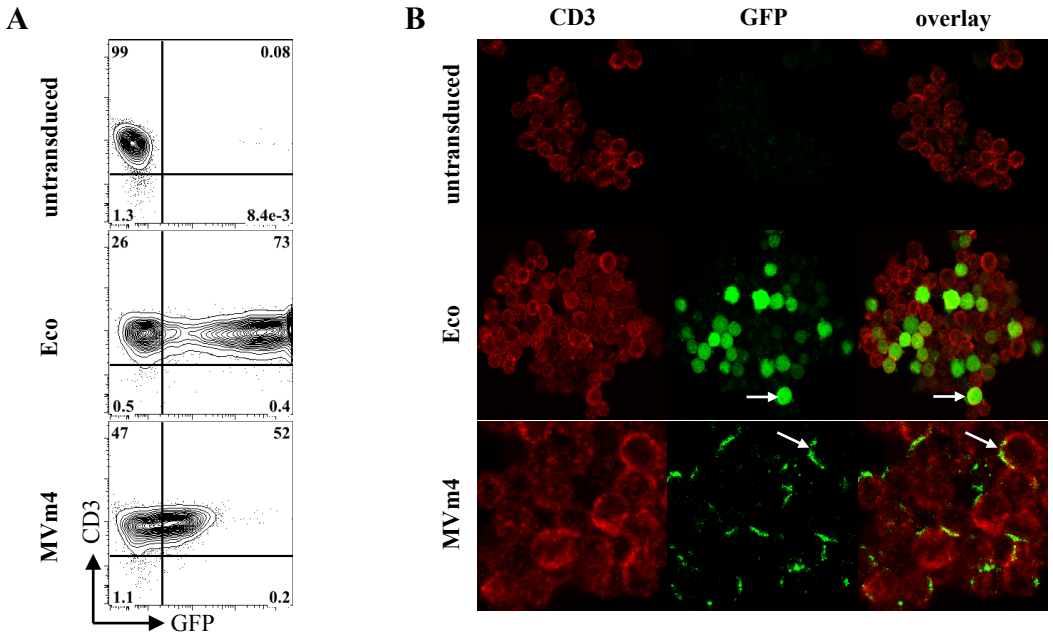

Fig.18 Transient GFP expression is emitted by membrane-bound vector particles
(A) GFP and CD3 expression of primary B6-derived T cells detected by flow cytometry on day one after transduction. Gates were set accordingly to unstained and untransduced controls. Numbers indicate percentages of positive cells. (B) Confocal microscopy of the same samples as in (A) on day one after transduction. White arrows mark examples of origin of GFP signals from the complete cell (Eco) or from the rim of the cell (MVm4). Magnification of untransduced and Eco: 40x, MVm4: 100x.

In contrast, membrane fusion is not impaired on 58m4 cells transduced by MVm4. The CD4 molecule used for generation of 58m4 is derived from B6 splenocytes and is identical in sequence. However, CD4 expression on 58m4 is driven by the strong viral MP71 promoter and is thus higher compared to B6 T cells. To analyze if cell entry is dependent on high

expression levels of CD4, CD4-sorted B6-derived splenocytes were transduced with MP71-CD4, which was also used to generate 58m4 cells. This led to an increase of CD4 expression on B6 T cells (Fig.19A). Next, B6 T cells, expressing endogenous (- MP71-CD4) and exogenous (+ MP71-CD4) levels of CD4, were tested for their transducability by MVm4. B6 T cells expressing endogenous levels of CD4 were not transduced by MVm4 gRV/GFP as observed in previous experiments. Surprisingly, identical MVm4 gRV/GFP vector stocks readily transduced B6 T cells expressing increased levels of CD4 (Fig.19B). A transduction rate of approximately 32% $CD4^+GFP^+$ cells was achieved and remained stable for 16 days after transduction (Fig.19C). General transducability of B6 T cells with low or high CD4 expression levels was shown by transduction using Eco-pseudotyped gRV/GFP vectors (Fig.19D).

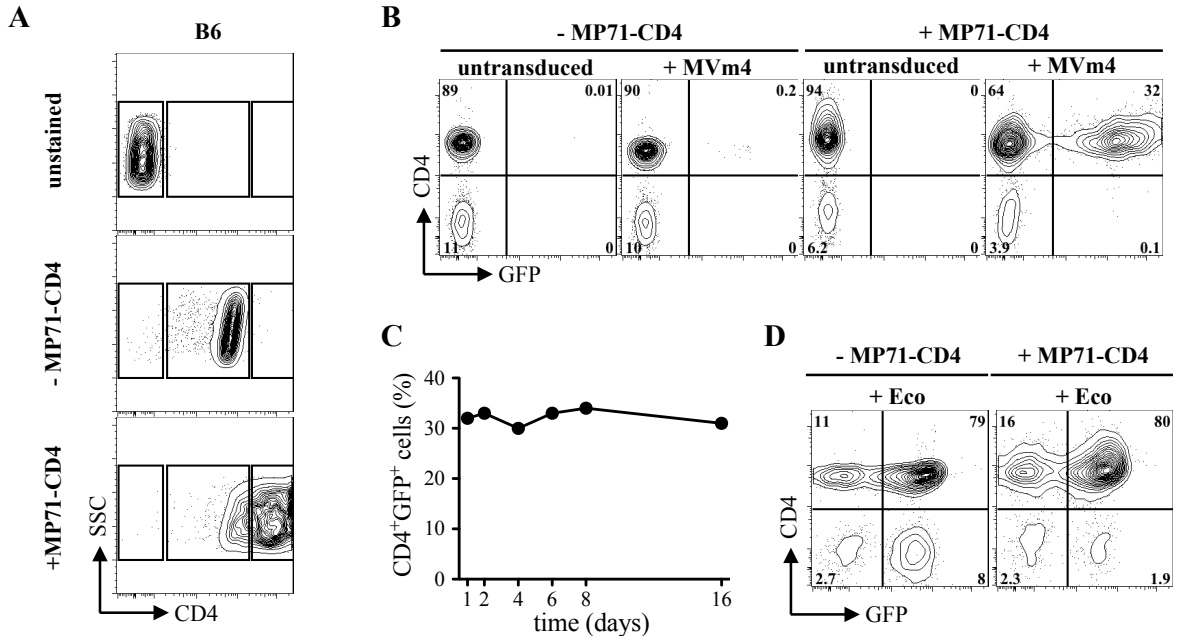

Fig.19 Increased levels of CD4 render B6-derived T cells permissive for MVm4-mediated stable transduction
(A) CD4 surface expression of B6-derived T cells analyzed by flow cytometry on day 1 after transduction with MP71-CD4. Unstained B6 T cells served as negative control. Plots are gated on $CD4^+$ cells. (B) GFP and CD4 expression of cells from (A), after transduction with MVm4 gRV/GFP analyzed by flow cytometry on day 2 after transduction with MP71-CD4. (C) Stable GFP expression of $CD4^+$ B6 T cells from B, right plot. Analyzed by flow cytometry on indicated days. (D) CD4 and GFP expression of B6 T cells transduced by either Eco gRV/GFP alone or by MP71-CD4 and Eco gRV/GFP. Analyzed by flow cytometry on day two after transduction with MP71-CD4. Numbers indicate percentages of positive cells.

3.3.3 Transduction of BALB/c-derived T cells

Unmanipulated B6-derived T cells can be transduced by MVm8 but not by MVm4, making this mouse model futile for the purpose of this study. We therefore analyzed BALB/c mice for their transducability by MVm4 and MVm8.

Unmanipulated CD4-sorted BALB/c-derived splenocytes were efficiently transduced by MVm4 gRV/GFP reaching transduction rates of 69% $CD4^+GFP^+$ cells with an MOI of 2. Eco gRV/GFP reached a transduction rate of 44% $CD4^+GFP^+$ cells with the identical MOI (Fig.20A). GFP expression in MVm4-transduced cells was stable over a time period of 16 days (Fig.20B). Regarding the results from Fig.19 we assumed that CD4 expression of BALB/c-derived splenocytes must be higher compared to B6-derived splenocytes. Flow cytometric analysis, however, showed that CD4 and CD8 expression levels before and two days after activation (time point of transduction) was identical in BALB/c- and B6-derived splenocytes (Fig.20C,D). Sequence analysis of BALB/c-derived CD4 cDNA showed no differences to B6-derived CD4 regarding the amino acid sequence (see appendix, 7.2 sequences).

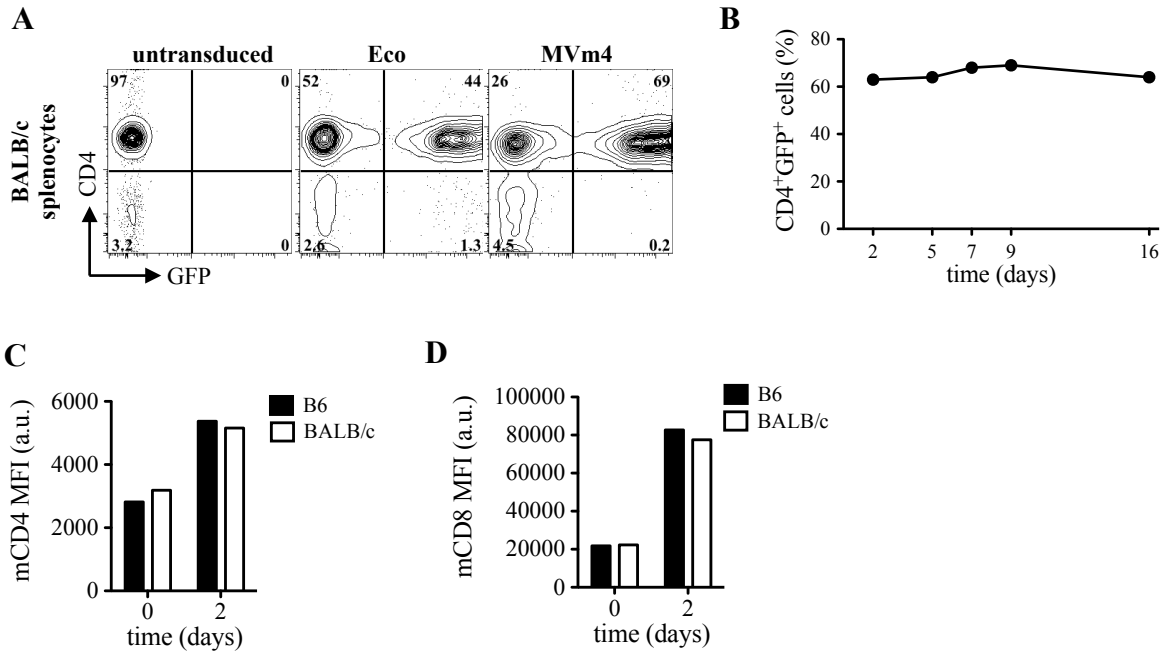

Fig.20 BALB/c-derived T cells are permissive for MVm4-mediated stable transduction
(A) GFP and CD4 expression of BALB/c-derived T cells transduced by MVm4 gRV/GFP or Eco gRV/GFP analyzed by flow cytometry on day two after transduction. Numbers indicate percentages of positive cells. (B) Stable GFP expression of BALB/c-derived T cells transduced with MVm4 gRV/GFP vector (A, right panel) as analyzed by flow cytometry on indicated days. (C) Expression levels of CD4 on resting (day 0) and activated T cells (day 2). (D) Expression levels of CD8 on resting (D0) and activated T cells (D2). Both (C) and (D) were analyzed by flow cytometry. a.u.: arbitratry units

Next, the ability of MVm8 and MVm4 to simultaneously transduce unsorted BALB/c T cells was assessed. To do so, MVm8 gRV/GFP and MVm4 gRV/mCherry vectors were mixed and the applied to activated T cells. Analysis of the transduced cells by flow cytometry showed an exclusive expression of GFP in $CD8^+$ and mCherry in $CD4^+$ T cells (Fig.21). The restricted expression of both marker genes in their respective target cell type confirmed the

feasibility of subset-specific transduction of primary T cells *in vitro* using the targeting vectors generated in this study.

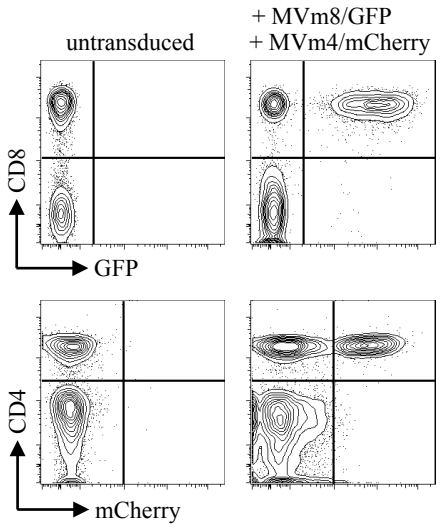

Fig.21 Simultaneous and exclusive transduction of primary CD4$^+$ and CD8$^+$ T cells by MVm4 and MVm8
Expression of CD4, CD8, GFP and mCherry in a single sample of BALB/c-derived T cells analyzed by flow cytometry two days after transduction. One representative experiment of two is shown.

3.4 *In vivo* T cell transduction

3.4.1 Intraperitoneal transduction of polyclonal T cells

Initial *in vivo* transduction experiments were performed with activated polyclonal B6-derived T cells injected into the peritoneal cavity of Rag2$^{-/-}$ mice. Two days later MVm8 gRV/GFP vectors or PBS was injected via the same route (intraperitoneally, i.p.). Mice were sacrificed on day four after injection of T cells and cells of the peritoneal cavity were analyzed for expression of GFP by flow cytometry (Fig.22A). In three out of three mice GFP$^+$ cells were detected. GFP signals were exclusively restricted to CD8$^+$ T cells (99%), whereas no GFP signal was detectable in CD8$^-$ cells from the peritoneal cavity (Fig.22B). Transduction efficiencies ranged from 1.2 to 5.8% CD3$^+$CD8$^+$GFP$^+$ cells among all cells of the peritoneum. Mice that got PBS instead of MVm8 showed no GFP signals at all. The average transduction efficiency of intraperitoneal T cells was around 3% (Fig.22C).

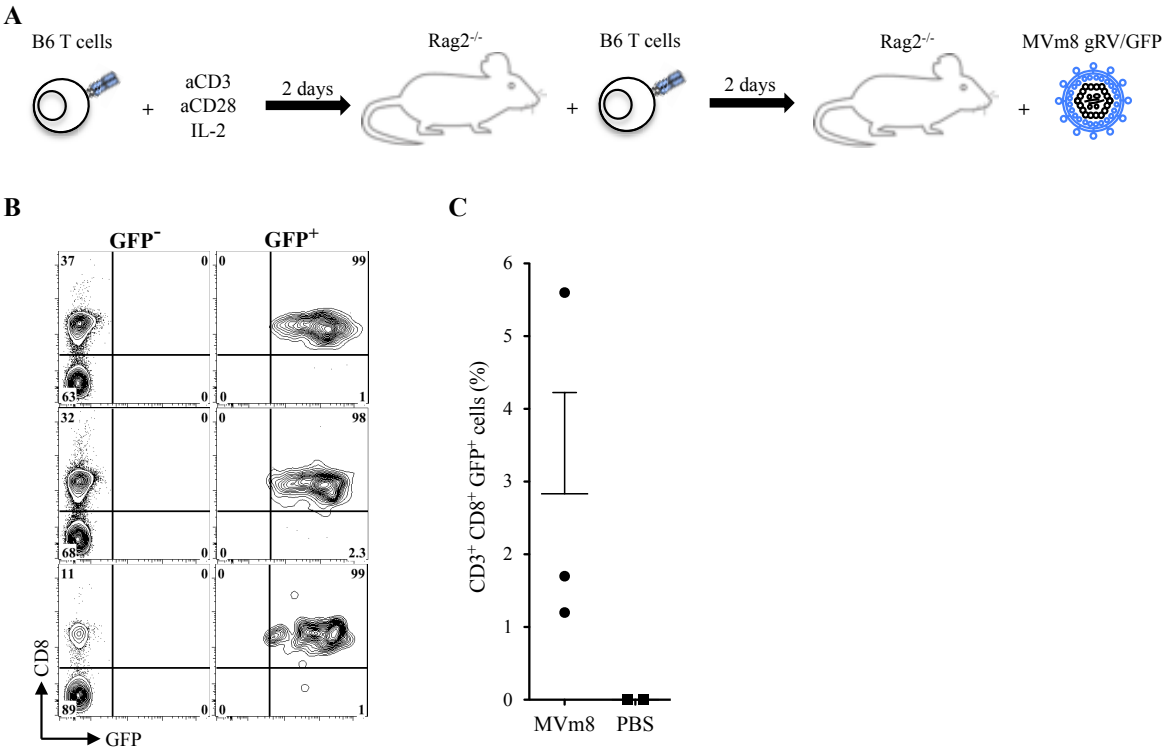

Fig.22 Intraperitoneal transduction of CD8$^+$ T cells by MVm8 gRV/GFP vectors
(A) Schematic overview of experimental procedure. B6-derived T cells were activated and two days later injected in Rag2$^{-/-}$ mice i.p. Another two days later MVm8 gRV/GFP vectors were injected into the same compartment. (B) Mice were sacrificed another two days later and cells of the peritoneal cavity were analyzed for expression of CD8 and GFP by flow cytometry. Left panel is gated on GFP$^-$ and right panel on GFP$^+$ cells. Numbers indicate percentages of positive cells. (C) Intraperitoneal transduction efficiency is shown as percentage of CD3$^+$CD8$^+$GFP$^+$ cells analyzed by flow cytometry. Datapoints represent individual mice.

3.4.2 *In vivo* transduction of polyclonal T cells by systemic application of MVm8

MVm8 successfully transduced CD8$^+$ T cells after being given i.p. To test its ability to transduce CD8$^+$ T cells also by systemic application, MVm8-pseudotyped gRV vectors encoding for the OVA-specific OT-I TCR and a luciferase (MVm8 gRV/OT-I-luc) were injected intravenously (i.v.) into Rag2$^{-/-}$ mice, which have been repopulated with activated B6-splenocytes beforehand. Five days after i.v.-injection of MVm8 gRV/OT-I-Luc mice were immunized with irradiated OVA$^+$ colon carcinoma cells (MC38-OVA) by subcutaneous (s.c.) injection into the flank. Flow cytometric analysis of peripheral blood obtained five days after immunization showed, that all 5 mice injected with MVm8 showed elevated levels of OT-I-$\alpha^+\beta^+$ T cells compared to mice that were injected with PBS. The percentage of OT-I-$\alpha^+\beta^+$ T cells ranged from 1.9 to 5.4% (subtracted by an average signal of 0.4% detected in PBS mice). In average approximately 3.2% of peripheral T cells were transduced by systemically applied MVm8 vector (Fig.23).

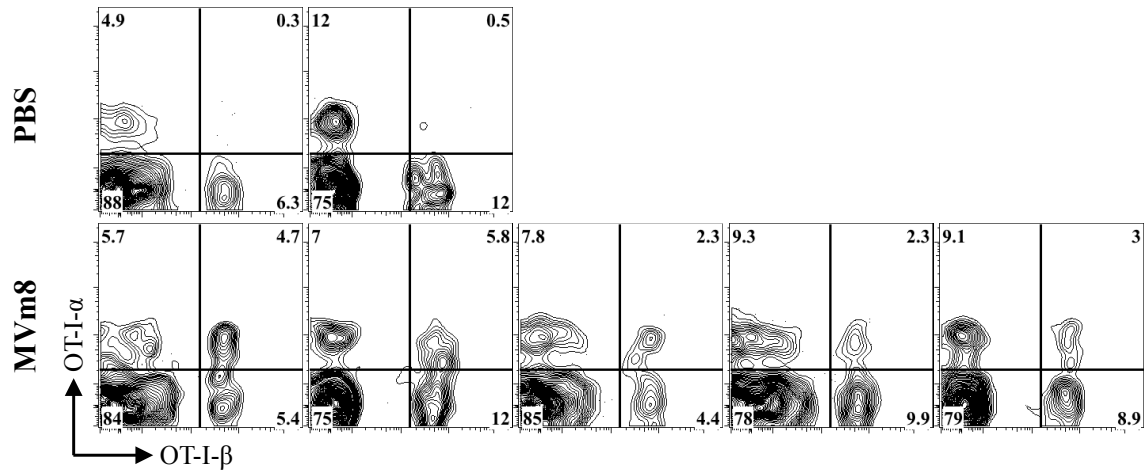

Fig.23 *In vivo*-transduced polyclonal T cells detected in peripheral blood after immunization
OT-I-αβ surface expression in peripheral blood of $Rag2^{-/-}$ mice repopulated with B6-derived splenocytes analyzed by flow cytometry on day 5 after immunization. Mice were i.v. injected with PBS or MVm8 gRV/OT-I-luc. Numbers indicate percentages of positive cells. FACS plots are gated on living cells.

The incorporation of a luciferase reporter gene into the vector construct allowed live imaging of *in vivo*-transduced T cells. Mice were imaged daily starting five days after immunization or boosting until the luciferase signal vanished. A recovery time of at least four weeks was scheduled between initial immunization (priming) and boostings. In each *in vivo* transduction experiment three groups were analyzed: (i) mice injected with PBS, (ii) MVm8 gRV/OT-I-luc or (iii) Eco gRV/OT-I-luc. All mice were repopulated with B6-derived T cells 2 days before injection. Identical vector titers for MVm8 and Eco were applied mostly (table 2).

Specific luciferase signals were detected in mice injected with MVm8 gRV/OT-I-luc, but not in mice that received PBS or titer-adjusted Eco gRV/OT-I-luc. After priming in most, but not all mice (5/7), an initial luciferase signal was detected in the draining lymph node of the injection site. During the course of the immune response the luciferase signal moved to the actual site of injection of irradiated MC38-OVA cells, where it increased over time before vanishing (Fig.24A). While PBS-injected mice did not show any luciferase signals, mice that received Eco gRV/OT-I-luc showed luciferase at the day of priming on the flank contralateral to immunization (day 0). Only on day seven a weak luciferase signals on the correct flank was detectable (Fig.24A). Subsequently, mice were boosted twice. Neither the PBS nor the Eco mice showed any luciferase signals during the course of the experiment. In mice injected with MVm8, however, specific luciferase signals were restored, even if the irradiated MC38-OVA cells were injected into the contralateral flank (Fig.24B).

Importantly, if mice were injected with elevated titers of Eco gRV/OT-I-luc ($7x10^6$ TU/mouse/200µl), high luciferase signals were detectable all over the mouse (Fig.24C). After adjusting the parameters for imaging distinct signals from multiple sites, probably resembling

inner organs, e.g. spleen, liver, etc., were visible (Fig.24C, red box). PBS-injected mice showed no luciferase signal at all, whereas MVm8-injected mice within the same experiment still emitted a restricted luciferase signal from the site of immunization, with similar kinetics as previously mentioned.

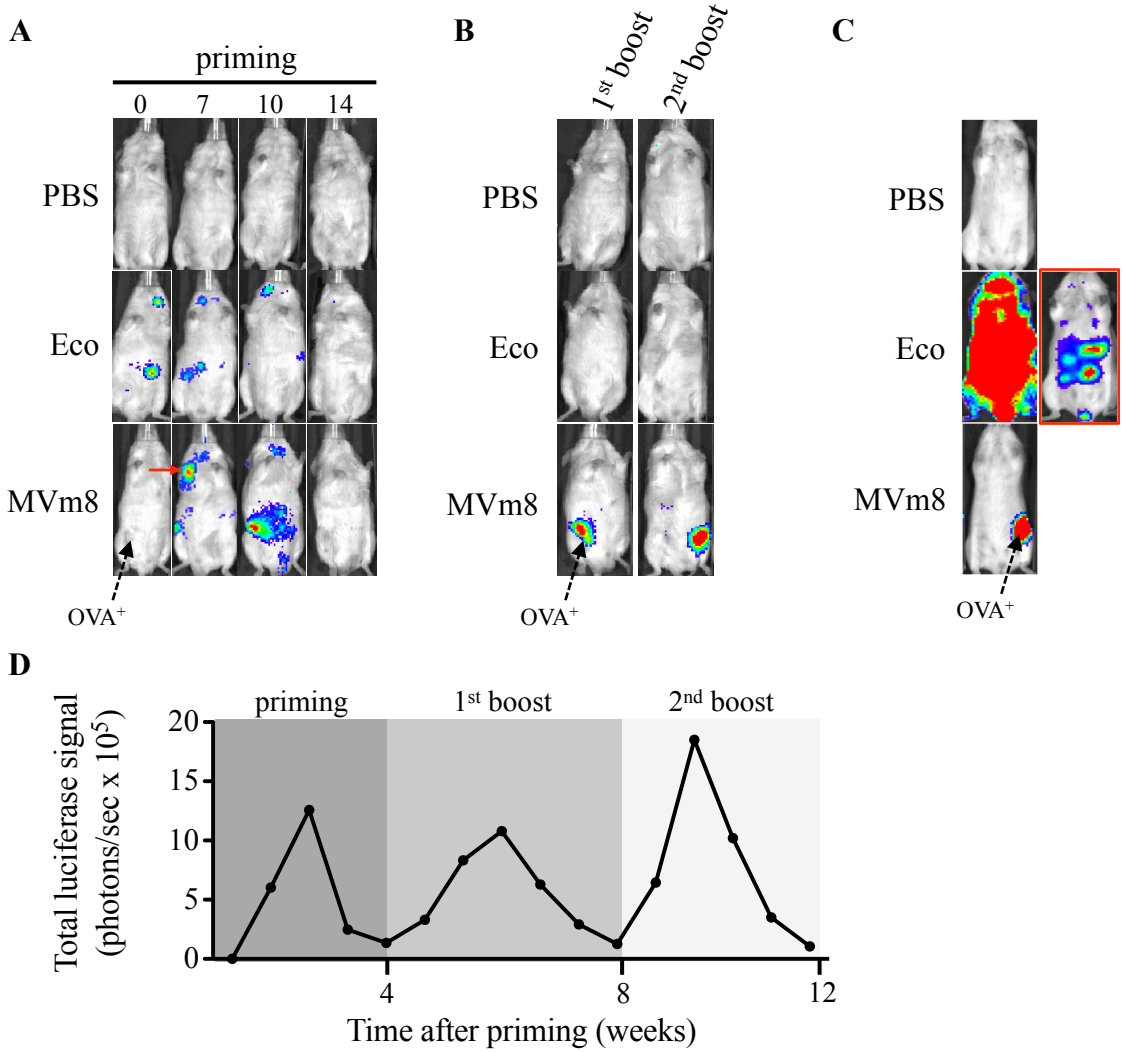

Fig.24 *In vivo*-transduced T cells home towards sites of antigenic stimulation and proliferate
Luciferase signals of representative Rag2$^{-/-}$ mice, repopulated by B6-derived splenocytes and injected by either PBS, Eco gRV/OT-I-luc or MVm8 gRV/OT-I-luc, imaged using IVIS, (A) after priming or (B) 1st (day 6) and 2nd (day 5) boosting with irradiated MC38-OVA cells. Numbers in (A) indicate days after priming. (C) Luciferase signals of Rag2$^{-/-}$ mice, repopulated by P14-derived splenocytes and injected by either PBS, Eco gRV/OT-I-luc or MVm8 gRV/OT-I-luc, imaged using IVIS. Day 8 after priming. IVIS-parameters: min=2.5x10^4 and max=1x10^5 (p/sec/cm^2/sr). IVIS-parameters for red box: min=2.5x10^5 and max=1.5x10^6 (p/sec/cm^2/sr). Red arrow marks signal from draining lymphnode. Black dashed arrow marks site of injection of irradiated MC38-OVA cells. (D) Course of luciferase signal over the complete duration of the experiment detected on the site of immunization or boosting from the MVm8-injected mouse shown in (A) using IVIS.

In conclusion, MVm8 was able to transduce T cells directly *in vivo* by systemic application. Transduced T cells were OT-I-TCR$^+$ and expressed luciferase. They homed towards sites of antigenic stimulation, expanded and contracted again, as shown by luciferase expression and live imaging of mice. Titer-adjusted Eco vectors were not able to transduce sufficient amounts of T cells *in vivo* to elicit similar effects.

Table 2 summarizes all *in vivo* transduction experiments using polyclonal B6-derived splenocytes. An average transduction efficiency of 37% was achieved by injection of approximately $0.7x10^6$ TU/mouse (mean of 4 experiments), meaning that a positive luciferase signal was observed in seven out of 19 mice that received MVm8-pseudotyped vector particles. Differences between the individual experimental settings were the origin of the luciferase and the nature of antigen used for stimulation. Ultimately, the firefly luciferase and irradiated MC38-OVA cells were used for all further *in vivo* transduction experiments (table 2).

Table 2: Summary of *in vivo* transduction experiments using B6-derived polyclonal T cells

#	donor	recipient	TCR	luciferase	TU/mouse	stimulus	positive mice
01	B6	$Rag2^{-/-}$	OT1	Renilla	$1.2x10^6$	MC38-OVA	2/3 (66%)
02	B6	$Rag2^{-/-}$	OT1	Renilla	$0.6x10^6$	SIINFEKL-pept.	2/5 (40%)
03	B6	$Rag2^{-/-}$	OT1	Firefly	$0.4x10^6$	irr. MC38-OVA	1/3 (33%)
04	B6	$Rag2^{-/-}$	OT1	Firefly	$0.7x10^6$	irr. MC38-OVA	2/8 (25%)
							7/19 (37%)

Next, the therapeutic potential of *in vivo*-transduced T cells was analyzed. MC38-OVA is a rapidly growing progressor tumor, which was chosen for immunization because of its high OVA expression levels (Fig.25A,B). $Rag2^{-/-}$ mice were injected with a tumorigenic dose of MC38-OVA cells, which formed an established tumor first palpable after eight days at which point T cells were i.v.-injected. 24 hours later MVm8 gRV/OT-I-luc vector or PBS was injected. Mice were, subsequently, imaged over a period of 17 days. *In vivo*-transduced T cells were detectable in two out of three mice (table 2, Fig.25C). They homed towards MC38-OVA and proliferated reflected by the steady increase of luciferase signal intensity over time. PBS-injected mice showed no detectable signs of luciferase expression beyond background. The increase of luciferase signal in MVm8-injected mice paralleled tumor growth with both peaking on day 17. Despite this, the *in vivo*-transduced T cells were not able to affect tumor outgrowth (Fig.25D). All mice had to be sacrificed 17 days after *in vivo* transduction.

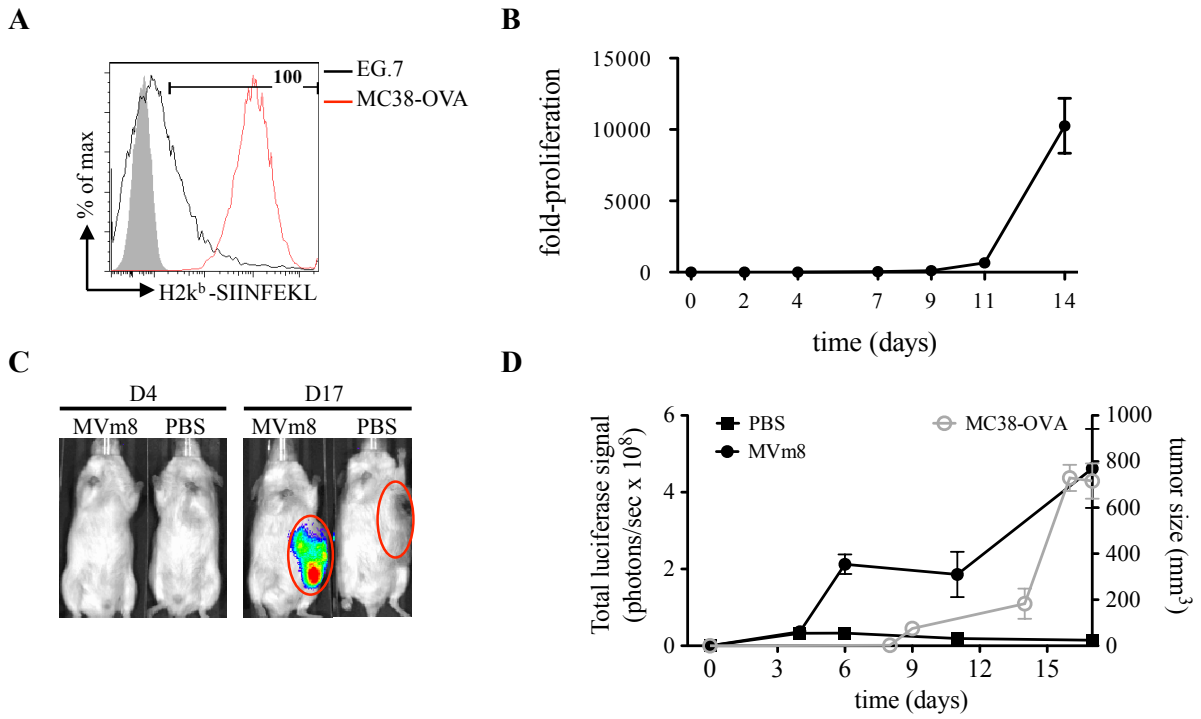

Fig.25 *In vivo*-transduced T cells homing to established tumors have no impact on tumor outgrowth
(A) Expression of H2k^b presenting SIINFEKL peptide on EG.7 and MC38-OVA tumor cell lines analyzed by flow cytometry. Gray filled curve is unstained MC38-OVA. Number indicates percentage of MC38-OVA$^+$ cells (B) *In vitro* growth kinetics of MC38-OVA cells over a time period of 14 days analyzed by viable cell counting. (C) Luciferase signals of Rag2$^{-/-}$ mice, repopulated by B6-derived splenocytes and injected by either PBS or MVm8 gRV/OT-I-luc on day four and day 17, imaged using IVIS. IVIS-parameters: min=2.5x10^4 and max=1x10^5 (p/sec/cm^2/sr). Red gates mark tumor area. Two representative mice out of five are shown. (D) Average luciferase signal of marked tumor areas from (C) are depicted over a time period of 17 days (black curves). The average tumorsize of all three mice that received MVm8 is depicted over the same time period (grey curve).

There were two assumptions why *in vivo*-transduced T cells failed to reject established MC38-OVA tumors: (i) the rapid growth kinetic, which possibly killed the mice before the *in vivo*-transduced T cells could become effective and (ii) the transduction of T cells after the tumor being established, which means that the still naïve *in vivo*-transduced T cells were at too low precursor frequencies at the time of tumor contact. The experimental setup was changed accordingly. T cells were transduced *in vivo* as described above and all mice, including the PBS-injected mice, underwent a prime-boost protocol. Four weeks after the second boost mice were challenged with a tumorigenic dose of MC38-OVA cells. However, in this case, all mice, including PBS-injected mice, rejected the tumor (Fig.26, iv-TD-03).

As mentioned above, MC38-OVA is a progressor tumor, which means that it is not rejected when injected into immune competent mice as opposed to regressor tumors, which do not manifest if a functional immune system is present (e.g. EG.7 tumor). Besides the high expression level of OVA, MC38-OVA was also chosen for tumor rejection experiments because Rag2$^{-/-}$ mice, which have been repopulated by a polyclonal B6-derived immune cell population, would not reject it. Thus, functional differences between mice injected with

MVm8 or PBS would be visible. But, the application of a harsh prime-boost protocol leads to a functional polyclonal immunity against MC38-OVA cells making this approach futile.

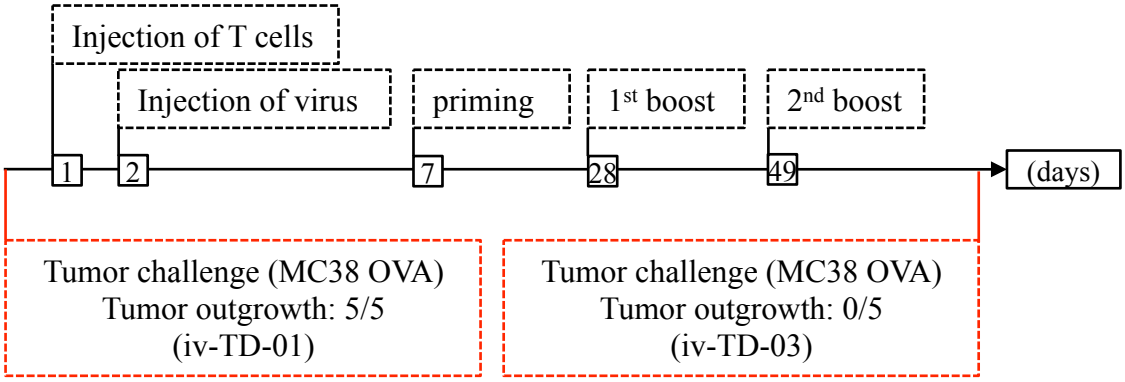

Fig.26 Timeline of tumor challenge experiments
Schematic overview of the chronology of tumor rejection experiments and prime-boost protocol used.

3.4.3 *In vivo* transduction of monoclonal T cells by systemic application of MVm8

Polyclonal T cells were not suitable to dissect the contributions of *in vivo*-transduced T cells to tumor rejection. Therefore, monoclonal T cells expressing the P14 TCR, specific for a lymphocytic choriomeningitis virus-derived gp33-epitope, were used for upcoming experiments described in this section. T cells derived from P14-Rag1$^{-/-}$ mice are strictly tolerant against MC38-OVA cells, since they harbor a single specificity. This means that any protective immunity against OVA^{+} tumor cells or pathogens in mice repopulated with P14 T cells can be traced back to *in vivo* OT1-TCR-transduced T cells.

Rag2$^{-/-}$ mice were repopulated with approximately 6x10^{6} CD3^{+}CD8^{+} T cells either derived from B6 or P14 mice. Flow cytometric analysis of identical volumes of peripheral blood on day two and day five revealed an approximately ten-fold better engraftment of B6-derived T cells compared to P14 T cells (Fig.27A). Nevertheless, P14-derived T cells were successfully transduced *in vivo*, in six out of six mice, by MVm8 gRV/OT-I-luc emitting strong luciferase signals from the site of antigenic stimulation, but not from the contralateral site, where irradiated antigen^{-} MC38 cells were injected. Overall, the efficacy of *in vivo* transduction increased from 37% to 94% by using monoclonal donor T cells (compare table 2 and table 3). In most but not all mice there was again an initial luciferase signal coming from the draining lymph node after priming but not after subsequent boostings, as observed in B6-repopulated mice. No luciferase signals were observed in PBS- or titer-adjusted Eco-injected mice (Fig.27B). In average, P14-repopulated mice emitted 20-fold stronger luciferase signals than B6-repopulated mice after *in vivo* transduction with 0.47x10^{6} TU/mouse (mean of three experiments) and subsequent priming (Fig.27C). Tetramer staining on day five after priming

showed a two-fold higher amount of $CD8^+Tet^+$ T cells in peripheral blood of P14-repopulated mice compared to B6-repopulated mice (Fig.27D).

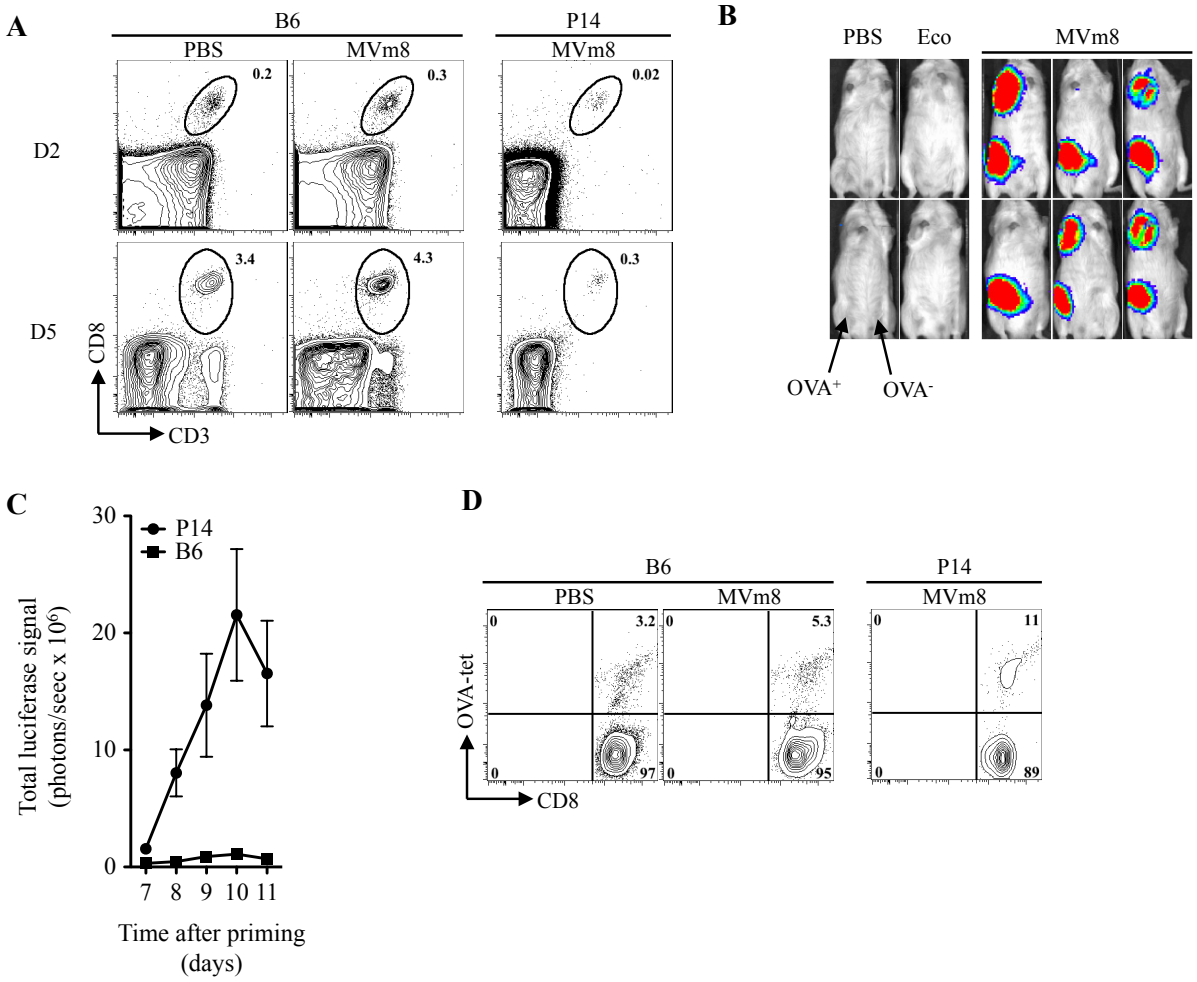

Fig.27 *In vivo* transduction of P14-derived splenocytes results in higher frequencies of OT-I-TCR$^+$ cells (A) CD3 and CD8 expression of B6- or P14-derived T cells in peripheral blood of Rag2$^{-/-}$ mice analyzed by FACS. Numbers indicate percentage of positive cells. One representative plot for each group is shown. (B) Luciferase-signal determined for each mouse by IVIS (day eight after priming). Black arrows indicate sites of injection of MC38 (right flank) or MC38-OVA (left flank). IVIS-parameters are: min=2.5x10^4 and max=1x10^5 (p/sec/cm^2/sr). (C) Total luciferase signal over time determined by IVIS. Shown is the average luciferase signal from mice repopulated with P14- (circles, n=6) or B6-derived (squares, n=3) splenocytes and primed with irradiated MC38-OVA cells. Automatic contour gates were set to define regions of interest. Total luciferase signal was calculated for each mouse. Mean ± SEM. (D) Tetramer staining of B6- or P14-derived T cells in peripheral blood of Rag2$^{-/-}$ mice analyzed by FACS (day five). Numbers indicate percentage of positive cells. One representative plot for each group is shown.

Table 3: Summary of *in vivo* transductions experiments using P14-derived monoclonal T cells

#	donor	recipient	TCR	luciferase	TU/mouse	stimulus	positive mice
01	P14	Rag2$^{-/-}$	OT1	Firefly	0.3x10^6	irr. MC38-OVA	5/6 (83%)
02	P14	Rag2$^{-/-}$	OT1	Firefly	0.6x10^6	irr. MC38-OVA	6/6 (100%)
03	P14	Rag2$^{-/-}$	OT1	Firefly	0.5x10^6	irr. MC38-OVA	6/6 (100%)
							17/18 (94%)

3.4.4 Protective immunity against *Listeria monocytogenes* by *in vivo*-transduced T cells

P14-repopulated mice showing strong luciferase signals indicating high levels of *in vivo*-transduced T cells were challenged with a tumorigenic dose of MC38-OVA cells after the first boost. As observed in B6-repopulated mice no functional immunity against MC38-OVA tumors could be observed, although *in vivo*-transduced T cells again homed to the site of injection and remained at the tumor until mice had to be sacrificed. Tumor growth was delayed in one mouse that received MVm8 gRV/OT-I-luc (Fig.28A,B)

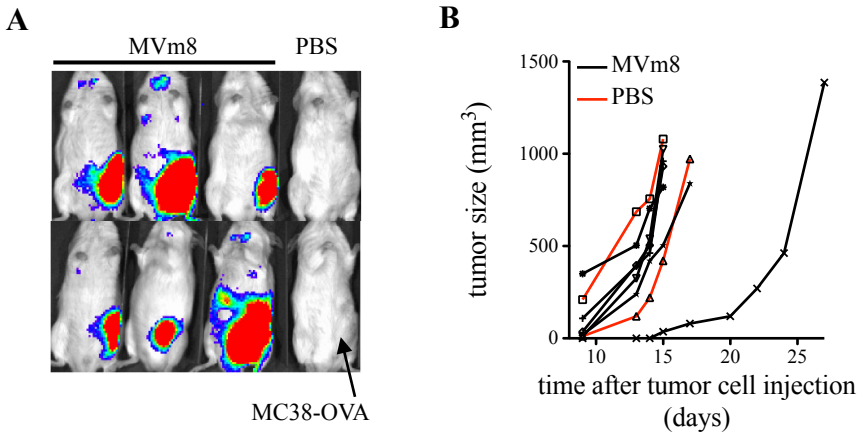

Fig.28 *In vivo*-transduced P14 T cells do not prevent tumor outgrowth
(A) Luciferase-signal determined for each mouse by IVIS (D8 after injection of MC38-OVA). Black arrow indicates site of injection of MC38-OVA. IVIS-parameters are: min=2.5x10^4 and max=1x10^5 (p/sec/cm^2/sr). (B) Tumor volumes were measured along three orthogonal axes (a, b, and c).

In parallel to tumor rejection experiments P14-repopulated and *in vivo*-transduced mice were also challenged with OVA transgenic *listeria monocytogenes* (LM-OVA) after priming. Although all mice that received MVm8 gRV/OT-I-luc were successfully transduced *in vivo*, the intensity of the luciferase signal differed strongly between individual mice. When challenged with LM-OVA those mice that show low luciferase signals (MVm8^{lo}) were not protected, whereas mice emitting strong luciferase signals exhibited a protective immunity. PBS- or titer-adjusted Eco-injected mice showed no luciferase activity and were not protected against LM-OVA (Fig.29).

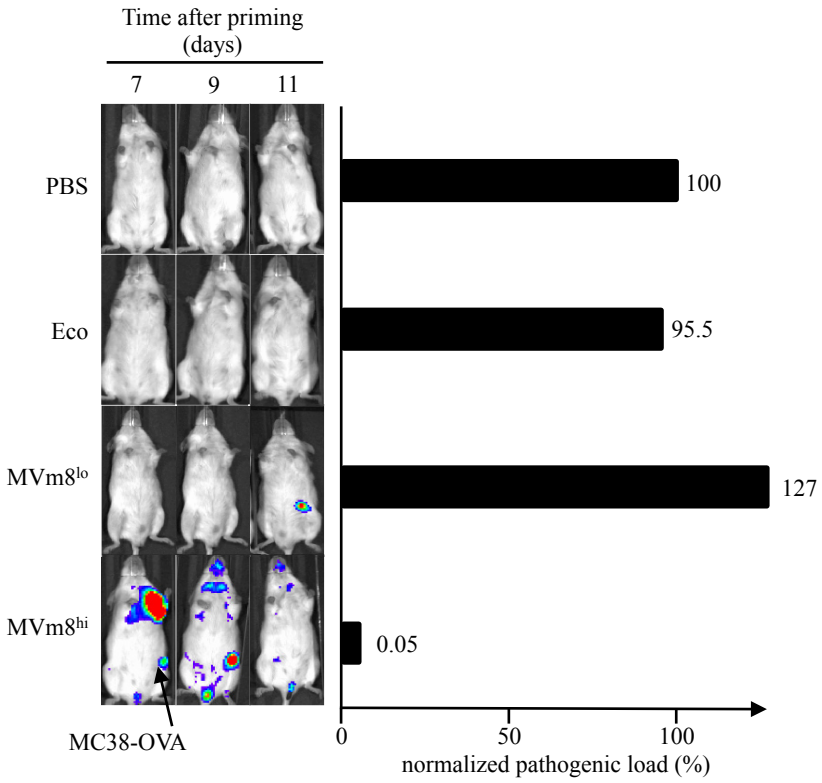

Fig.29 Protective immunity depends on *in vivo* transduction efficiency
Luciferase signal determined for each mouse by IVIS (day eight after injection of MC38-OVA, left panel). Black arrow indicates site of injection of MC38-OVA. IVIS-parameters are: min=2.5x10^4 and max=1x10^5 (p/sec/cm^2/sr). One mouse per group is shown. Percentage of colony forming units (CFU) derived from single cell suspensions from each individual mouse is shown normalized to the PBS-injected mouse (right panel). Rag2$^{-/-}$ mice were challenged with pathogenic doses of LM-OVA. Three days later, mice were sacrificed, spleens isolated and fractions of single-cell-suspensions were plated. 24 hrs later CFUs were counted and calculated back to whole organ of individual mice.

Next, mice emitting strong luciferase signals after *in vivo* transduction were generated and challenged with LM-OVA. Compared to PBS control mice, MVm8-injected mice were significantly better protected against LM-OVA infection, with approximately 100-fold less colony forming units, thereby proving that *in vivo*-transduced T cells are functional and can build up a protective immunity (Fig.30).

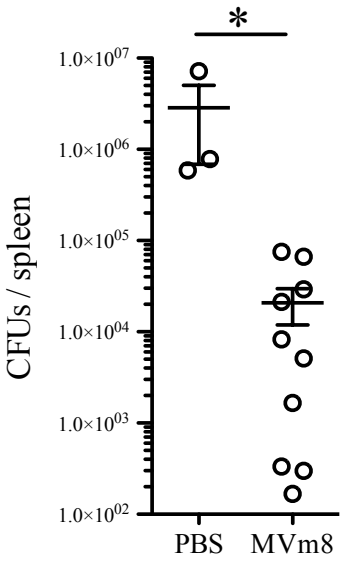

Fig.30 Mice harboring *in vivo*-transduced T cells are protected against LM-OVA
Number of colony forming units (CFU) derived from single cell suspensions from each individual mouse is shown. Rag2$^{-/-}$ mice were challenged with pathogenic doses of LM-OVA. Three days later, mice were sacrificed, spleens isolated and fractions of single cell suspensions were plated. 24 hrs later CFUs were counted and calculated back to whole organ of individual mice. Pooled data of two independent experiments. PBS (n=3), MVm8 (n=10). Asterisk indicates a p value < 0.05.

4 Discussion

T cell based immunotherapies are the most promising therapeutic strategies for cancer patients refractory to classical treatments. While most approaches, e.g. checkpoint inhibitors or DC vaccination, rely on the presence of functional tumor-reactive T cell populations in the autologous repertoire of patients, TCR and CAR engineering can create those populations and thereby fill in immunological gaps. Thus, genetic engineering of T cells is the most straightforward immunotherapeutic approach. The introduced antigen receptors can redirect the cytotoxic activities of autologous T cells to almost any desired specificity, including pathogen-derived antigens. Generation of receptor-engineered T cells is performed in two steps. First, viral vector particles encoding for the tumor-reactive receptor have to be generated, second, patient-derived T cells have to be isolated from peripheral blood, activated, transduced and expanded to sufficient numbers before reinjection. All steps have to be performed under GMP conditions. While the viral particles are quality-controlled off-the-shelf products, the condition of the T cells may vary strongly from patient to patient, depending on the nature and stage of disease, as well as previous treatment regimes. Long *ex vivo* cultures, potentially needed for engineering and generation of therapeutic numbers might further reduce the *in vivo* functionality of T cells.[89] Thus, a lot of effort is put in identifying, isolating and artificially generating "young" T cell phenotypes, such as naïve, stem cell memory or central memory T cells, or by inducing pluripotency followed by engineering and re-differentiation.[93–95,152,153] Including these strategies into above-mentioned GMP production cycles will require even further efforts and expand the time period needed for manufacturing the final therapeutic T cell product.

Non-viral gene transfer techniques may be able to reduce the time needed for production of engineered T cells. Most promising and advanced farthest in clinical development is the Sleeping Beauty transposon/transposase system, but other non-viral techniques such as zinc-finger nucleases, transcription activator-like effector nucleases (TALENs), and the clustered regularly interspersed short palindromic repeat (CRISPR)-Cas9 system, might also be interesting options in future.[154,155] However, like all viral vectors used in clinic so far, non-viral vectors are not able to distinguish between subsets of T cells, as for example $CD8^+$ and $CD4^+$ T cells. Most preclinical and clinical studies focused on $CD8^+$ Tc cells. The importance of including $CD4^+$ Th1 or Th17 cells into the design of clinical trials is underlined by many studies in recent years.[156,157] Based on this data, it is likely that combining tumor-reactive $CD4^+$ and $CD8^+$ T cells results in better therapeutic outcomes when translated to clinics. Technically, this critical endeavor demands techniques allowing the transfer of different

transgenes into both T cell subsets, e.g. an MHC I-restricted TCR in $CD8^+$ Tc and an MHC II-restricted TCR into $CD4^+$ Th cells. Owing to the inability of current gene transfer platforms to discriminate both T cell subsets, the only option is to separate them and transduce both individually. This can be achieved either by labeled magnetic beads or by staining and subsequent flow cytometry assisted sorting. However, both ways add another level of complexity to the highly demanding production procedure of engineered T cells described above, potentially decreasing *in vivo* efficacy further.

This thesis provides a viral vector-based technology, allowing the simultaneous delivery of distinct transgenes into both $CD8^+$ and $CD4^+$ T cells without any further manipulation. Beyond that, it also fulfills the primary requirement for transducing both T cell subsets *in vivo*, which is the exclusive specificity of MVm4 and MVm8. By doing so, *ex vivo* culture and accompanying negative effects can be excluded. Further, it has been shown, that MVm8-pseudotyped vector particles are able to transduce T cells by systemic application retargeting them to desired specificities. *In vivo*-transduced T cells homed specifically towards sites of antigenic stimulation, expanded and retracted in population size, were maintained over a long period of time and where able to exhibit protective immunity when challenged with LM-OVA.

4.1 Overcoming low titers of MV-pseudotyped retroviral vectors

Pseudotyping - the incorporation of glycoproteins, derived from other enveloped viruses - is a phenomenon occurring during viral assembly in cells infected with more than one virus.[158] The technological exploitation of this phenomenon has to a large extend, but not exclusively, focused on lentiviral vectors and allows the alteration of natural viral tropisms. HIV-1 was among the first viruses where pseudotyping through phenotypic mixing was shown.[159–162] Owing to its high stability and broad tropism, VSV-g became one of todays most commonly used LV pseudotypes.[163–166] VSV-pseudotyped LV vectors yield very high titers and are stable enough to be further concentrated by ultracentrifugation. This way, titers up to 10^9 TU/ml can be achieved. Nevertheless, by retargeting VSV only a relative specificity is achieved, since both the wild type as well as the modified glycoprotein have to be incorporated in one vector particle.[167] On the other hand, high viral titers are indispensable for efficient transgene delivery *in vitro* and especially *in vivo*. As outlined in the introduction, two-component envelopes, like the MV envelope, are ideally suited for retargeting retroviral vector particles and achieve complete and exclusive specificities. However, not all envelope vector combinations are compatible. For example, pseudotyping LV vectors with wild type MV envelope glycoproteins results in titers of less than 30 TU/ml most probably due to steric

interferences between the intracellular domains of the MV glycoproteins and the LV-derived matrix proteins, which are lining the inner part of the cell membrane. This is confirmed by the fact that the usage of MV envelope tail variants does not lead to a higher expression of the glycoproteins in vector producing cells, but to an improved incorporation into the budding vector particles.[128] Screening of eleven combinations of H and F tail variants revealed that the HΔ18-FΔ30 combination yields the highest titer when pseudotyping LV vectors.[128] Applying the same H-F combination to gRV vectors could not exceed titers of ca. 10^4 TU/ml after concentration by ultracentrifugation, while usage of the HΔ21A-FΔ24 combination yielded titers in the range of 10^6-10^7 TU/ml. We observed that efficient pseudotyping of gRV vectors by MV envelopes is mainly mediated by the FΔ24 tail variant. From all eight tail variant combinations that yielded an at least 10-fold higher transduction rate than the HΔ18-FΔ30 combination when pseudotyping gRV vectors, only one did utilize FΔ30 instead of FΔ24. Interestingly, in this case FΔ30 paired with HΔ21A. Thus, it seems logical that pairing of FΔ24 and HΔ21A resulted in such an extraordinary good production of vector particles. Surprisingly, the structurally most closely related H tail variants, HΔ21 and HΔ22, resulted in substantially lower titers when combined with FΔ24. HΔ21A-FΔ24 yielded approximately 10-fold higher titers than HΔ21-FΔ24 (10^6 TU/ml) and even 100-fold higher titers than HΔ22-FΔ24 (10^5 TU/ml). Thus, an amazingly little variation, in this case the substitution of one single amino-acid, can lead to tremendous changes in viral vector titers. The different usage of H and F tail variants on the other hand can be attributed to structural differences of the matrix proteins of LV and gRV vectors, although in our hands the HΔ21A-FΔ24-combination, which has not been analyzed by Funke *et al.*, also increased LV titers substantially.[128]

The range of titer achieved in this thesis was sufficient to transduce T cells both *in vitro* and *in vivo* in mice. However, when translating this technology to humans increasing the titer further is desirable. Measles virus belongs to the *Morbillivirus* genus within the *Paramyxovirus* family. All paramyxoviruses have a similar virion structure including the use of two distinct envelope glycoproteins. Thus, in theory, other members of the paramyxovirus family are also eligible for being redirected towards new specificities and pseudotyping RV vectors. This has already been shown for the Tupaia paramyxovirus, which is not a member of the *Morbillivirus* genus.[168] In this study, LV vectors were successfully pseudotyped with Tupaia virus-derived envelope glycoproteins redirected against human CD20, not substantially increasing titers compared to MV-pseudotyped LV vectors. However, this observation proves that other members of the paramyxovirus family are suitable pseudotypes for LV vectors, proving once again the flexibility of this system. In addition, Bender *et al.*

have shown that Nipah virus glycoproteins are more effective in pseudotyping LV vectors leading to an increase in titer compared to MV and Tupaia virus pseudotypes (oral presentation, XXI. Annual Meeting of German Society for Gene Therapy). Thus, for clinical application in humans Nipah virus pseudotypes might be the more valuable vector choice.

Another aspect of consideration is the source of targeting domains. In most cases targeting domains used for redirection of RV vectors are single chain antibody fragments specific for their respective target.[146] But theoretically any specific protein binding domain could be used. The usage of DARPINs as targeting domains has been shown to result in a more stabilized H protein leading to improved titers.[147,169]

After obtaining the final configuration of the targeting vector, concerning tail variants, glycoprotein ancestry and nature of targeting domain, the development of a stable packaging cell line is worthwhile. Stable production conditions enable higher titers, because in contrast to transient production conditions all cells are producing virus and are derived from a single clone tested for its efficiency. In contrast to wild type MV glycoproteins, redirected MV envelopes do not induce formation of syncytia, making this approach feasible. Thus, large scale flow-through or steady-state systems could be developed producing large volumes of virus-containing supernatant which can be further purified and concentrated in down-stream processes while maintaining the biological activity of the viral vectors.[170] Examples of such methods are gradient centrifugation through sucrose or CsCl, PEG precipitation, membrane ultrafiltration or chromatographic approaches, partly being commercially available. One purification method being relevant for *in vivo* applications is the pretreatment of virus-containing supernatant with poly-L-lysine resulting in complexes that can be isolated by low-speed centrifugation. Conventional ultracentrifugation requires 18 rounds of centrifugation and more than 50 hrs to process three liters of supernatant, compared to a single centrifugation and two hrs using poly-L-lysine with low-speed centrifuges.[171] A second option is to use continuous flow centrifugation methods developed for the concentration of viral particles, which also allows the processing of large quantities of supernatant.[172]

Finally, while from a regulatory and animal welfare perspective the maximum volume being injected i.v. into a single mouse is restricted to appr. 200 µl, it is possible to inject 500 – 1000 ml into a patient if necessary. Thus, based on an average titer of appr. $1x10^6$ TU/ml we would inject around $2x10^5$ virus particles into a single mouse, whereas a human individual would receive virus particles in the range of $5x10^8$ to $1x10^9$ in a single dose.

4.2 Simultaneous transduction of $CD8^+$ and $CD4^+$ T cells *in vitro*

The key role of $CD8^+$ Tc cells in anti-tumor and anti-viral immunity is undisputed. $CD8^+$ Tc cells are capable of recognizing and destroying infected as well as transformed MHC I^+ cells in a direct cell-to-cell manner. Since most tumor cells do not express MHC II molecules the role of $CD4^+$ Th cells in anti-tumor immunity has been long underestimated. However, in 1970´s and 1980´s first experimental data showed that also $CD4^+$ Th cells can exhibit anti-tumor activities, by preventing virus-induced sarcomas, eradicating disseminated leukemia and rejecting transplantable tumors.[173–176] MHC II expression is rarely found on tumor cells and may be induced in some tumor entities by IFNγ stimulation.[177–179] In such cases efficient elimination of tumor cells mediated by $CD4^+$ Th cells *in vivo* has been reported.[152,180,181] Mechanisms of direct tumor cell killing by $CD4^+$ Th cells include Fas-FasL-interaction as well as expression of granzyme B and perforin.[182,183] The majority of tumors, however, lack MHC II expression. In these cases $CD4^+$ Th cell-mediated tumor rejection has been associated with the activation and recruitment of tumor-infiltrating APCs or the modulation of the tumor stroma.[44,181] The existence of tumor-derived epitopes presented on MHC II molecules is now well established, with approximately 137 identified and validated pMHC II complexes, from which 86 are considered to be tumor-specific or cancer-testis antigens.[184] Although no clinical study has so far analyzed the potential of engineered $CD4^+$ Th cells alone, there is one case study of a melanoma patient being in complete remission upon a single infusion of an *ex vivo*-generated clonal population of tumor-reactive $CD4^+$ Th cells.[185] This population recognized an NY-ESO1-derived HLA-DOB1*04:01-restricted epitope, which was present in 50-75% of all tumor cells. Complete remission was associated with epitope spreading, which is attributed to tumor-reactive $CD4^+$ Th but not $CD8^+$ Tc cells, further strengthening the importance of combining both T cell subsets.[185,186] The most practical and straightforward way to generate mixed tumor-reactive T cell products is the simultaneous engineering of both T cell subsets.

MV-pseudotyped retargeted vector particles have proven to be a highly flexible and efficient technology.[146] However, the simultaneous delivery of transgenes into different types of cells adds another level of complexity to this system and has never been tried before. The fundamental feature for delivering distinct transgenes into two different types of cells simultaneously is the exclusive specificity of both targeting vectors. Two experiments within this thesis prove that MVm4 and MVm8 are highly specific and deliver transgenes exclusively to the desired target cells. First, we determined CD4 and CD8 being the true entry gates for MVm4- and MVm8-pseudotyped vector particles by incubating target cells with blocking antibodies. This resulted in a dose-dependent decrease of transduction efficiency in both cases. Second, selective transduction of receptor-positive cells was shown when MVm4-

or MVm8-pseudotyped vector particles were added to mixed cultures of cells. This mixture consisted of receptor-positive cells and the receptor-negative parental cell line. Thus, transduction is solely attributed to the presence of CD4 or CD8 on the respective target cell line. Finally, we show that the simultaneous transduction of mixed receptor-positive cell lines as well as primary cells is feasible using MVm4- and MVm8-pseudotyped vector particles. By mixing supernatants containing both viral particles before applying them to a single sample of mixed cells we observed no decrease in specificity at all. In both cases – cell lines and primary cells – signals were detected exclusively in the desired subset of cells. In addition to that, analysis of *in vivo*-transduced cells by application of MVm8-pseudotyped vector particles i.p. showed that 100% of cells expressing GFP were also $CD8^+$. Thus, the specificity of the targeting vectors is retained *in vivo*.

To our knowledge this thesis describes for the first time the genetic engineering of two different subsets of cells simultaneously with different transgenes.

However, above-mentioned simultaneous application of MVm4- and MVm8-pseudotyped vector particles to primary T cell subsets only succeeded when those cells originated from mice of BALB/c but not of B6 background. This surprising observation will be discussed in the next paragraph.

4.3 Identification of a suitable mouse strain for MVm4-mediated transduction

Initial attempts to transduce primary B6-derived $CD4^+$ T cells by MVm4-pseudoytped vector particles failed although high-titer supernatants were applied.

Culture conditions used in our laboratory to activate and propagate primary murine T cells favor expansion of $CD8^+$ over $CD4^+$ T cells, resulting in purely $CD8^+$ T cell cultures after approximately five to seven days. Thus, it seemed likely that the inability of MVm4 to transduce its target cells is due to inadequate activation of $CD4^+$ T cells preventing proliferation, which is crucial for the ability of gRV vectors to transduce cells. As a consequence we sorted primary $CD4^+$ T cells using magnetic beads reaching purities of more than 95% in average. These cells were properly activated and also proliferated as observed by an increase in granularity, cell size and number of cells, analyzed by microscopy and flow cytometry. However, they were again mostly refractory to MVm4-mediated transduction. The level of transduction efficiency achieved throughout all experiments was in the range of 1-8% of GFP^+CD4^+ cells. Regarding the fact that we used MOIs up to four, we expected much higher transduction rates.

We next hypothesized that possibly a special feature of the mAB GK1.5-derived targeting domain leads to prevention or hampering of fusion-mediated cell entry. Strangely, this feature should only be effective on primary cells but not on the 58m4 cell line. Nevertheless, to rule out that it was a GK1.5-derived effect we generated three other CD4-specific targeting domains and grafted them on the H protein. All three new MVm4 envelopes were incorporated into vector particles and were able to transduce the 58m4 cell line. However, again none of those CD4 targeting vector particles reached transduction rates above 1-7% on primary B6-derived $CD4^+$-sorted samples.

The repeated failure of transducing primary $CD4^+$ T cells using targeting domains derived from different CD4-specific antibodies led us to put more effort in analyzing the different steps of the transduction process to narrow down the problem. We focused on the transient shift of $CD4^+$ T cells towards GFP expression after transduction with MVm4-pseudotyped vectors. This observation could be explained by pseudotransduction of cells. Pseudotransduction is a phenomenon provoked by random packaging, in this case, of GFP proteins during vector production into budding vector particles. These GFP proteins are then released into the cytosol of target cells and can be detected as false-positive signals. Pseudotransduction is transient because proteins that are subsequently degraded with a kinetic depending on their half-life mediate it. Pseudotransduction can occur with or without additional packaging of the transfer vector that in contrast mediates stable transduction of cells. From experiments with the 58m4 cell line, which were stably transduced by identical supernatants used for transduction of primary B6-derived T cells we reasoned that also transfer vectors were readily packaged into vector particles, being in general able to mediate integration and stable transduction. Beyond that, when identical transfer vectors were delivered into the same B6-derived $CD4^+$ T cells using entry gates other than CD4, they were easily and efficiently transduced leading to stable expression of the transgene. Taken together, we assumed that GFP protein-harboring MVm4-pseudotyped vector particles were binding to CD4 on the surface of B6-derived T cells but failed to initiate the fusion process for unknown reasons.

Confocal microscopy analysis supported this hypothesis. Application of Eco-pseudotyped vectors led to a GFP signal distributed all over the cells, possibly originating from the cytosol, whereas GFP signals were only detectable at the rim of the cells, co-localized with the expression of CD3, when MVm4 was applied. This result conforms to the transient shift of $CD4^+$ populations towards GFP expression detected by flow cytometry. Based on this data we concluded that the uptake of MVm4-pseudotyped vector particles bound to CD4 on the cell surface is impaired. Since the complete process of binding of redirected H protein,

recruitment of F Protein to the binding site and subsequent fusion and cell entry was in principal successful the problem must have been allocated to B6-derived $CD4^+$ T cells.

In an attempt to understand if CD4 as an entry gate can be functional on B6-derived T cells we artificially increased the surface expression level of B6-derived CD4 molecules by genetic engineering. The transgene used for this experiment is originally derived from B6 T cells. When MVm4-pseudotyped vector particles where used for transduction of these B6-derived T cells stable and long-term transduction was achieved.

Although this loop way approach enabled us to transduce finally B6-derived T cells *in vitro* it was not an option for *in vivo* transduction experiments for obvious reasons. Therefore, we analyzed other mouse strains for receptivity for transduction via CD4 including BALB/c mice. Although expression levels and sequence of CD4 is identical to B6-mice, BALB/c-derived $CD4^+$ T cells were surprisingly permissive for transduction mediated by MVm4-pseudotyped vector particles.

Lipid rafts are known to play a pivotal role in T cell signaling and formation of the immunological synapse after TCR engagement.[187,188] It is obvious that also the T cell co-receptors CD4 and CD8 have to be present in lipid rafts at a certain point of time.[189] Differences in lipid raft organization between $CD8^+$ and $CD4^+$ T cells as well as between mice of different genetic backgrounds have been described and also attributed to differences in immunological reactions towards pathogens observed between B6 and BALB/c mice for example.[190–192] These observations and the data generated within this thesis lead to the hypothesis that the CD4 molecule, although being identical in sequence and similarly expressed, is differently compartmentalized in B6 compared to BALB/c mice. While in B6 mice CD4 is mostly located within the more rigid lipid rafts, in BALB/c mice it is located outside of lipid rafts. Since by definition lipid rafts are areas of higher rigidity and molecules in lipid rafts have less degree of freedom it seems likely that viruses binding to entry gates located permanently in lipid rafts are not able to initiate fusion of the viral and (in this case highly rigid) cell membrane. Although direct evidence is missing, this hypothesis explains all observations made during the course of experiments performed in this study. First, confocal microscopy revealed that GFP expression, indicating virus bound to CD4, is not evenly distributed on the surface of the cell, but rather concentrated at distinct parts of the surface. Second, the artificial increase of CD4 expression on B6-derived T cells probably led to such high levels of CD4 molecules on the cell surface, exceeding the capacity of lipid rafts. Thus, surplus CD4 molecules resided in non lipid raft areas leading to successful transduction of B6-derived T cells.

Direct evidence for above-mentioned speculations can be obtained either by staining of CD4 molecules and lipid raft markers like e.g. GM1 to identify co-localization in B6-derived T cells or by isolating lipid rafts from B6 and BALB/c mice by detergent extraction and sucrose gradient fractionation and analyzing molecules present by mass spectrometry.

One fundamental idea of this project was to transduce both main T cell subsets, $CD4^+$ and $CD8^+$, simultaneously *in vitro* and *in vivo* with different transgenes and to subsequently analyze the potential benefits of this approach for immunotherapy of cancer and infectious disease. During the course of experiments, however, B6 has proven futile for our intentions. Nevertheless, BALB/c-derived $CD4^+$ and $CD8^+$ T cells were permissive for transduction mediated by MVm4- and MVm8-pseudotyped vector particles, respectively. As a consequence a tumor model on BALB/c background, including two antigen-positive (Influenza hemagglutinin protein) progressor tumor cell lines, two MHC I-restricted antigen-reactive TCRs with different affinities and one MHC II-restricted antigen-reactive TCR was established in our lab (C.P. Kemna, unpublished data).[193–195] This system allowed first successful *in vivo* transductions of $CD8^+$ and $CD4^+$ T cells and will enable us to analyze the interplay of both subsets in tumor immunotherapies.

4.4 $CD8^+$ T cells are transduced *in vivo* and built up a protective immunity

4.4.1 Kinetics of *in vivo*-transduced T cells mimic natural immune responses

Within the scope of this thesis we were able transduce B6-derived T cells *in vivo* by systemic application of MVm8-pseudotyped vector particles and analyze their effector functions.

To be able to analyze successful *in vivo* transduction events, a read-out system based on luciferase expression and $Rag2^{-/-}$ mice was established. MVm8-pseudotyped vector particles harboring genes encoding for the OT-I TCRαβ chains and a firefly luciferase were i.v. injected into $Rag2^{-/-}$ mice, which were previously repopulated either with B6-derived polyclonal or P14-$Rag^{-/-}$ mice-derived monoclonal T cells. Comparing both donor T cells, using similar amounts of viral particles and $CD8^+$ T cells per recipient mouse, *in vivo* transduction was more successful in the monoclonal setting (table 2 & 3). This was probably not due to differences in initial transduction efficiencies but rather because of less competition between endogenous tumor-reactive and transduced T cells favoring the outgrowth and thus the increase in luciferase signal of the transduced T cell population in the monoclonal setting. In order to detect rare *in vivo* transduction events irradiated OVA^+ tumor cells are injected s.c.

into the flank of recipient mice. This leads to an accumulation and expansion of T cells reactive against OVA and other foreign tumor antigens in B6 mice.[196] Thus, transduced T cells have to compete with endogenous tumor-reactive T cells present in the polyclonal repertoire of B6 mice for survival factors and antigen HLA complexes. In the monoclonal setting, however, there is no competition since all T cells harbor a TCR reactive to LCMV-gp33, which is not present in the irradiated tumor cells. Thus, the full potential of *in vivo*-transduced T cells can be visualized and luciferase signals in the monoclonal setting reached values approximately ten-fold higher than in the polyclonal setting. In retrospective, the efficiency of *in vivo* transduction in the polyclonal setting was presumably underestimated.

Nevertheless, in both settings *in vivo* transduction was stable over time in terms of transgene expression as well as presence of transduced T cells. Kinetics and homing of T cells developed as expected. Initial luciferase signals were mostly detected in the draining lymph nodes. Analogous to a natural infection, where naïve antigen-specific T cells are primed by APCs in secondary lymphoid organs, e.g. lymph node, we assume that APCs took up antigen at the injection site from irradiated MC38-OVA cells and homed and transported to the draining lymph nodes where they primed naïve transduced T cells. Next, primed T cells homed towards the site of antigenic stimulation and expanded until reaching a peak value after which the population contracted again. Finally, no luciferase signal in mice was detectable anymore. In cases, where irradiated MC38-OVA cells were injected into one flank and OVA^- MC38 cells were injected into the contralateral flank luciferase signals were only detectable at the site of OVA^+ tumor cells and respective draining lymph nodes, proving the antigen-specific homing of transduced T cells. Subsequent boosting of mice using irradiated OVA^+ tumor cells resulted in reconstitution of the luciferase signal again at site of stimulation directly without any detectable signals from draining lymph nodes. Both, onset and extinction of the luciferase signal was faster relative to initial priming. The omission of the draining lymph node as well as the faster kinetics hints towards a memory response.

Transduced T cells were detectable up to 69 days after *in vivo* transduction in the polyclonal setting and up to 90 days in the monoclonal setting.

4.4.2 Alternative tumor models to study *in vivo*-transduced T cell-mediated tumor immunity

First attempts to show the protective capacity of *in vivo*-transduced T cells against MC38-OVA cells failed. Either the tumor was given too early and grew out in all mice, irrespective of injection of MVm8-pseudotyped vectors or PBS, or the tumor cells were given after a prime-boost protocol and did not form in any of the mice. In these experiments polyclonal T cells were used and as mentioned above they endogenously harbor OVA-reactive T cells.

However, the precursor frequency of these cells was probably not high enough to fight an aggressive progressor tumor with fast growth kinetics such as MC38-OVA. Only after a prime-boost protocol, the endogenous T cells were capable of preventing the formation of MC38-OVA tumors. In conclusion, in the polyclonal setting it was not possible to discriminate between the anti-tumoricidal effects of the endogenous and transduced tumor-reactive T cells.

Therefore, we turned to the monoclonal setting. In this experiment six out of six mice showed luciferase signals after injection of MVm8-pseudotyped vector particles, whereas two mice that received PBS showed no signal at all. All mice were primed and boosted once. Next, we s.c. injected a tumorigenic dose of MC38-OVA tumor cells into the flank of each mice. In contrast to our expectations tumors formed in all mice with similar kinetics, although luciferase signals coming from the site of the tumor was detectable over the complete period of the experiment. This means that transduced T cells successfully homed to the tumor but had no impact on tumor outgrowth. MC38 has been described to express PD-L1 and to form a suppressive tumor microenvironment. Usage of anti-PD-1 and anti-CTLA-4 treatments resulted in significantly more potent therapies of MC38 tumors.[197,198] Therefore functional analysis of *in vivo*-transduced T cells should be repeated with less aggressive tumors as for example EG.7, an OVA-expressing derivative of EL4.[199] Another option is to combine immunotherapy using *in vivo*-transduced T cells with checkpoint inhibitors, which have been shown to be effective if a tumor-reactive population of T cells is present. *In vivo* transduction might generate this population.

4.4.3 Protective immunity against bacterial infections by *in vivo*-transduced T cells

In parallel to tumor models we also used an infectious disease model to gain insights into the functionality of *in vivo*-transduced T cells. It was shown that few OT-I TCR^+ $CD8^+$ T cells are sufficient to mediate protective immunity against an otherwise lethal infection by LM-OVA.[200,201] *In vivo*-transduced as well as control mice were systemically infected with LM-OVA. Luciferase signal, with varying intensities, was detectable in all mice injected with MVm8-pseudotyped vector particles but not in control mice. Four to five days after injection of LM-OVA, mice were sacrificed and bacterial colony forming units per spleen were analyzed. Mice showing substantial amounts if *in vivo*-transduced T cells, assessed by luciferase imaging, were approximately ten times better protected against LM-OVA compared to control mice. This experiment has been performed twice so far and will be repeated. We assume that longer incubation times of infected mice will result in even more pronounced differences between treated and control mice. This protection experiment was

performed in the monoclonal setting, meaning that untreated mice (PBS) have no protective immunity against LM-OVA, whereas the transduced T cells present in the treated group might need longer than four to five days to execute their full protective functionality. In addition to the analysis of bacterial colony forming units in spleen, a survival experiment will also be performed. By this, we should be able to more precisely characterize the protective functionality of *in vivo*-transduced T cells.

Taken together, this thesis provides the first evidence that *in vivo* transduction of $CD8^+$ T cells by systemic application of targeting vectors leads to functionally engineered T cells.

4.5 Targeting vectors in clinical applications

Adoptive immunotherapy using *ex vivo* engineered T cells has proven to be a powerful and feasible tool to treat leukemias and will further expand to create similar results for solid cancers in near future. Solid tumors are harder to treat because (i) tumor cells are not readily accessible because of the surrounding tumor stroma and (ii) an established tumor creates a microenvironment impinging on immune cells. One possible way to break tolerance of solid tumors is the combination of tumor-reactive $CD4^+$ and $CD8^+$ T cells.

This thesis provides the tool to generate a combinatorial therapeutic T cell product without the need of further manipulations, like for example cell sorting procedures.

The potential use of *in vivo* transduction for immunotherapy, in the light of the recent successes of *ex vivo* engineered T cells, has to be further validated. However, also for *ex vivo* transduction it took decades to be now a valuable therapeutic approach.[202] One possible use might be prevention of tumor formation in high-risk cancer patients using TCRs targeting shared tumor-specific mutations identified for their tumor entities. In this case, it might also be of interest to include elements down-regulating the expression of checkpoint molecules like PD-1 or CTLA-4, e.g. by RNA interference. This would lead to engineered tumor-reactive T cells being refractory to suppressive features of a newly developing tumor. In addition, the selective inhibition of checkpoints using this approach avoids negative side effects attributed to systemic application and broad range activation of T cells by current antibody-based checkpoint inhibitions. A setting that can be tested in future mouse experiments including $PD\text{-}L1^+$ or $CTLA\text{-}4^+$ tumor cell line, otherwise being refractory immunotherapy.

In therapeutic settings *in vivo* transduction might also be worthwhile for patients with life expectancies less than 6 months and not being suitable for lymphodepletion.[203] In this case,

transducing T cells directly *in vivo* with tumor-reactive TCRs and down regulating checkpoint molecules, either paralleled by *ex vivo* approaches or alone, might lead to a prolonged survival and possibly a curative effect.

In vivo transduction in immune-competent hosts is subject to a number of obstacles, beyond reaching sufficient titers and targeting the correct type of cell subset. Almost every individual has MV-reactive antibody titers either due to vaccination or to natural infections.[204] Therefore, systemically applied MV-pseudotyped vector particles are likely to be neutralized by the hosts' adaptive immunity before reaching their respective target cells. Immunity is almost exclusively directed against a limited number of epitopes present on MV envelope H protein.[205,206] Analysis of natural MV escape variants led to the discovery of specific mutations in two immunodominant epitopes and altered glycosylation patterns.[207–212] Based on this observations mutated variants of MV H protein were developed, which are not neutralized by blood derived from immunized individuals allowing them to transduce their targets *in vivo*.[213] Another report has demonstrated that addition of a targeting domain, in this case three different scFvs, to mutated H protein blinded for its natural receptors partially protects MV-pseudotyped vector particles from neutralization.[214] Retargeted MV vector particles maintained their transduction abilities at low serum concentrations, whereas wild type MV variants were neutralized. At higher concentrations retargeted vector particles still performed appr. four-times better compared to wild type variants. Protection probably results from the targeting domains sterically hindering neutralizing antibodies to bind and by deletion of antibody binding sites by insertion of four distinct point mutations for blinding of the H protein.[144] Specifically mutating the two most dominant epitopes and altering the glycosylation pattern of retargeted H proteins might result in complete protection of MV-pseudotyped vector particles and their untroubled use for *in vivo* transduction in human individuals.

As mentioned above, in the light of increase of viral titers, envelope glycoproteins derived from other members of the paramyxovirus family can also be used as retargeted pseudotypes for LV, and most probably also for gRV, vectors.[168] Nipah viruses, together with Hendra and Cedar virus, form the genus *henipavirus* within the paramyxovirus family. Natural hosts are fruit bats of Pteropodidae family, Pteropus genus. Although seldom Nipah virus can infect humans, being asymptomatic to causing fatal encephalitis. It can be transmitted by uptake of fruits contaminated by infected bats, by intermediate hosts like pigs or even by human-to-human transmission.[215] Tupaia viruses on the other hand have not been reported to infect

humans so far. As part of gene transfer tools, both, Nipah- and Tupaia-derived envelope glycoproteins might be highly valuable. First, because infection is very rare or absent and second, there are no immunizations known to elicit immunity against those glycoproteins, although after *in vivo* transduction immunity against those pseudotypes might develop. But, if a certain treatment demands successive injections of targeting vectors the sequential use of differently pseudotyped vector particles might avoid neutralization of the targeting vectors induced by preceding injections. Thus, they might be highly valuable alternatives for MV-pseudotyped targeting vectors, especially sine retargeting was already successful using Nipah and Tupaia envelopes.

Probably the biggest challenge of translating the targeting technology from murine model systems to humans in clinical settings will be the efficient transduction of high numbers of non-dividing cells, in our case of T cells, *in vivo*. LV vectors are able to transduce resting primary human T cells under certain conditions *in vitro*, but if that is also the case *in vivo* still has to be proven.[216–218] On the other hand, adeno-associated vectors (AAV) can infect non-dividing cells and have also been already successfully redirected to new specificities.[219] Disadvantages of AAV systems are their high immunogenicity and mostly episomal being.[220,221]

In conclusion, the retargeting technology has made great advances in the recent years. It is a highly flexible system, regarding its targets, the type of targeting domains, the type of transfer vectors, the origin of glycoproteins as well as the indications it can be useful for. Crossing the boarder from basic to translational science, the targeting technology will soon be a valuable tool in clinical settings.

4.6 Costs of immunotherapies and ethical considerations

Individualized medicine is regarded to revolutionize the ability of man to manipulate and sustain health. Recent successes especially, but not exclusively, in the field of cancer immunotherapies, have raised expectations of experts from academia as well as industry and also reached popularity in general public, maybe comparable to the complete sequencing of the human genome in 2000.[222–226] The journal *Science* has declared cancer immunotherapy as breakthrough of the year 2013 and the genome editing technology CRISPR breakthrough of the year 2015.[227,228] Both announcements are highly important for the current and future status of adoptive therapy using TCR- or CAR-engineered T cells. In the midst of all this (justified) enthusiasm, however, also critical voices are breaching through. From the scientific

and individual patient point-of-view individualized medicine has enormous power to understand and treat diseases, which were inaccessible to scientists and medical doctors a few years ago. But from the public view the therapeutic benefits have to be in accordance to the resources being invested.

Medical products have never been as expensive as in the era of immunotherapies.[229] This is mostly due to the nature of individualized medical cell products, which have to be generated again and again for each patient and his unique disease (e.g. tumors) as opposed to off-the-shelf products, which can be produced once in large amounts for everyone. Being a fundamentally new approach also infrastructure is lacking. So, far, it is not clear how such infrastructures for individualized cancer therapies might look like. Two scenarios are possible: (i) decentralized small units evolve, each comprising the expertise, facilities and staff needed or (ii) a central (e.g. national or Europe-wide) unit is established, handling the physical generation of the therapeutic cell product, which is then distributed to smaller units, where the patients are treated. Nevertheless, investing huge amounts of money is necessary to develop aforementioned structures. The ideal individualized course of therapy for a cancer patient starts with the sequencing of his cancer genome in order to identify molecular targets for either checkpoint inhibitors or for adoptive T cell therapy. In case of engineered T cell therapy, the next step includes the identification of at least one suitable TCR or CAR, optimally being tumor-specific. Last, autologous T cells from the patient are stably engineered to express the given receptor, expanded to therapeutical numbers and reinfused. A form of therapy that will cost 100.000s of Euros per patient and treatment cycle.

Undisputedly, the interest of big pharma and industry to invest in the field of T cell therapy has increased remarkably since the recent successes of CD19-CARs in ALL.[102,229] But reimbursement-orientated companies want to know if the national health care systems are willing to finance each patient. Regarding the ever-increasing amount of cancer patients this is not likely. Rather, the national health care systems will require information about the efficacy of treatment for each patient - an individualized risk assessment. This requirement is partly met by prescreening of patients, for example by analyzing their tumor biopsies for expression of inhibitory ligands or mutations, but that might not be sufficient to decrease the amount of eligible patients to a number that is bearable by society. At one point the health care system has to decide which patient has better chances for survival, and thus is worth to be invested in, and which one is not. Ultimately this leads to the necessity of being able to measure health itself. The national institute of care & health excellence (NICE) in Great Britain has developed a tool meant to do so. The so-called “Quali-System” is a tool to measure health in terms of duration and quality of years of lives extended by a certain

therapy.[230] For example if a therapy extends patients life for one year without any decrease in life quality, that equals 1 quali. If life is extended for a year but the quality of life is decreased by 50%, that equals 0.5 quali and so on. Each quali is financed with 20 – 30.000 £. The quality of life is assessed by question-based interviews. Although one can discuss the actual use of such a tool, it highlights the need of authorities to find objective rules to adapt to the changing conditions in medicine.

Finally, being driven by nature to extend our lives and to maintain our physical integrity, we have to decide as society how much of the value we generate we are willing to invest into each individual. Certainly, from the patients or family members point-of-view it might seem superfluous and even cruel, but keeping the bigger picture of functioning societies in mind it is an inevitable discussion.

5 Material and Methods

5.1 Molecular biology

5.1.1 Generation of MP71 plasmids

A description of MP71 plasmid constructs generated in this thesis is summarized in table 4. Details regarding the cloning procedure are described in subsequent paragraphs.

Table 4 • List of plasmids

Plasmid (MP71-)	Origin of insert	Type of cloning	Restriction enzyme	Use
-mCD8α	murine T cell	sticky-end	EcoRI, NotI	58m8 cell line
-mCD4	murine T cell	sticky-end	EcoRI, NotI	58m4 cell line
-hCD8α	human T cell	sticky-end	EcoRI, NotI	J76S8 cell line
-hCD150	human T cell	sticky-end	EcoRI, NotI	J76S8 cell line
-mCherry	plasmid	sticky-end	EcoRI, NotI	marker gene
-trOVA-IRES-GFP	plasmid	sticky-end	SalI, NotI	MC38-trOVA Glia-trOVA
-cOVA-IRES-GFP	plasmid	sticky-end	SalI, NotI	MC38-cOVA Glia-cOVA
-OT1-RLuc	plasmid	sticky-end	DraIII, EcoRI	*in vivo* transduction
-OT1-FLuc	plasmid	sticky-end	DraIII, EcoRI	*in vivo* transduction

RNA-extraction and cDNA generation was performed in order to isolate genes from primary tissue origin. Cells were pelleted, lysed and RNA was extracted (RNeasy Mini Kit, Qiagen, Hilden, Germany). Total cell RNA was reverse transcribed into cDNA using SuperScript® II Reverse Transcriptase and oligo$(dT)_{20}$ primers (both Invitrogen, Life Technologies, CA, USA). All steps were performed according to manufacturer´s instructions.

Polymerase chain reaction (PCR) was performed to amplify gene sequences from cDNA or template DNA plasmids using gene specific primers (Eurofins MWG Operon, Martinsried, Germany) harboring individual restriction sites, and the Phusion (Thermo Scientific, MA, USA) or Taq (Invitrogen) DNA Polymerase.

Restriction digest of inserts and plasmid backbones generated compatible overhangs (sticky-end). To prevent relegation of plasmid backbones after linearization alkaline phosphatase treatment (Roche, Basel, Switzerland) was performed twice for 30 mins at 37°C.

Both, the amplicons and the plasmid backbones were purified by gel electrophoresis using Invisorb Fragment CleanUp kit (Stratec, Berlin, Germany).

Ligation of inserts and linearized plasmid backbones took place at a molar ratio of 3:1 using the Rapid DNA Ligation Kit (Roche).

All plasmids were verified by sequence analysis (Eurofins MWG Operon & SourceBioscience, Nottingham, UK).

DNA preparations were performed to propagate plasmid DNA in transformed bacteria. DNA was isolated using either Invisorb Spin Plasmid Mini Two Kit (Stratec) or Qiagen Plasmid Maxi Kit (Qiagen).

5.1.2 Generation of targeting domains

Targeting domains presented in this thesis and their specific characteristics are summarized in table 5.

Table 5 • List of hybridomas for generation of targeting domains

hybridoma	Origin of B cell	Origin of myeloma	specificity	Iotype	ATCC / PHE
2.43[231]	rat	mouse	mLyt2.2	IgG2b	TIB-210
GK1.5[232]	ratx	mouse (BALB/c)	mL3T4	IgG2b	TIB-207
YTS 177.9.6.1[233]	rat	rat (Y3.AG.1.2.3)	mL3T4B	IgG2a	11060819
YTS 191.1.1.2[234]	rat	rat (Y3.AG.1.2.3)	mL3T4B	IgG2b	87072282
YTA 3.1.2[235]	rat	rat (Y3.AG.1.2.3)	mL3T4B	IgG2b	89040603

GK1.5 and 2.43 hybridomas were a kind gift from Prof. Thomas Blankenstein (MDC, Charité, Berlin). Other hybridomas were purchased from Public health England (PHE, Salesbury, UK).

All targeting domains were generated identically. RNA was isolated from $1x10^7$ hybridoma cells, as described above, and cDNA was generated by Taq DNA polymerase (Invitrogen) derived from using gene specific primers rIgck and rIgG2ab (table 6). [236,237]

Table 6 • List of primers used for identification of antibody sequences

name	abbreviation	sequence (5´→ 3)	template
rat Ckappa	rIgck	TGC CAT CAA TCT TCC ACT TGA CA	mRNA
rat IgG2a/2b	rIgG2ab	AAY TTT CTT GTC CAC CTT GG	mRNA
rat kC643-rev	rCk-rev	AGG ATG ATG TCT TAT GAA CAA	cDNA
rat IgG2b-rev	rG2b-rev	CGT CAT GTC GAC GGA TCC AAG CTT GTC ACG GTG ACT GGC TCA GG	cDNA
rat IgG2a-rev	rG2a-rev	CGT CAT GTC GAC GGA TCC AAG CTT AAT AGC CCT TGA CCA GGC AT	cDNA
ANGTAIL	ATL	CGT CGA TGA GCT CTA GAA TTC GCA TGT GCA AGT CCG ATG GTC GGG GGG GGG GGG G	cDNA

Resulting cDNAs were elongated with a poly-C-tail using a terminal deoxynucleotidyl transferase (TDT) and subsequently deployed to 5´-RACE-PCR (Thermo Fisher Scientific, Dreieich, Germany) using the primers rCK-rev, rG2b-rev, rG2a-rev and ATL (table 6). Purified amplicons were ligated into the pCR4Blunt-TOPO® vector using the Zero Blunt TOPO PCR Cloning Kit for Sequencing and transformed into One Shot chemically competent bacteria (Invitrogen, Life Technologies). Plasmid DNA from individual bacterial colonies were prepared and sent for sequencing in order to obtain heavy and light chain variable region sequences depicted in table 7 (Eurofins MWG Operon & SourceBioscience).

Resulting sequences were *in silico* analyzed by comparing their sequences with deposit amino acid sequences from IMGT (performed by Irene Schenider, PEI, Langen). Heavy and light chain variable region sequences were fused using a glycine-serine-linker ($(G_4S)_3$) *in silico* in order to generate scFv fragments. Complete constructs harboring respective cloning-sites (Not1, Sfi1) were ordered from GeneArt (Thermo Fisher Scientific) and cloned into the pHL3 vector harboring a blinded variant of the MVvc H protein, which was a kind gift of Prof. Christian J. Buchholz (PEI, Langen).

Table 7 • List of scFvs

hybridoma	sequence
2.43[231]	EVQLVESGGGLVQPGRSLKLSCAASGFTFSNYYMAWVRQAPTKGLEWV AYINTGGGTTYYRDSVKGRFTISRDDAKSTLYLQMDSLRSEDTATYYC*T TAIGYYFDY*WGQGVMVTVSSGGGGSGGGGSGGGGSDIQMTQSPASLSAS LGETVSIECLASEDIYSYLAWYQQKPGKSPQVLIYAANRLQDGVPSRFSG SGSGTQYSLKISGMQPEDEGDYFC*LQGSKFPYT*FGAGTKLELKR
GK1.5[232]	EVQLVQSGAELVKPGASVKLSCKVSDYNIRRTYMHWVRQRPGKGLEWI GRIDPANGNTIYGEKFKSKATLTADTSSNTAYMQLSQLKSDDTAIYYC*AI GVQYLDY*WGQGTTVTVSSGGGGSGGGGSGGGGSDIVLTQSPALAVSPGE RVTISCRATESVSTLIHWYQQRPGQQPKLLIYLTSHLDSGVPARFSGSGSG TDFTLTIDPVEADDTATYYC*QQTWNDPWT*FGGGTKLELKR
YTS 177.9.6.1[233]	QVQLVESGPGLVQPGQTLSLTCTVSGFSLTSNSVHWVRQAPGKGLEWM GGIWGDGSTDYNSALKGRLSISRDTSKSQVYLKMNSLQTEDTAIYYC*TR YYNSYIYEGWYFDF*WGQGTTVTVSSGGGGSGGGGSGGGGSDIVMTQSPSS LSASLGDRVTITCLASQDIGNYLSWYQQKPGKAPKLLIYGATNLEDGVPS RFSGSGSGTDYTLTINSLGPEDFATYHC*HQYYEYPLT*FGSGTKLEIKR
YTS 191.1.1.2[234]	EVQLVESGGGLVQPGGSLKLSCAASGFTFSDYNMAWVRQAPKKGLEW VATIDYDGSTTYYRDSVKGRFTISRDNTKNTLYLQMNSLKSEDTAMYYC *AKQAYYDGFYHVDYFAY*WGQGVVVTVSSGGGGSGGGGSGGGGSDIVLTQ SPALAVSLGQRVTISCKASESVSSSRYSYMHWYQQKPGQQPKLLIYHAS NLESGVPARFSGSGSGTDFTLTIDPVEADDIATYYC*QQSWNDPPT*FGGGT KLELKR
YTA 3.1.2[235]	QVQLVQSGPELKKPGGSVKISCKASGYTFTNYGMYWVRQAPGQGLEW MGWINTETGKPTYADDFKGRFTFSLDTSASTAYLQINNLKNEDTATYYC *ARPSRYYDGPNWFGY*WGQGTTVTVSSGGGGSGGGGSGGGGSDIVMTQSP ASLSASLGETVSIECLASEGISNYLAWYQQKPGKSPQLLIYYASSLQDGV PSRFSGSGSGTQYSLKISNMQPEDVATYYC*QQAYKFPLT*FGSGTKLEIKR

Underlined: linker. Italic: CDR3 region

5.1.3 Generation of H tail variants

Hm8-Δ18 was used as a template to generate two PCR products (368 bp and 186 bp), which were subsequently fused together by an annealing-PCR to generate an amplicon harboring the Δ21A tail variation (531 bp). The phusion DNA polymerase (Thermo Fisher scientific) was used for each of the three PCRs.

The final amplicon as well as Hm8-Δ18 and Hm4-Δ18 were digested by MunI and XbaI and ligated (sticky end) to yield Hm8-Δ21A and Hm4-Δ21A.

Table 8 • List of primers used for generation of HΔ21A variants

primer	sequence
f-Hd18-MunI	GAA*CAATTG*TTTATAATTAAATGATAAGGTA
r-Hd18	TTAATGACTATGGCCATTATCGATGATGATCTTGCACCCTAAGTTTTA ATTAAC
f-Hd18	ATCGATAATGGCCATAGTCATTAACAGAGAACATCTTATGATTGATA GAC
r-Hd18-XbaI	ACA*TCTAGA*TTGGTGCTGAGGCTTTTATGG

Italic: restriction sites, underlined: additional alanine

5.2 Cell culture

5.2.1 Virus production protocols

Small-scale virus production was performed for all viral particles generated in this thesis except those that were pseudotyped with MV-derived glycoproteins. PlatE and 293T cells were seeded 24 hrs before transfection at a concentration of $0.8x10^6$ cells per well to reach an optimal confluence of ca. 80% at the timepoint of transfection. Ecotropic vector particles were generated by transiently transfecting 18 µg of transfer-vector plasmid DNA into 293T-based PlatE retroviral packaging cells, already harboring gag, pol and env genes, by calciumphosphate precipitaion.[238] Accordingly, amphotropic (10A1) or pantropic (VSV) vector particles were generated by transiently transfecting transgene-encoding (gRV, SIN-gRV or SIN-LV harboring marker genes or TCRs), env- (pALF-10A1; pMD2.G, a gift from Didier Trono)[239] and gag/pol-encoding (pcDNA3.1-MLVg/p, provided by C. Baum, Medical School, Hannover; psPAX2, a gift from Didier Trono) plasmids (6 µg of each plasmid) into 293T cells. Therefore, DNA-containing 250 mM calcium chloride solution (Sigma Aldrich, Seelze, Germany) was mixed with the same volume of transfection buffer (1% HEPES, 1.5 mM Na_2HPO_4, 270 mM NaCl, 10 mm KCl, pH 6.76, all: Sigma Aldrich), incubated for 15 mins and added to the cells. After 6 hours medium was exchanged and cells were cultured for additional 42 hrs before harvesting the virus-containing supernatant. The supernatant was filtered (0.45 µm) and either used directly for transduction or frozen at -80°C or concentrated via ultracentrifugation and then frozen.

Large-scale virus production was performed for all MV-pseudotyped vector particles. $1.4x10^7$ 293T cells were seeded into one T175 flask 24 hrs before to reach an optimal confluence of ca. 80% at the timepoint of transfection. Then medium was exchanged with 11 ml FCS-free medium. Transfection was mediated by polyethylenimine (PEI, SigmaAldrich). Therefore four plasmids, the transfer-vector (gRV, SIN-gRV or SIN-LV harboring marker-

genes or TCRs), the gag/pol-encoding pcDNA3.1-MLVg/p or psPAX2 and the MV-H- and F-encoding plasmids (total: 70µg; H:F:g/p:MP71 = 0.06:0.31:0.95:1) were mixed together with 310 µl of 5% glucose (Merck, Darmstadt, Germany). In parallel 70 µl of PEI was mixed with 310 µl of 5% glucose in another tube. Both solutions were vortexed at intermediate to low speed and incubated at room temperature for ten mins before being mixed with each other, vortexed and incubated for additional ten mins. Finally, 2.25 ml of FCS-free medium was added to the transfection-solution (total volume: 3 ml). The resulting transfection-reagent is added to the cells. Six hrs later 10% FCS (PAN Biotech, Aidenbach, Germany) is added. Additional 48 hrs later the supernatant is harvested, filtered (0.45 µm), concentrated via ultracentrifugation, aliquoted and frozen at –80°C.

Ultracentrifugation was performed using an Optima XPN-80 Ultracentrifuge (Beckman-Coulter, Brea, CA, USA). 16-18 ml of virus-containing supernatant was filtered and collected into one Ultracentrifugation tube and underplayed with 4.5 ml of 20%-sucrose (Sigma, Kawasaki, Japan). After three hrs at 4°C and 100,000g the supernatant was discarded and the virus pellet was resuspended in 50 or 100 µl of DPBS (Gibco, Thermo Fisher Scientific) by pipetting up to 40-times. Supernatant derived from 12 T175 flasks could be concentrated in one round of centrifugation. Virus-containing DPBS was pooled and aliquoted again before freezing and use.

End-point titration of virus stocks was performed by transducing susceptible cell lines in a serial dilution. 2.5-50 µl of virus-containing DPBS was filled up to 200 µl with medium in the first well and then diluted in 1:2 steps in a 96-well plate in medium. Each well comprised a volume of 100 µl in the end. Then $1x10^4$ cells in 100 µl were added to each well. Additionally, protaminesulfate (4µg/ml final, SigmaAldrich) was added to aid transduction of target cells. The cells were cultured for 48-72 hrs before FACS analysis. Titer was determined by calculating the amount of functional viral particles per ml in each well with transduction rates between 1-30%, ensuring single-copy transductions. For each titration the average of calculated values was determined as final value for TU/ml. Each titration was performed at least in duplicates.

5.2.2 Generation of cell lines

Cells were transduced by vector particles harboring the respective transgenes (tables 4 & 9) either generated by transfecting PlatE (murine) or 293T (human) cells. Bulk-transduced cells were analyzed for the presence of the transgene via flow cytometry. If necessary cell surface expression of the transgenes was verified by antibody staining and flow cytometry. Bulk

populations of cells were then single-cell sorted into 96-well plates (flat bottom) prefilled with 200 µl of respective medium via flow cytometry assisted cell-sorting on an Aria II-device (BD Biosciences). In each case a life-dead staining was performed using Sytox-blue (Biolegend, San Dieso, CA, USA). The 96-well plates were then incubated for ca. 10-14 days at 37°C and 5% CO_2. Cell populations derived from single cells were analyzed for clonality and transgene-expression via FACS. Selection criteria included a uniform forward and sideward scatter profile as well as high and stable transgene-expression. Candidate clones were analyzed repeatedly over a time period of at least four weeks. The final clone was expanded to high cell numbers and frozen at two different time points.

Table 9 • List of cell lines

Cell line	Cell type	purpose
58m4	Murine thymoma	Indicator cell line for testing viral supernatants
58m8	Murine thymoma	Indicator cell line for testing viral supernatants
J76S8	Human T cell (ALL)	Indicator cell line for testing viral supernatants
MC38-cOVA-iGFP	Murine colon carcinoma	Target cell line for OTI-TCR-transduced T cells
MC38-trOVA-iGFP	Murine colon carcinoma	Target cell line for OTI-TCR-transduced T cells
Glia-cOVA-iGFP	Murine glioma	Target cell line for OTI-TCR-transduced T cells
Glia-trOVA-iGFP	Murine glioma	Target cell line for OTI-TCR-transduced T cells

5.2.3 Isolation and culture of primary murine T cells

C57BL/6 and BALB/c (Charles River, Wilmington, MA, USA & Taconic, Boston, MA,USA) mice were killed by cervical dislocation and spleens were prepared as single cell suspensions. Removal of red blood cells was achieved by ammonium chloride treatment (150 mM NH_4Cl (Merck), 1 mM $KHCO_3$, 100 nM Na_2EDTA (both: Roth, Karlsruhe, Germany)). Cell density was adjusted to $2x10^6$ cells/ml in T cell medium (RPMI, 10% FCS, 1% Penicillin/Streptomycin, 1% Sodium-pyruvate, 1% non-essential aminoacids; all Gibco, Thermo Fisher Scientific) and supplemented with 1 µg/ml anti-mouse CD3 and 0.1 µg/ml anti –mouse CD28 monoclonal antibodies (BD Biosciences, Pharmingen, Heidelberg, Germany) and 10 U/ml recombinant IL-2 (Chiron, Marburg, Germany) 24 hrs after isolation cells were either adoptively transferred into mice or transduced *in vitro*. Each two to three days the supernatant of primary T cell cultures were exchanged completely with fresh T cell medium containing IL-2 and cell density was adjusted to $2x10^6$ cells/ml.

5.2.4 *Ex vivo* transduction protocols

Primary T cells ($1x10^6$/well/ml) and cell lines ($1x10^5$/well/ml) were transduced in their respective culture medium in RetroNectin-coated (12.5 µg/ml, TaKaRa, Saint-German-en-Laye, France) 24-well non-tissue culture plates. In case of primary T cells beads coated with anti-mouse CD3 and anti-mouse CD28 antibodies were added ($1x10^4$/ml). After addition of 1 ml virus supernatant, supplemented with protamine-sulfate (final: 4 µg/ml) the plates were centrifuged for 90 mins at 800g and 32°C. Cells were incubated at 37°C and 5%CO_2 as described above. Transduction efficiency was measured earliest 48 hrs after centrifugation and functional assays were performed 10-14 days later.

5.2.5 Antibody blocking experiments

Monoclonal antibodies blocking either mCD4 or mCD8a (Santa Cruz Biotechnologies, Dallas, TX, USA) or an IgG2b-Isotype (Biolegend) were serially diluted in 1:2 steps in 25 µl T cell medium in a 96-well round-bottom plate before $1x10^4$ 58m4 or 58m8 cells/25µl/well were added. The plates were incubated for two hrs at 37°C and 5% CO_2 and washed twice before 200 µl of titer-equilibrated (MOI=1) MVm4- or MVm8-pseudotyped GFP-encoding vector particles supplemented with protamine sulfate (final: 4µg/ml) were added. Transduction efficiency was analyzed 48 hrs later by flow cytometry.

5.2.6 Confocal microscopy

Primary B6-derived T cells were activated and transduced with MVm4 gRV/GFP or Eco gRV/GFP as. One day later cells were stained for expression of CD3 with a brilliant violet conjugated antibody (Biolegend) and imaged using two-photon microscopy and a Leica SP 5 microscope and LAS AF software (Leica microsystems, Heerbrugg, Switzerland).

5.3 Functional assays

5.3.1 Flow cytometry

Expression of surface antigens was detected by incubation of $5x10^5$ to $1x10^6$ cells with 1 µg of specific monoclonal antibodies conjugated with either allophycocyanine (APC), phycoerythrine (PE), fluorescin isothiocyanate (FITC) or brilliant violet (BV) in 50 µl PBS for 30 mins at 4°C (see table 10). Cells were washed twice with phosphate-buffered saline (PBS) and analyzed by FACS (MacsQuant, Miltenyi, Teterow, Germany). Data was analyzed with FlowJo (Treestar, Ashland, Oregon, USA). Discrimination of living and dead cells was accomplished by incubation of stained cells with Sytox-Blue (Biolegend) 5-10 mins before data acquisition. Detection of functional TCR expression on transduced T cells was achieved by incubation with MHC multimers for 40 mins at 4°C prior to incubation with antibodies.

Table 10 • List of antibodies and multimers used for flow cytometry

specificity	conjugate	manufacturer
hCD150	PE	BD Biosciences
hCD8	APC	BD Biosciences
hCD8	PE	BD Biosciences
His-Tag	PE	MACS
CD3	FITC	
mCD4	PE	BD Biosciences
mCD8	PE	Biolegend
mCD8	APC.Cy7	Biolegend
Vα2	APC	
Vβ5	PE	
H2k^b-SIINFEKL	PE	Biolegend
OVA-Tetramer	PE	Beckman-Coulter

5.3.2 Coculture and cytokine release assay

OT-I-TCR-transduced primary T cells and ovalbumin positive tumor cells (table 9) were seeded into 96-well round-bottom plates in a 1:1 ratio (each 5x10^4 cells/well/100µl) in T cell medium and incubated at 37°C and 5%CO_2 for 16-24 hrs to stimulate antigen-specific cytokine release by effector T cells. Coculture supernatant was either frozen at -20°C or immediately analyzed for presence and concentration of Interferon γ (IFNγ) by enzyme-linked immunosorbent assay according to manufacturers instructions (ELISA, BD Biosciences). Untransduced effector cells and ovalbumin$^-$ tumor cells were used as controls. TCR-independent stimulation was achieved by incubating effector T cells with 1 µM ionomycin (Calbiochem, Darmstadt, Germany) and 5 ng/ml phorbol-12-myristate-13-acetate (Promega, Mannhein, Germany). All coculture samples were performed in duplicates.

5.4 *In vivo* experiments

5.4.1 *In vivo* transduction protocol

B6- and P14-derived splenocytes were isolated and activated as described above.

Splenocytes were washed twice with PBS and injected intravenously into Rag2$^{-/-}$-white mice (Rag2$^{-/-}$) either via the tail-vein or retro-orbitally 24 hrs after isolation. In case of B6 donor mice ½ a spleen in 200 µl DPBS was injected into one recipient Rag$^{-/-}$ mouse. In case of P14 donor mice one spleen in 200 µl DPBS was injected into one recipient Rag$^{-/-}$ mouse. Thus similar numbers of CD8$^+$ T cells were transferred (appr. 6x10^6 CD8$^+$ T

cells/mouse/200µl). Mice were allowed to rest for 24 hrs before 200 µl DPBS with or without viral particles encoding for the OT-I-TCR and a luciferase were injected into the contralateral side retro-orbitally. Mice were anesthetized by continuous flow administration of an Isofluran-O_2-mixture prior to retro-orbital injections.

On day 5 after injection of viral particles mice were primed either by subcutaneous injection of SIINFEKL-peptide (Biosyntan, Berlin, Germany) in conjunction with CpG and IFA or by injection of irradiated MC38-OVA cells ($5x10^6$ cells/mouse/200 µl, 65 Gy). In some experiments OVA^- parental cell lines were s.c. injected into the collateral flanks. Imaging of mice started on day 12 after injection of viral particles and was performed daily until loss of signal. Repeated immunizations (boostings) were performed in four-week intervals.

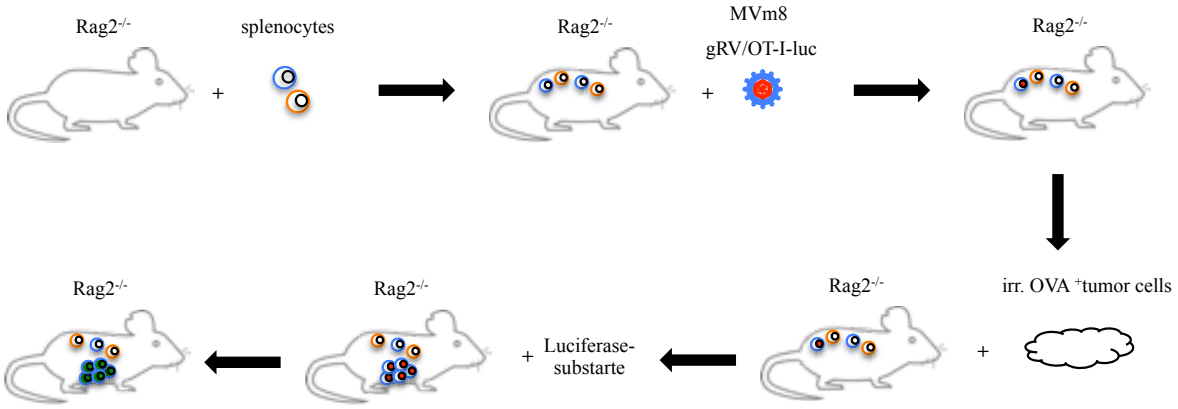

Fig.31 Mouse model for visualization of successful *in vivo* transduction events

5.4.2 Live imaging of mice

Mice were anesthetized prior to retro-orbital injection of 100 µl D-Luciferin (Biosynth, Staad, Switzerland) i.v. (300 mg/g body weight prepared in PBS) in case of Firefly-Luciferase (FLuc) or coelenterazin (Biosynth) dissolved in DMSO (Sigma) and diluted in PBS (100 µg/100 µL per mouse) in case of Renilla-Luciferase (RLuc). Mice were exposed for 60 sec using Xenogen IVIS 200 (Caliper Life Science, Hopkinton, MA, USA). mages were acquired for 1 min using medium binning. Images were analyzed using LivingImage analysis software (Caliper Life Science). The dimensions of the region of interestvaried based on the tumor and mouse size and were set for each experiment at the time point when the tumor was largest.

5.4.3 Tumor challenge

Mice were injected s.c. with $1x10^5$ living MC38-trOVA tumor cells into one flank. Tumor growth was measured using a caliper and tumor volume was calculated by multiplying all three dimensions.

5.4.4 LM-OVA challenge

Mice were injected i.v. with appr. 4-5x10^6 OVA-transgenic *Listeria monocytogenes* per mouse. Three days after injection mice were killed by cervical dislocation and the spleen was isolated. Single cell suspensions of the individual spleens were prepared and different dilutions were plated on Agar. After 24 hrs at 37°C the resulting colonies were counted.

5.5 Statistical analysis

All data are displayed as mean and the standard error of the mean. Statistical significance between 2 groups was determined using unpaired Student *t* tests. *P* values are given in the figure legends. A p value of less than .05 was considered significant. One asterisk indicates a p value of less than 0.05, two asterisks indicate a p value of less than 0.01. GraphPad Prism 5 (GrapPad, La Jolla, CA, USA) was used for statistical analysis.

6 References

1. Flajnik, M. F. & Kasahara, M. Origin and evolution of the adaptive immune system: genetic events and selective pressures. *Nat. Rev. Genet.* **11,** 47–59 (2010).
2. Feldman, S. A., Assadipour, Y., Kriley, I., Goff, S. & Rosenberg, S. A. Adoptive Cell Therapy – TIL, TCRs and CARs. *Semin. Oncol.* **42,** 626–39 (2015).
3. Mombaerts, P. *et al.* RAG-1-deficient mice have no mature B and T lymphocytes. *Cell* **68,** 869–77 (1992).
4. Shinkai, Y. *et al.* RAG-2-deficient mice lack mature lymphocytes owing to inability to initiate V(D)J rearrangement. *Cell* **68,** 855–67 (1992).
5. Murphy, K. *Janeway's immunobiology*. (Garland Science, Taylor & Francis Group, 2011).
6. Paul WE. *Fundamental Immunology*. (Lippincott, Williams 6 Wilkins, Wolters Kluwer, 2012).
7. Davis, M. M. & Bjorkman, P. J. T-cell antigen receptor genes and T-cell recognition. *Nature* **334,** 395–402 (1988).
8. ZINKERNAGEL, R. M. & DOHERTY, P. C. Immunological surveillance against altered self components by sensitised T lymphocytes in lymphocytes choriomeningitis. *Nature* **251,** 547–548 (1974).
9. ZINKERNAGEL, R. M. & DOHERTY, P. C. Restriction of in vitro T cell-mediated cytotoxicity in lymphocytic choriomeningitis within a syngeneic or semiallogeneic system. *Nature* **248,** 701–702 (1974).
10. Tikhonova, A. N. *et al.* αβ T Cell Receptors that Do Not Undergo Major Histocompatibility Complex-Specific Thymic Selection Possess Antibody-like Recognition Specificities. *Immunity* 1–13 (2011). doi:10.1016/j.immuni.2011.11.013
11. Collins, E. J. & Riddle, D. S. TCR-MHC docking orientation: natural selection, or thymic selection? *Immunol. Res.* **41,** 267–94 (2008).
12. Van Laethem, F. *et al.* Deletion of CD4 and CD8 coreceptors permits generation of alphabetaT cells that recognize antigens independently of the MHC. *Immunity* **27,** 735–50 (2007).
13. Starr, T. K., Jameson, S. C. & Hogquist, K. A. Positive and negative selection of T cells. *Annu. Rev. Immunol.* **21,** 139–76 (2003).
14. Kim, J. M. & Rudensky, A. The role of the transcription factor Foxp3 in the development of regulatory T cells. *Immunol. Rev.* **212,** 86–98 (2006).
15. Picca, C. C. & Caton, A. J. The role of self-peptides in the development of CD4+

CD25+ regulatory T cells. *Curr. Opin. Immunol.* **17,** 131–6 (2005).

16. Burnet, F. M. A modification of Jerne's theory of antibody production using the concept of clonal selection. *CA. Cancer J. Clin.* **26,** 119–21
17. Richards, D. M., Kyewski, B. & Feuerer, M. Re-examining the Nature and Function of Self-Reactive T cells. *Trends Immunol.* (2016). doi:10.1016/j.it.2015.12.005
18. Hogquist, K. A. & Jameson, S. C. The self-obsession of T cells: how TCR signaling thresholds affect fate 'decisions' and effector function. *Nat. Immunol.* **15,** 815–23 (2014).
19. Mueller, D. L. Mechanisms maintaining peripheral tolerance. *Nat. Immunol.* **11,** 21–7 (2010).
20. Yu, W. *et al.* Clonal Deletion Prunes but Does Not Eliminate Self-Specific αβ CD8(+) T Lymphocytes. *Immunity* **42,** 929–41 (2015).
21. Melief, C. J. M. Cancer immunotherapy by dendritic cells. *Immunity* **29,** 372–83 (2008).
22. Schwartz, R. H. Models of T cell anergy: is there a common molecular mechanism? *J. Exp. Med.* **184,** 1–8 (1996).
23. Walunas, T. L. *et al.* CTLA-4 can function as a negative regulator of T cell activation. *Immunity* **1,** 405–13 (1994).
24. Smyth, M. J. & Trapani, J. A. Granzymes: exogenous proteinases that induce target cell apoptosis. *Immunol. Today* **16,** 202–6 (1995).
25. Pipkin, M. E. & Lieberman, J. Delivering the kiss of death: progress on understanding how perforin works. *Curr. Opin. Immunol.* **19,** 301–8 (2007).
26. Young, J. D., Clark, W. R., Liu, C. C. & Cohn, Z. A. A calcium- and perforin-independent pathway of killing mediated by murine cytolytic lymphocytes. *J. Exp. Med.* **166,** 1894–9 (1987).
27. Rouvier, E., Luciani, M. F. & Golstein, P. Fas involvement in Ca(2+)-independent T cell-mediated cytotoxicity. *J. Exp. Med.* **177,** 195–200 (1993).
28. Ju, S. T., Cui, H., Panka, D. J., Ettinger, R. & Marshak-Rothstein, A. Participation of target Fas protein in apoptosis pathway induced by CD4+ Th1 and CD8+ cytotoxic T cells. *Proc. Natl. Acad. Sci. U. S. A.* **91,** 4185–9 (1994).
29. Berke, G. The CTL's kiss of death. *Cell* **81,** 9–12 (1995).
30. Kolb, W. P. & Granger, G. A. Lymphocyte in vitro cytotoxicity: characterization of human lymphotoxin. *Proc. Natl. Acad. Sci. U. S. A.* **61,** 1250–5 (1968).
31. Carswell, E. A. *et al.* An endotoxin-induced serum factor that causes necrosis of tumors. *Proc. Natl. Acad. Sci. U. S. A.* **72,** 3666–70 (1975).

32. Wheelock, E. F. Interferon-Like Virus-Inhibitor Induced in Human Leukocytes by Phytohemagglutinin. *Science* **149,** 310–1 (1965).
33. Caza, T. & Landas, S. Functional and Phenotypic Plasticity of CD4(+) T Cell Subsets. *Biomed Res. Int.* **2015,** 521957 (2015).
34. Schoenborn, J. R. & Wilson, C. B. Regulation of interferon-gamma during innate and adaptive immune responses. *Adv. Immunol.* **96,** 41–101 (2007).
35. Weiss, R. A. How does HIV cause AIDS? *Science* **260,** 1273–9 (1993).
36. Mosmann, T. R., Cherwinski, H., Bond, M. W., Giedlin, M. A. & Coffman, R. L. Two types of murine helper T cell clone. I. Definition according to profiles of lymphokine activities and secreted proteins. *J. Immunol.* **136,** 2348–57 (1986).
37. Mosmann, T. R. & Sad, S. The expanding universe of T-cell subsets: Th1, Th2 and more. *Immunol. Today* **17,** 138–46 (1996).
38. Harrington, L. E., Mangan, P. R. & Weaver, C. T. Expanding the effector CD4 T-cell repertoire: the Th17 lineage. *Curr. Opin. Immunol.* **18,** 349–56 (2006).
39. Breitfeld, D. *et al.* Follicular B helper T cells express CXC chemokine receptor 5, localize to B cell follicles, and support immunoglobulin production. *J. Exp. Med.* **192,** 1545–52 (2000).
40. Schaerli, P. *et al.* CXC chemokine receptor 5 expression defines follicular homing T cells with B cell helper function. *J. Exp. Med.* **192,** 1553–62 (2000).
41. Ma, C. S., Deenick, E. K., Batten, M. & Tangye, S. G. The origins, function, and regulation of T follicular helper cells. *J. Exp. Med.* **209,** 1241–53 (2012).
42. Veldhoen, M. *et al.* Transforming growth factor-beta 'reprograms' the differentiation of T helper 2 cells and promotes an interleukin 9-producing subset. *Nat. Immunol.* **9,** 1341–6 (2008).
43. Eyerich, S. *et al.* Th22 cells represent a distinct human T cell subset involved in epidermal immunity and remodeling. *J. Clin. Invest.* **119,** 3573–85 (2009).
44. Qin, Z. & Blankenstein, T. CD4+ T cell--mediated tumor rejection involves inhibition of angiogenesis that is dependent on IFN gamma receptor expression by nonhematopoietic cells. *Immunity* **12,** 677–86 (2000).
45. Sommermeyer, D. *et al.* Chimeric antigen receptor-modified T cells derived from defined CD8(+) and CD4(+) subsets confer superior antitumor reactivity in vivo. *Leukemia* (2015). doi:10.1038/leu.2015.247
46. Schietinger, a., Philip, M., Liu, R. B., Schreiber, K. & Schreiber, H. Bystander killing of cancer requires the cooperation of CD4+ and CD8+ T cells during the effector phase. *J. Exp. Med.* (2010). doi:10.1084/jem.20092450

47. Kerkar, S. P. *et al.* Genetic engineering of murine CD8+ and CD4+ T cells for preclinical adoptive immunotherapy studies. *J. Immunother.* **34,** 343–52 (2011).
48. Hoepner, S. *et al.* Synergy between CD8 T cells and Th1 or Th2 polarised CD4 T cells for adoptive immunotherapy of brain tumours. *PLoS One* **8,** e63933 (2013).
49. Tran, E. *et al.* Cancer immunotherapy based on mutation-specific CD4+ T cells in a patient with epithelial cancer. *Science* **344,** 641–5 (2014).
50. Muranski, P. & Restifo, N. P. Adoptive immunotherapy of cancer using CD4(+) T cells. *Curr. Opin. Immunol.* **21,** 200–8 (2009).
51. Kamphorst, A. O. & Ahmed, R. CD4 T-cell immunotherapy for chronic viral infections and cancer. *Immunotherapy* **5,** 975–87 (2013).
52. Zanetti, M. Tapping CD4 T cells for cancer immunotherapy: the choice of personalized genomics. *J. Immunol.* **194,** 2049–56 (2015).
53. Coley, W. B. The treatment of malignant tumors by repeated inoculations of erysipelas. With a report of ten original cases. 1893. *Clin. Orthop. Relat. Res.* 3–11 (1893).
54. Little, C. C. & Tyzzer, E. E. Further experimental studies on the inheritance of susceptibility to a Transplantable tumor, Carcinoma (J. W. A.) of the Japanese waltzing Mouse. *J. Med. Res.* **33,** 393–453 (1916).
55. Currie, G. A. Eighty years of immunotherapy: a review of immunological methods used for the treatment of human cancer. *Br. J. Cancer* **26,** 141–53 (1972).
56. Powles, R. L. The application of immunotherapy to the treatment of cancer. *Pharmacol. Ther.* **4,** 281–306 (1979).
57. Clowes, G. H. & Baeslack, F. W. ON THE INFLUENCE EXERTED ON THE VIRULENCE OF CARCINOMA IN MICE BY SUBJECTING THE TUMOR MATERIALS TO INCUBATION PREVIOUS TO INOCULATION. *J. Exp. Med.* **8,** 481–503 (1906).
58. Strong, L. C. The Origin of Some Inbred Mice. *Cancer Res.* **2,** 531–539 (1942).
59. Old, L. J. & Boyse, E. A. Specific antigens of tumors and leukemias of experimental animals. *Med. Clin. North Am.* **50,** 901–12 (1966).
60. CRI. http://www.cancerresearch.org/news-publications/our-blog/april-2015/fda-approved-cancer-immunotherapies-and-cri-impact.
61. American Cancer Society. Cancer Immunotherapy What is cancer immunotherapy ? (2014).
62. Gross, J. A., St John, T. & Allison, J. P. The murine homologue of the T lymphocyte antigen CD28. Molecular cloning and cell surface expression. *J. Immunol.* **144,** 3201–10 (1990).

63. Lotze, M. T. *et al.* High-dose recombinant interleukin 2 in the treatment of patients with disseminated cancer. Responses, treatment-related morbidity, and histologic findings. *JAMA* **256,** 3117–24 (1986).

64. Rosenberg, S. A. IL-2: the first effective immunotherapy for human cancer. *J. Immunol.* **192,** 5451–8 (2014).

65. Goldstein, D. & Laszlo, J. The Role of Interferon in Cancer Therapy: A Current Perspective. *CA. Cancer J. Clin.* **38,** 258–277 (1988).

66. Gelao, L., Criscitiello, C., Esposito, A., Goldhirsch, A. & Curigliano, G. Immune checkpoint blockade in cancer treatment: a double-edged sword cross-targeting the host as an 'innocent bystander'. *Toxins (Basel).* **6,** 914–33 (2014).

67. Hodi, F. S. *et al.* Improved survival with ipilimumab in patients with metastatic melanoma. *N. Engl. J. Med.* **363,** 711–23 (2010).

68. Robert, C. *et al.* Ipilimumab plus dacarbazine for previously untreated metastatic melanoma. *N. Engl. J. Med.* **364,** 2517–26 (2011).

69. Topalian, S. L. *et al.* Survival, durable tumor remission, and long-term safety in patients with advanced melanoma receiving nivolumab. *J. Clin. Oncol.* **32,** 1020–30 (2014).

70. Robert, C. *et al.* Anti-programmed-death-receptor-1 treatment with pembrolizumab in ipilimumab-refractory advanced melanoma: a randomised dose-comparison cohort of a phase 1 trial. *Lancet* **384,** 1109–17 (2014).

71. Blankenstein, T., Leisegang, M., Uckert, W. & Schreiber, H. Targeting cancer-specific mutations by T cell receptor gene therapy. *Curr. Opin. Immunol.* **33,** 112–9 (2015).

72. FDA. http://www.fda.gov/Drugs/DevelopmentApprovalProcess/HowDrugsareDevelopedandApproved/ApprovalApplications/TherapeuticBiologicApplications/ucm080591.htm.

73. FDA. http://www.fda.gov/Drugs/InformationOnDrugs/ApprovedDrugs/ucm340913.htm.

74. FDA. http://www.fda.gov/Drugs/DrugSafety/PostmarketDrugSafetyInformationforPatientsandProviders/ucm109106.htm.

75. Weiner, G. J. Rituximab: mechanism of action. *Semin. Hematol.* **47,** 115–23 (2010).

76. Kantoff, P. W. *et al.* Sipuleucel-T immunotherapy for castration-resistant prostate cancer. *N. Engl. J. Med.* **363,** 411–22 (2010).

77. FDA. http://www.fda.gov/BiologicsBloodVaccines/CellularGeneTherapyProducts/Approved

Products/ucm210012.htm.

78. Gillison, M. L., Chaturvedi, A. K. & Lowy, D. R. HPV prophylactic vaccines and the potential prevention of noncervical cancers in both men and women. *Cancer* **113,** 3036–46 (2008).
79. Markowitz, L. E. *et al.* Human papillomavirus vaccine introduction--the first five years. *Vaccine* **30 Suppl 5,** F139-48 (2012).
80. DELORME, E. J. & ALEXANDER, P. TREATMENT OF PRIMARY FIBROSARCOMA IN THE RAT WITH IMMUNE LYMPHOCYTES. *Lancet (London, England)* **2,** 117–20 (1964).
81. Fefer, A. Immunotherapy and chemotherapy of Moloney sarcoma virus-induced tumors in mice. *Cancer Res.* **29,** 2177–83 (1969).
82. Morgan, D. A., Ruscetti, F. W. & Gallo, R. Selective in vitro growth of T lymphocytes from normal human bone marrows. *Science* **193,** 1007–8 (1976).
83. Cohen, C. J. *et al.* Isolation of neoantigen-specific T cells from tumor and peripheral lymphocytes. *J. Clin. Invest.* **125,** 3981–91 (2015).
84. Bonini, C. & Mondino, A. Adoptive T-cell therapy for cancer: The era of engineered T cells. *Eur. J. Immunol.* **45,** 2457–69 (2015).
85. Dudley, M. E. *et al.* Cancer regression and autoimmunity in patients after clonal repopulation with antitumor lymphocytes. *Science* **298,** 850–4 (2002).
86. Rosenberg, S. A. *et al.* Use of tumor-infiltrating lymphocytes and interleukin-2 in the immunotherapy of patients with metastatic melanoma. A preliminary report. *N. Engl. J. Med.* **319,** 1676–80 (1988).
87. Rosenberg, S. A. & Restifo, N. P. Adoptive cell transfer as personalized immunotherapy for human cancer. *Science (80-.).* **348,** 62–68 (2015).
88. Yannelli, J. R. *et al.* Growth of tumor-infiltrating lymphocytes from human solid cancers: summary of a 5-year experience. *Int. J. Cancer* **65,** 413–21 (1996).
89. Gattinoni, L. *et al.* Acquisition of full effector function in vitro paradoxically impairs the in vivo antitumor efficacy of adoptively transferred CD8+ T cells. *J. Clin. Invest.* **115,** 1616–26 (2005).
90. Leisegang, M. *et al.* Eradication of large solid tumors by gene therapy with a T cell receptor targeting a single cancer-specific point mutation. *Clin. Cancer Res.* (2015). doi:10.1158/1078-0432.CCR-15-2361
91. Leisegang, M., Kammertoens, T., Uckert, W. & Blankenstein, T. Targeting human melanoma neoantigens by T cell receptor gene therapy. *J. Clin. Invest.* (2016). doi:10.1172/JCI83465

92. Dembic, Z. *et al.* Transfer of specificity by murine alpha and beta T-cell receptor genes. *Group* (1986).

93. Hinrichs, C. S. *et al.* Human effector CD8+ T cells derived from naive rather than memory subsets possess superior traits for adoptive immunotherapy. *Blood* **117,** 808–14 (2011).

94. Berger, C. *et al.* Adoptive transfer of effector CD8+ T cells derived from central memory cells establishes persistent T cell memory in primates. *J. Clin. Invest.* **118,** 294–305 (2008).

95. Klebanoff, C. A. *et al.* Central memory self/tumor-reactive CD8+ T cells confer superior antitumor immunity compared with effector memory T cells. *Proc. Natl. Acad. Sci. U. S. A.* **102,** 9571–6 (2005).

96. Morgan, R. A. *et al.* Cancer Regression and Neurological Toxicity Following Anti-MAGE-A3 TCR Gene Therapy. *J. Immunother.* **36,** 133–151 (2013).

97. Robbins, P. F. *et al.* Tumor regression in patients with metastatic synovial cell sarcoma and melanoma using genetically engineered lymphocytes reactive with NY-ESO-1. *J. Clin. Oncol.* **29,** 917–24 (2011).

98. Parkhurst, M. R. *et al.* T cells targeting carcinoembryonic antigen can mediate regression of metastatic colorectal cancer but induce severe transient colitis. *Mol. Ther.* **19,** 620–6 (2011).

99. Johnson, L. A. *et al.* Gene therapy with human and mouse T-cell receptors mediates cancer regression and targets normal tissues expressing cognate antigen. *Blood* **114,** 535–46 (2009).

100. Morgan, R. A. *et al.* Cancer regression in patients after transfer of genetically engineered lymphocytes. *Science* **314,** 126–9 (2006).

101. Maus, M. V, Grupp, S. A., Porter, D. L. & June, C. H. Antibody-modified T cells: CARs take the front seat for hematologic malignancies. *Blood* **123,** 2625–35 (2014).

102. Maude, S. L. *et al.* Chimeric Antigen Receptor T Cells for Sustained Remissions in Leukemia. *N. Engl. J. Med.* **371,** 1507–1517 (2014).

103. Kochenderfer, J. N. *et al.* Chemotherapy-refractory diffuse large B-cell lymphoma and indolent B-cell malignancies can be effectively treated with autologous T cells expressing an anti-CD19 chimeric antigen receptor. *J. Clin. Oncol.* **33,** 540–9 (2015).

104. Louis, C. U. *et al.* Antitumor activity and long-term fate of chimeric antigen receptor-positive T cells in patients with neuroblastoma. *Blood* **118,** 6050–6 (2011).

105. Morgan, R. a *et al.* Case report of a serious adverse event following the administration of T cells transduced with a chimeric antigen receptor recognizing ERBB2. *Mol. Ther.*

18, 843–51 (2010).

106. Kershaw, M. H. *et al.* A phase I study on adoptive immunotherapy using gene-modified T cells for ovarian cancer. *Clin. Cancer Res.* **12,** 6106–15 (2006).
107. Lamers, C. H. *et al.* Treatment of metastatic renal cell carcinoma with CAIX CAR-engineered T cells: clinical evaluation and management of on-target toxicity. *Mol. Ther.* **21,** 904–12 (2013).
108. Offringa, R. Antigen choice in adoptive T-cell therapy of cancer. *Curr. Opin. Immunol.* **21,** 190–9 (2009).
109. Kunert, A. *et al.* TCR-Engineered T Cells Meet New Challenges to Treat Solid Tumors: Choice of Antigen, T Cell Fitness, and Sensitization of Tumor Milieu. *Front. Immunol.* **4,** 363 (2013).
110. Obenaus, M. *et al.* Identification of human T-cell receptors with optimal affinity to cancer antigens using antigen-negative humanized mice. *Nat. Biotechnol.* **33,** 402–7 (2015).
111. Wilde, S. *et al.* Generation of allo-restricted peptide-specific T cells using RNA-pulsed dendritic cells: A three phase experimental procedure. *Oncoimmunology* **1,** 129–140 (2012).
112. Wilde, S. *et al.* Dendritic cells pulsed with RNA encoding allogeneic MHC and antigen induce T cells with superior antitumor activity and higher TCR functional avidity. *Blood* **114,** 2131–9 (2009).
113. Hebeisen, M. *et al.* Identifying Individual T Cell Receptors of Optimal Avidity for Tumor Antigens. *Front. Immunol.* **6,** 582 (2015).
114. Engels, B. & Uckert, W. Redirecting T lymphocyte specificity by T cell receptor gene transfer--a new era for immunotherapy. *Mol. Aspects Med.* **28,** 115–42 (2007).
115. ZINDER, N. D. & LEDERBERG, J. Genetic exchange in Salmonella. *J. Bacteriol.* **64,** 679–99 (1952).
116. Shimotohno, K. & Temin, H. M. No apparent nucleotide sequence specificity in cellular DNA juxtaposed to retrovirus proviruses. *Proc. Natl. Acad. Sci. U. S. A.* **77,** 7357–61 (1980).
117. Miller, A. D. & Buttimore, C. Redesign of retrovirus packaging cell lines to avoid recombination leading to helper virus production. *Mol. Cell. Biol.* **6,** 2895–902 (1986).
118. Poznansky, M., Lever, A., Bergeron, L., Haseltine, W. & Sodroski, J. Gene transfer into human lymphocytes by a defective human immunodeficiency virus type 1 vector. *J. Virol.* **65,** 532–6 (1991).
119. Tatum, E. L. Molecular biology, nucleic acids, and the future of medicine. *Perspect.*

Biol. Med. **10,** 19–32 (1966).

120. Ltd, J. W. and S. http://www.abedia.com/wiley/vectors.php.
121. Landau, N. R., Page, K. A. & Littman, D. R. Pseudotyping with human T-cell leukemia virus type I broadens the human immunodeficiency virus host range. *J. Virol.* **65,** 162–9 (1991).
122. Colin, A. *et al.* Engineered lentiviral vector targeting astrocytes in vivo. *Glia* **57,** 667–79 (2009).
123. Miletic, H. *et al.* Selective transduction of malignant glioma by lentiviral vectors pseudotyped with lymphocytic choriomeningitis virus glycoproteins. *Hum. Gene Ther.* **15,** 1091–100 (2004).
124. Russell, S. J., Hawkins, R. E. & Winter, G. Retroviral vectors displaying functional antibody fragments. *Nucleic Acids Res.* **21,** 1081–5 (1993).
125. Buchholz, C. J., Mu, M. D. & Cichutek, K. Lentiviral vectors with measles virus glycoproteins – dream team for gene transfer ? *Trends Biotechnol.* 259–265 (2009). doi:10.1016/j.tibtech.2009.02.002
126. Yang, L. *et al.* Engineered lentivector targeting of dendritic cells for in vivo immunization. *Nat. Biotechnol.* **26,** 326–34 (2008).
127. Morizono, K. *et al.* Lentiviral vector retargeting to P-glycoprotein on metastatic melanoma through intravenous injection. *Nat. Med.* **11,** 346–52 (2005).
128. Cichutek & Buchholz, C. J. Targeted cell entry of lentiviral vectors. *Am. Soc. Gene Ther. Orig.* **16,** 1427–1436 (2008).
129. Plattet, P. & Plemper, R. K. Envelope protein dynamics in paramyxovirus entry. *MBio* **4,** (2013).
130. Jardetzky, T. S. & Lamb, R. A. Activation of paramyxovirus membrane fusion and virus entry. *Curr. Opin. Virol.* **5,** 24–33 (2014).
131. Russell, C. J., Jardetzky, T. S. & Lamb, R. A. Membrane fusion machines of paramyxoviruses: capture of intermediates of fusion. *EMBO J.* **20,** 4024–34 (2001).
132. Porotto, M. *et al.* Spring-loaded model revisited: paramyxovirus fusion requires engagement of a receptor binding protein beyond initial triggering of the fusion protein. *J. Virol.* **85,** 12867–80 (2011).
133. Noyce, R. S. *et al.* Tumor cell marker PVRL4 (nectin 4) is an epithelial cell receptor for measles virus. *PLoS Pathog.* **7,** e1002240 (2011).
134. Noyce, R. S. & Richardson, C. D. Nectin 4 is the epithelial cell receptor for measles virus. *Trends Microbiol.* **20,** 429–39 (2012).
135. Pirquet, C. Das Verhalten der kutanen Tuberkulinreaktion während der Masern. *DMW*

- *Dtsch. Medizinische Wochenschrift* **34,** 1297–1300 (2009).

136. ENDERS, J. F. & PEEBLES, T. C. Propagation in tissue cultures of cytopathogenic agents from patients with measles. *Proc. Soc. Exp. Biol. Med.* **86,** 277–86 (1954).
137. ENDERS, J. F., KATZ, S. L., MILOVANOVIC, M. V & HOLLOWAY, A. Studies on an attenuated measles-virus vaccine. I. Development and preparations of the vaccine: technics for assay of effects of vaccination. *N. Engl. J. Med.* **263,** 153–9 (1960).
138. SCHWARZ, A. J. Preliminary tests of a highly attenuated measles vaccine. *Am. J. Dis. Child.* **103,** 386–9 (1962).
139. Yanagi, Y., Ono, N., Tatsuo, H., Hashimoto, K. & Minagawa, H. Measles virus receptor SLAM (CD150). *Virology* **299,** 155–61 (2002).
140. Massé, N., Barrett, T., Muller, C. P., Wild, T. F. & Buckland, R. Identification of a second major site for CD46 binding in the hemagglutinin protein from a laboratory strain of measles virus (MV): potential consequences for wild-type MV infection. *J. Virol.* **76,** 13034–8 (2002).
141. Funke, S. *et al.* Pseudotyping lentiviral vectors with the wild-type measles virus glycoproteins improves titer and selectivity. *Gene Ther.* **16,** 700–5 (2009).
142. Vongpunsawad, S., Oezgun, N., Braun, W. & Cattaneo, R. Selectively receptor-blind measles viruses: Identification of residues necessary for SLAM- or CD46-induced fusion and their localization on a new hemagglutinin structural model. *J. Virol.* **78,** 302–13 (2004).
143. Blechacz, B. & Russell, S. J. Measles virus as an oncolytic vector platform. *Curr. Gene Ther.* **8,** 162–75 (2008).
144. Nakamura, T. *et al.* Rescue and propagation of fully retargeted oncolytic measles viruses. *Nat. Biotechnol.* **23,** 209–14 (2005).
145. Moll, M., Klenk, H. & Maisner, A. Importance of the Cytoplasmic Tails of the Measles Virus Glycoproteins for Fusogenic Activity and the Generation of Recombinant Measles Viruses. **76,** 7174–7186 (2002).
146. Buchholz, C. J., Friedel, T. & Büning, H. Surface-Engineered Viral Vectors for Selective and Cell Type-Specific Gene Delivery. *Trends Biotechnol.* **33,** 777–90 (2015).
147. Zhou, Q. *et al.* Exclusive Transduction of Human CD4+ T Cells upon Systemic Delivery of CD4-Targeted Lentiviral Vectors. *J. Immunol.* **195,** 2493–2501 (2015).
148. Zhou, Q. *et al.* T-cell receptor gene transfer exclusively to human CD8+ cells enhances tumor cell killing. *Blood* **120,** 4334–42 (2012).
149. Engels, B. *et al.* Retroviral vectors for high-level transgene expression in T

lymphocytes. *Hum. Gene Ther.* **14,** 1155–68 (2003).

150. Schambach, a *et al.* Overcoming promoter competition in packaging cells improves production of self-inactivating retroviral vectors. *Gene Ther.* **13,** 1524–1533 (2006).
151. Letourneur, F. & Malissen, B. Derivation of a T cell hybridoma variant deprived of functional T cell receptor alpha and beta chain transcripts reveals a nonfunctional alpha-mRNA of BW5147 origin. *Eur. J. Immunol.* **19,** 2269–74 (1989).
152. Xie, Y. *et al.* Naive tumor-specific CD4(+) T cells differentiated in vivo eradicate established melanoma. *J. Exp. Med* **207,** 651–667 (2010).
153. Nishimura, T. *et al.* Generation of rejuvenated antigen-specific T cells by reprogramming to pluripotency and redifferentiation. *Cell Stem Cell* **12,** 114–26 (2013).
154. LaFountaine, J. S., Fathe, K. & Smyth, H. D. C. Delivery and Therapeutic Applications of Gene Editing Technologies ZFNs, TALENs, and CRISPR/Cas9. *Int. J. Pharm.* **494,** 180–94 (2015).
155. Ammar, I., Izsvák, Z. & Ivics, Z. The Sleeping Beauty transposon toolbox. *Methods Mol. Biol.* **859,** 229–40 (2012).
156. Nishimura, T. *et al.* Distinct role of antigen-specific T helper type 1 (Th1) and Th2 cells in tumor eradication in vivo. *J. Exp. Med.* **190,** 617–27 (1999).
157. Muranski, P. *et al.* Tumor-specific Th17-polarized cells eradicate large established melanoma. *Blood* **112,** 362–73 (2008).
158. Závada, J. The pseudotypic paradox. *J. Gen. Virol.* **63 (Pt 1),** 15–24 (1982).
159. Canivet, M., Hoffman, A. D., Hardy, D., Sernatinger, J. & Levy, J. A. Replication of HIV-1 in a wide variety of animal cells following phenotypic mixing with murine retroviruses. *Virology* **178,** 543–51 (1990).
160. Lusso, P. *et al.* Expanded HIV-1 cellular tropism by phenotypic mixing with murine endogenous retroviruses. *Science* **247,** 848–52 (1990).
161. Chesebro, B., Wehrly, K. & Maury, W. Differential expression in human and mouse cells of human immunodeficiency virus pseudotyped by murine retroviruses. *J. Virol.* **64,** 4553–7 (1990).
162. Spector, D. H. *et al.* Human immunodeficiency virus pseudotypes with expanded cellular and species tropism. *J. Virol.* **64,** 2298–308 (1990).
163. Zhu, Z. H., Chen, S. S. & Huang, A. S. Phenotypic mixing between human immunodeficiency virus and vesicular stomatitis virus or herpes simplex virus. *J. Acquir. Immune Defic. Syndr.* **3,** 215–9 (1990).
164. Akkina, R. K. *et al.* High-efficiency gene transfer into CD34+ cells with a human

immunodeficiency virus type 1-based retroviral vector pseudotyped with vesicular stomatitis virus envelope glycoprotein G. *J. Virol.* **70,** 2581–5 (1996).

165. Naldini, L. *et al.* In vivo gene delivery and stable transduction of nondividing cells by a lentiviral vector. *Science* **272,** 263–7 (1996).
166. Reiser, J. *et al.* Transduction of nondividing cells using pseudotyped defective high-titer HIV type 1 particles. *Proc. Natl. Acad. Sci. U. S. A.* **93,** 15266–71 (1996).
167. Höfig, I. *et al.* Systematic improvement of lentivirus transduction protocols by antibody fragments fused to VSV-G as envelope glycoprotein. *Biomaterials* **35,** 4204–12 (2014).
168. Enkirch, T. *et al.* Targeted lentiviral vectors pseudotyped with the Tupaia paramyxovirus glycoproteins. *Gene Ther.* 1–8 (2012). doi:10.1038/gt.2011.209
169. Münch, R. C. *et al.* DARPins: an efficient targeting domain for lentiviral vectors. *Mol. Ther.* **19,** 686–93 (2011).
170. Morenweiser, R. Downstream processing of viral vectors and vaccines. *Gene Ther.* **12 Suppl 1,** S103-10 (2005).
171. Zhang, B. *et al.* A highly efficient and consistent method for harvesting large volumes of high-titre lentiviral vectors. *Gene Ther.* **8,** 1745–51 (2001).
172. Uckert, W., Sydow, G., Hertling, I., Rudolph, M. & Wunderlich, V. Comparison of different methods for large-volume concentration of a type D retrovirus (PMFV). *Arch. für Geschwulstforsch.* **52,** 541–9 (1982).
173. Cantor, H. & Boyse, E. A. Functional subclasses of T-lymphocytes bearing different Ly antigens. I. The generation of functionally distinct T-cell subclasses is a differentiative process independent of antigen. *J. Exp. Med.* **141,** 1376–89 (1975).
174. Leclerc, J. C. & Cantor, H. T cell-mediated immunity to oncornavirus-induced tumors. II. Ability of different T cell sets to prevent tumor growth in vivo. *J. Immunol.* **124,** 851–4 (1980).
175. Greenberg, P. D., Kern, D. E. & Cheever, M. A. Therapy of disseminated murine leukemia with cyclophosphamide and immune Lyt-1+,2- T cells. Tumor eradication does not require participation of cytotoxic T cells. *J. Exp. Med.* **161,** 1122–34 (1985).
176. Fujiwara, H., Fukuzawa, M., Yoshioka, T., Nakajima, H. & Hamaoka, T. The role of tumor-specific Lyt-1+2- T cells in eradicating tumor cells in vivo. I. Lyt-1+2- T cells do not necessarily require recruitment of host's cytotoxic T cell precursors for implementation of in vivo immunity. *J. Immunol.* **133,** 1671–6 (1984).
177. Mach, B., Steimle, V., Martinez-Soria, E. & Reith, W. Regulation of MHC class II genes: lessons from a disease. *Annu. Rev. Immunol.* **14,** 301–31 (1996).

178. Steimle, V., Siegrist, C. A., Mottet, A., Lisowska-Grospierre, B. & Mach, B. Regulation of MHC class II expression by interferon-gamma mediated by the transactivator gene CIITA. *Science* **265,** 106–9 (1994).

179. Martin-Orozco, N. *et al.* Melanoma cells express ICOS ligand to promote the activation and expansion of T-regulatory cells. *Cancer Res.* **70,** 9581–90 (2010).

180. Perez-Diez, A. *et al.* CD4 cells can be more efficient at tumor rejection than CD8 cells. *Blood* **109,** 5346–54 (2007).

181. Corthay, A. *et al.* Primary antitumor immune response mediated by CD4+ T cells. *Immunity* **22,** 371–83 (2005).

182. Lundin, K. U. *et al.* CD4+ T cells kill Id+ B-lymphoma cells: FasLigand-Fas interaction is dominant in vitro but is redundant in vivo. *Cancer Immunol. Immunother.* **53,** 1135–45 (2004).

183. Quezada, S. A. *et al.* Tumor-reactive CD4(+) T cells develop cytotoxic activity and eradicate large established melanoma after transfer into lymphopenic hosts. *J. Exp. Med.* **207,** 637–50 (2010).

184. Vigneron, N., Stroobant, V., Van den Eynde, B. J. & van der Bruggen, P. Database of T cell-defined human tumor antigens: the 2013 update. *Cancer Immun.* **13,** 15 (2013).

185. Hunder, N. N. *et al.* Treatment of metastatic melanoma with autologous CD4+ T cells against NY-ESO-1. *N. Engl. J. Med.* **358,** 2698–703 (2008).

186. Kim, H. & Cantor, H. CD4 T-cell Subsets and Tumor Immunity: The Helpful and the Not-so-Helpful. *Cancer Immunol. Res.* **2,** 91–98 (2014).

187. MAGEE, T., PIRINEN, N., ADLER, J., PAGAKIS, S. N. & PARMRYD, I. Lipid rafts: cell surface platforms for T cell signaling. *Biol. Res.* **35,** 127–131 (2002).

188. Luo, C., Wang, K., Liu, D. Q., Li, Y. & Zhao, Q. S. The functional roles of lipid rafts in T cell activation, immune diseases and HIV infection and prevention. *Cell. Mol. Immunol.* **5,** 1–7 (2008).

189. Nagafuku, M. *et al.* CD4 and CD8 T cells require different membrane gangliosides for activation. *Proc. Natl. Acad. Sci. U. S. A.* **109,** E336-42 (2012).

190. Huang, H. *et al.* Lipid-based signaling modulates DNA repair response and survival against Klebsiella pneumoniae infection in host cells and in mice. *Am. J. Respir. Cell Mol. Biol.* **49,** 798–807 (2013).

191. de Mello Coelho, V. *et al.* Quantitative differences in lipid raft components between murine CD4+ and CD8+ T cells. *BMC Immunol.* **5,** 2 (2004).

192. Kovacs, B. *et al.* Human CD8+ T cells do not require the polarization of lipid rafts for activation and proliferation. *Proc. Natl. Acad. Sci. U. S. A.* **99,** 15006–11 (2002).

193. Morgan, D. J. *et al.* CD8(+) T cell-mediated spontaneous diabetes in neonatal mice. *J. Immunol.* **157,** 978–83 (1996).

194. Wong, S. B. J., Bos, R. & Sherman, L. A. Tumor-specific CD4+ T cells render the tumor environment permissive for infiltration by low-avidity CD8+ T cells. *J. Immunol.* **180,** 3122–31 (2008).

195. Taylor, A. H., Haberman, A. M., Gerhard, W. & Caton, A. J. Structure-function relationships among highly diverse T cells that recognize a determinant from influenza virus hemagglutinin. *J. Exp. Med.* **172,** 1643–51 (1990).

196. Steinaa, L., Rasmussen, P. B., Gautam, A. & Mouritsen, S. Breaking B-cell tolerance and CTL tolerance in three OVA-transgenic mouse strains expressing different levels of OVA. *Scand. J. Immunol.* **67,** 113–20 (2008).

197. Korman, A. *et al.* Activity of Anti-PD-1 in Murine Tumor Models: Role of 'Host' PD-L1 and Synergistic Effect of Anti-PD-1 and Anti-CTLA-4. *J. Immunol.* **178,** S82 (2007).

198. Deng, L. *et al.* Irradiation and anti-PD-L1 treatment synergistically promote antitumor immunity in mice. *J. Clin. Invest.* **124,** 687–95 (2014).

199. Moore, M. W., Carbone, F. R. & Bevan, M. J. Introduction of soluble protein into the class I pathway of antigen processing and presentation. *Cell* **54,** 777–85 (1988).

200. Buchholz, V. R., Schumacher, T. N. M. & Busch, D. H. T Cell Fate at the Single-Cell Level. *Annu. Rev. Immunol.* (2015). doi:10.1146/annurev-immunol-032414-112014

201. Stemberger, C. *et al.* Lowest numbers of primary CD8(+) T cells can reconstitute protective immunity upon adoptive immunotherapy. *Blood* **124,** 628–37 (2014).

202. Gilham, D. E. *et al.* Adoptive T-cell therapy for cancer in the United kingdom: a review of activity for the British Society of Gene and Cell Therapy annual meeting 2015. *Hum. Gene Ther.* **26,** 276–85 (2015).

203. Houot, R., Schultz, L. M., Marabelle, A. & Kohrt, H. T-cell-based Immunotherapy: Adoptive Cell Transfer and Checkpoint Inhibition. *Cancer Immunol. Res.* **3,** 1115–22 (2015).

204. World health organization. WHO | Measles immunization coverage. (2016). Available at: http://www.who.int/gho/mdg/child_mortality/situation_trends_measles_immunization/en/. (Accessed: 16th February 2016)

205. de Swart, R. L., Yüksel, S. & Osterhaus, A. D. M. E. Relative contributions of measles virus hemagglutinin- and fusion protein-specific serum antibodies to virus neutralization. *J. Virol.* **79,** 11547–51 (2005).

206. Ertl, O. T., Wenz, D. C., Bouche, F. B., Berbers, G. A. M. & Muller, C. P. Immunodominant domains of the Measles virus hemagglutinin protein eliciting a neutralizing human B cell response. *Arch. Virol.* **148,** 2195–206 (2003).

207. Fournier, P. *et al.* Antibodies to a new linear site at the topographical or functional interface between the haemagglutinin and fusion proteins protect against measles encephalitis. *J. Gen. Virol.* **78,** 1295–1302 (1997).

208. Finsterbusch, T. *et al.* Measles viruses of genotype H1 evade recognition by vaccine-induced neutralizing antibodies targeting the linear haemagglutinin noose epitope. *J. Gen. Virol.* **90,** 2739–45 (2009).

209. Shi, J. *et al.* Measles incidence rate and a phylogenetic study of contemporary genotype H1 measles strains in China: is an improved measles vaccine needed? *Virus Genes* **43,** 319–26 (2011).

210. Domínguez, A. *et al.* Large outbreak of measles in a community with high vaccination coverage: implications for the vaccination schedule. *Clin. Infect. Dis.* **47,** 1143–9 (2008).

211. Kremer, J. R. *et al.* High genetic diversity of measles virus, World Health Organization European Region, 2005-2006. *Emerg. Infect. Dis.* **14,** 107–14 (2008).

212. Zhang, Y. *et al.* New measles virus genotype associated with outbreak, China. *Emerg. Infect. Dis.* **16,** 943–7 (2010).

213. Lévy, C. *et al.* Lentiviral vectors displaying modified measles virus gp overcome pre-existing immunity in in vivo-like transduction of human T and B cells. *Mol. Ther.* **20,** 1699–712 (2012).

214. Kneissl, S. *et al.* Measles virus glycoprotein-based lentiviral targeting vectors that avoid neutralizing antibodies. *PLoS One* **7,** e46667 (2012).

215. WHO. WHO | Nipah Virus (NiV) Infection. Available at: http://www.who.int/csr/disease/nipah/en/. (Accessed: 16th February 2016)

216. Frecha, C., Lévy, C., Cosset, F.-L. & Verhoeyen, E. Advances in the field of lentivector-based transduction of T and B lymphocytes for gene therapy. *Mol. Ther.* **18,** 1748–57 (2010).

217. Frecha, C. *et al.* Stable transduction of quiescent T cells without induction of cycle progression by a novel lentiviral vector pseudotyped with measles virus glycoproteins. *Blood* **112,** 4843–52 (2008).

218. Verhoeyen, E., Costa, C. & Cosset, F.-L. Lentiviral vector gene transfer into human T cells. *Methods Mol. Biol.* **506,** 97–114 (2009).

219. Münch, R. C. *et al.* Off-target-free gene delivery by affinity-purified receptor-targeted

viral vectors. *Nat. Commun.* **6,** 6246 (2015).

220. Daya, S. & Berns, K. I. Gene therapy using adeno-associated virus vectors. *Clin. Microbiol. Rev.* **21,** 583–93 (2008).
221. Zhang, W. *et al.* Hybrid adeno-associated viral vectors utilizing transposase-mediated somatic integration for stable transgene expression in human cells. *PLoS One* **8,** e76771 (2013).
222. Huffington Post. Conquering Cancer: Personalized Medicine Is the Future. (2015). Available at: http://www.huffingtonpost.com/dr-david-samadi/conquering-cancer-personalized-medicine-is-the-future_b_7585544.html. (Accessed: 16th February 2016)
223. Huffington Post. Genomics Moves From the Lab to the Doctor's Office. (2015). Available at: http://www.huffingtonpost.com/footnote/genomics-moves-from-the-l_b_8287586.html. (Accessed: 16th February 2016)
224. Huffington Post. Tailoring Treatment, One Cancer Patient At A Time. (2015). Available at: http://www.huffingtonpost.com/footnote/tailoring-treatment-one-c_b_8334244.html. (Accessed: 16th February 2016)
225. Huffington Post. An Open Letter About Cancer and Other Weird Stuff. (2015). Available at: http://www.huffingtonpost.com/brigitte-cutshall/an-open-letter-about-my-c_b_8577972.html. (Accessed: 16th February 2016)
226. Huffington Post. Top 10 Medical Research Issues and Trends to Watch in 2016. (2015). Available at: http://www.huffingtonpost.com/margaret-anderson/top-10-medical-research-i_b_8924856.html. (Accessed: 16th February 2016)
227. Science. Science: 342 (6165). *Science (80-.).* **342,** (2013).
228. Science. Science: 350 (6267). *Science (80-.).* **350,** (2015).
229. Barrett, D. M., Grupp, S. A. & June, C. H. Chimeric Antigen Receptor- and TCR-Modified T Cells Enter Main Street and Wall Street. *J. Immunol.* **195,** 755–61 (2015).
230. Health, N. I. of C. &. https://www.nice.org.uk/. (2016).
231. Sarmiento, M., Glasebrook, A. L. & Fitch, F. W. IgG or IgM monoclonal antibodies reactive with different determinants on the molecular complex bearing Lyt 2 antigen block T cell-mediated cytolysis in the absence of complement. *J. Immunol.* **125,** 2665–72 (1980).
232. Wilde, D. B., Marrack, P., Kappler, J., Dialynas, D. P. & Fitch, F. W. Evidence implicating L3T4 in class II MHC antigen reactivity; monoclonal antibody GK1.5 (anti-L3T4a) blocks class II MHC antigen-specific proliferation, release of lymphokines, and binding by cloned murine helper T lymphocyte lines. *J. Immunol.* **131,** 2178–83 (1983).

233. Qin, S. X. *et al.* Induction of tolerance in peripheral T cells with monoclonal antibodies. *Eur. J. Immunol.* **20,** 2737–45 (1990).

234. Cobbold, S. P., Jayasuriya, A., Nash, A., Prospero, T. D. & Waldmann, H. Therapy with monoclonal antibodies by elimination of T-cell subsets in vivo. *Nature* **312,** 548–51

235. Qin, S., Cobbold, S., Tighe, H., Benjamin, R. & Waldmann, H. CD4 monoclonal antibody pairs for immunosuppression and tolerance induction. *Eur. J. Immunol.* **17,** 1159–65 (1987).

236. Brady, J. L., Corbett, A. J., McKenzie, B. S. & Lew, A. M. Rapid specific amplification of rat antibody cDNA from nine hybridomas in the presence of myeloma light chains. *J. Immunol. Methods* **315,** 61–7 (2006).

237. Gilliland, L. K. *et al.* Rapid and reliable cloning of antibody variable regions and generation of recombinant single chain antibody fragments. *Tissue Antigens* **47,** 1–20 (1996).

238. Morita, S., Kojima, T. & Kitamura, T. Plat-E: an efficient and stable system for transient packaging of retroviruses. *Gene Ther.* **7,** 1063–6 (2000).

239. Uckert, W. *et al.* Efficient gene transfer into primary human CD8+ T lymphocytes by MuLV-10A1 retrovirus pseudotype. *Hum. Gene Ther.* **11,** 1005–14 (2000).

7 Appendix

7.1 Abbreviations

AAV	adeno-associated virus/vector
ADC	antibody-drug-conjugates
AIDS	acquired immunodeficiency syndrome
ALL	acute lymphoblastic leukemia
APC	antigen presenting cell
B6	C57BL/6
CD	cluster of differentiation
CAR	chimeric antigen receptor
cDNA	complementary DNA
CDR	complementary determining region
cPPT	central poly-purine tract
CRISPR	clustered regularly interspersed short palindromic repeat
CT	cytoplasmic tail
CTLA-4	cytotoxic T-lymphocyte antigen 4
D	diversity gene segment
DARPin	designed ankyrin repeat protein
DC	dendritic cell
DMSO	dimethyl sulfoxide
DNA	deoxyribonucleid acid
DP	double positive
Eco	ecotropic viral envelope
ED	ectodomain
EGFR	epidermal growth factor receptor
Env	envelope
F	fusion
F1	fusion domain 1
F2	fusion domain 2
FACS	fluorescence-activated cell sorting
FDA	U.S. food and drug administration
Fluc	Firefly luciferase
FP	fusion protein
Gag	group-specific antigen
GALV	gibbon ape leukemia virus
GFP	green fluorescent protein
GMP	good manufacturing practice
GOI	gene of interest
Gp33	LCMV glycoprotein 33
gRV	gamma-retrovirus
H	hemagglutinin
HBV	hepatitis B virus
HER2	human EGF receptor 2

His	histidin
HIV	human immunodeficiency virus
HLA	human leukocyte antigen
HPV	human papillomavirus
IFN	interferon
IL	interleukin
IRES	internal ribosomal entry site
J	joining gene segment
Kb	kilobase
LM-OVA	OVA-transgenic Listeria monocytogenes
LTR	long terminal repeats
Luc	Luciferase
LV	Lentivirus
mAB	monoclonal antibody
MACS	magnetic-activated cell sorting
MFI	mean fluorescence intensity
MHC	major histocompatibility complex
MLV	murine leukemia virus
MOI	multiplicity of infection
MPSV	mouse proliferative sarcoma virus
MP71	MPSV-derived promoter variant
MV	measles virus
MVvc	Edmonston strain of measles virus used for vaccination
MVm4	murine CD4-specific targeting envelope
MVm8	murine CD8-alpha-specific targeting envelope
NICE	national institute of care & health excellence
OT-I	OVA-specific TCR
OVA	ovalbumine
P14	lymphocytic choriomeningitis virus-derived gp33-specific TCR
PAP	prostatic acid phosphatase
PAMP	pathogen-associated molecular pattern
PBS	phosphate-buffered saline
PCR	polymerase chain reaction
PD-1	programmed death protein 1
PD-L1	programmed death ligand 1
PEG	polyethylene glycol
PEI	polyethylenimine
pMHC	peptide-MHC complex
pol	polymerase
PRE	post-transcriptional regulatory element
RACE	rapid amplification of cDNA ends
Rluc	Renilla luciferase
Rag	recombination-activating gene
RNA	ribonucleid acid
RRE	rev-responsive element
RSV	rous-sarcoma-virus

RV	retrovirus
scFv	single chain antibody fragment
SIN	self-inactivating
SLAM	signaling lymphocyte activation molecule
TALEN	transcription activator-like effector nucleases
TCR	T cell receptor
Tc	cytotoxic T cell
Tfh	T follicular helper cell
Th	T helper cell
TIL	tumor infiltrating lymphocyte
TM	transmembrane domain
TNF	tumor necrosis factor
Treg	regulatory T cell
V	variable gene segment
VH	variable region of heavy chain
VL	variable region of light chain
VSV	vesicular stomatitis virus

7.2 Sequences

MP71-mCD4 (B6-derived)

Nucleotide sequence

ATGTGCCGAGCCATCTCTCTTAGGCGCTTGCTGCTGCTGCTGCTGCAGCTGTCACAACTC
CTAGCTGTCACTCAAGGGAAGACGCTGGTGCTGGGGAAGGAAGGGGAATCAGCAGAACT
GCCCTGCGAGAGTTCCCAGAAGAAGATCACAGTCTTCACCTGGAAGTTCTCTGACCAGAG
GAAGATTCTGGGGCAGCATGGCAAAGGTGTATTAATTAGAGGAGGTTCGCCTTCGCAGTT
TGATCGTTTTGATTCCAAAAAAGGGGCATGGGAGAAAGGATCGTTTCCTCTCATCATCAA
TAAACTTAAGATGGAAGACTCTCAGACTTATATCTGTGAGCTGGAGAACAGGAAAGAGG
AGGTGGAGTTGTGGGTGTTCAAAGTGACCTTCAGTCCGGGTACCAGCCTGTTGCAAGGGC
AGAGCCTGACCCTGACCTTGGATAGCAACTCTAAGGTCTCTAACCCCTTGACAGAGTGCA
AACACAAAAAGGGTAAAGTTGTCAGTGGTTCCAAAGTTCTCTCCATGTCCAACCTAAGGG
TTCAGGACAGCGACTTCTGGAACTGCACCGTGACCCTGGACCAGAAAAAGAACTGGTTC
GGCATGACACTCTCAGTGCTGGGTTTTCAGAGCACAGCTATCACGGCCTATAAGAGTGAG
GGAGAGTCAGCGGAGTTCTCCTTCCCACTCAACTTTGCAGAGGAAAACGGGTGGGGAGA
GCTGATGTGGAAGGCAGAGAAGGATTCTTTCTTCCAGCCCTGGATCTCCTTCTCCATAAA
GAACAAAGAGGTGTCCGTACAAAAGTCCACCAAAGACCTCAAGCTCCAGCTGAAGGAAA
CGCTCCCACTCACCCTCAAGATACCCCAGGTCTCGCTTCAGTTTGCTGGTTCTGGCAACCT
GACTCTGACTCTGGACAAAGGGACACTGCATCAGGAAGTGAACCTGGTGGTGATGAAAG
TGGCTCAGCTCAACAATACTTTGACCTGTGAGGTGATGGGACCTACCTCTCCCAAGATGA
GACTGACCCTGAAGCAGGAGAACCAGGAGGCCAGGGTCTCTGAGGAGCAGAAAGTAGTT
CAAGTGGTGGCCCCTGAGACAGGGCTGTGGCAGTGTCTACTGAGTGAAGGTGATAAGGT
CAAGATGGACTCCAGGATCCAGGTTTTATCCAGAGGGGTGAACCAGACAGTGTTCCTGGC
TTGCGTGCTGGGTGGCTCCTTCGGCTTTCTGGGTTTCCTTGGGCTCTGCATCCTCTGCTGTG
TCAGGTGCCGGCACCAACAGCGCCAGGCAGCACGAATGTCTCAGATCAAGAGGCTCCTC
AGTGAGAAGAAGACCTGCCAGTGCCCCCACCGGATGCAGAAGAGCCATAATCTCATCTG
A

Amino acid sequence

MCRAISLRRLLLLLLQLSQLLAVTQGKTLVLGKEGESAELPCESSQKKITVFTWKFSDQRKI
LGQHGKGVLIRGGSPSQFDRFDSKKGAWEKGSFPLIINKLKMEDSQTYICELENRKEEVELWV
FKVTFSPGTSLLQGQSLTLTLDSNSKVSNPLTECKHKKGKVVSGSKVLSMSNLRVQDSDFWN
CTVTLDQKKNWFGMTLSVLGFQSTAITAYKSEGESAEFSFPLNFAEENGWGELMWKAEKDS
FFQPWISFSIKNKEVSVQKSTKDLKLQLKETLPLTLKIPQVSLQFAGSGNLTLTLDKGTLHQEV
NLVVMKVAQLNNTLTCEVMGPTSPKMRLTLKQENQEARVSEEQKVVQVVAPETGLWQCLL
SEGDKVKMDSRIQVLSRGVNQTVFLACVLGGSFGFLGFLGLCILCCVRCRHQQRQAARMSQI
KRLLSEKKTCQCPHRMQKSHNLI*

BALB/c cDNA

Nucleotide sequence

ATGTGCCGAGCCATCTCTCTTAGGCGCTTGCTGCTGCTGCTGCTGCAGCTGTCACAACTC
CTAGCTGTCACTCAAGGGAAGACGCTGGTGCTGGGGAAGGAAGGGGAATCAGCAGAACT
GCCCTGCGAGAGTTCCCAGAAGAAGATCACAGTCTTCACCTGGAAGTTCTCTGACCAGAG
GAAGATTCTGGGGCAGCATGGCAAAGGTGTATTAATTAGAGGAGGTTCGCCTTCGCAGTT
TGATCGTTTTGATTCCAAAAAAGGGGCATGGGAGAAAGGATCGTTTCCTCTCATCATCAA
TAAACTTAAGATGGAAGACTCTCAGACTTATATCTGTGAGCTGGAGAACAGGAAAGAGG
AGGTGGAGTTGTGGGTGTTCAAAGTGACCTTCAGTCCGGGTACCAGCCTGTTGCAAGGGC
AGAGCCTGACCCTGACCTTGGATAGCAACTCTAAGGTCTCTAACCCCTTGACAGAGTGCA
AACACAAAAAGGGTAAAGTTGTCAGTGGTTCCAAAGTTCTCTCCATGTCCAACCTAAGGG
TTCAGGACAGCGACTTCTGGAACTGCACCGTGACCCTGGACCAGAAAAAGAACTGGTTC
GGCATGACACTCTCAGTGCTGGGTTTTCAGAGCACAGCTATCACGGCCTATAAGAGTGAG
GGAGAGTCAGCGGAGTTCTCCTTCCCACTCAACTTTGCAGAGGAAAACGGGTGGGGAGA
GCTGATGTGGAAGGCAGAGAAGGATTCTTTCTTCCAGCCCTGGATCTCCTTCTCCATAAA
GAACAAAGAGGTGTCCGTACAAAAGTCCACCAAAGACCTCAAGCTCCAGCTGAAGGAAA
CGCTCCCACTCACCCTCAAGATACCCCAGGTCTCGCTTCAGTTTGCTGGTTCTGGCAACCT
GACTCTGACTCTGGACAAAGGGACACTGCATCAGGAAGTGAACCTGGTGGTGATGAAAG
TGGCTCAGCTCAACAATACTTTGACCTGTGAGGTGATGGGACCTACCTCTCCCAAGATGA
GACTGACCCTGAAGCAGGAGAACCAGGAGGCCAGGGTCTCTGAGGAGCAGAAAGTAGTT
CAAGTGGTGGCCCCTGAGACAGGGCTGTGGCAGTGTCTACTGAGTGAAGGTGATAAGGT
CAAGATGGACTCCAGGATCCAGGTTTTATCCAGAGGGGTGAACCAGACAGTGTTCCTGGC
TTGCGTGCTGGGTGGCTCCTTCGGCTTTCTGGGTTTCCTTGGGCTCTGCATCCTCTGCTGTG
TCAGGTGCCGGCACCAACAGCGCCAGGCAGCACGAATGTCTCAGATCAAGAGGCTCCTC
AGTGAGAAGAAGACCTGCCAGTGCCCCCACCGGATGCAGAAGAGCCATAATCTCATCTG
A

Amino acid sequence

MCRAISLRRLLLLLLQLSQLLAVTQGKTLVLGKEGESAELPCESSQKKITVFTWKFSDQRKI
LGQHGKGVLIRGGSPSQFDRFDSKKGAWEKGSFPLIINKLKMEDSQTYICELENRKEEVELWV
FKVTFSPGTSLLQGQSLTLTLDSNSKVSNPLTECKHKKGKVVSGSKVLSMSNLRVQDSDFWN
CTVTLDQKKNWFGMTLSVLGFQSTAITAYKSEGESAEFSFPLNFAEENGWGELMWKAEKDS
FFQPWISFSIKNKEVSVQKSTKDLKLQLKETLPLTLKIPQVSLQFAGSGNLTLTLDKGTLHQEV
NLVVMKVAQLNNTLTCEVMGPTSPKMRLTLKQENQEARVSEEQKVVQVVAPETGLWQCLL
SEGDKVKMDSRIQVLSRGVNQTVFLACVLGGSFGFLGFLGLCILCCVRCRHQQRQAARMSQI
KRLLSEKKTCQCPHRMQKSHNLI*

8 Acknowledgements

I would like to thank my supervisor Wolfgang Uckert for giving me the opportunity to earn my PhD in the exciting field of cancer immune therapy. He found a perfect balance between outlining the path to go and giving the freedom to develop projects independently.

Great thanks to Christian Buchholz and his team for having me in their lab at PEI in Langen to learn techniques indispensable for running this project. Especially Qi Zhou and Irene Schneider taught me a lot.

Special thanks to the whole AG Uckert team. I have learned many valuable things from you during my PhD, not all being related with science. Especially, Michaela Naschke and her expertise were of utmost importance for the complete project. Her calm and considerate nature generated a pleasant atmosphere everyday and made working with her a joyful experience. Christoph Kemna not only broadened my horizon in medicine but also in literature. Nese Cakmak-Görür earned special thanks for her continuous support and friendship in the last years. A big shout-out to my bro-workers Julian Clauß and Felix Lorenz. Great times we had. Even better times ahead.

I am very thankful to be a part of the SFB TR 36 and the BIH consortium here in Berlin. I enjoyed the close collaborations and discussions with all members from Munich and Berlin. It is a great experience to see how the field of TCR gene therapy is driven from bench to bedside at the moment.

The path I have taken would not have been possible without the support of my family. I am grateful to have parents that gave me the opportunity to study. My brothers always challenged and looked after me. Most of all, I wish to thank Setareh. Her strong character and big heart make her my role model. Finally, I wish to thank Allegra. Just the thought of you puts a smile on my face.

9 Publications

Edes I, Schneider I, Zhou Q, Buchholz VR, Busch DH, Buchholz CJ and Uckert W. (2016) *In vivo* TCR engineering of $CD8^+$ T cells generates a protective immune response. *Manuscript in preparation.*

Ku MC, **Edes I**, Bendix I, Pohlmann A, Waiczies H, Prozorovski T, Günter M, Pagés G, Wolf SA, Kettenmann H, Uckert W, Niendorf T and Waiczies S. (2016) ERK1 as a Therapeutic Target for Dendritic Cell Vaccination against High-Grade Gliomas. *Submitted.*

Zhou Q, Schneider I, **Edes I**, Honegger A, Bach P, Schönfeld K, Schambach A, Wels WS, Kneissl S, Uckert W and Buchholz CJ. (2012) T-cell receptor gene transfer exclusively to human $CD8^+$ cells enhances tumor cell killing. *Blood* (doi:10.1182/blood-2012-02-412973)

Inan Edes

Berlin, March 14, 2016

10 Selbständigkeitserklärung

Hiermit erkläre ich, die vorliegende Dissertation mit dem Titel:

„Targeted transduction of T cell subsets for immunotherapy of cancer and infectious disease“

selbständig und nur unter Verwendung der angegebenen Hilfen und Hilfsmittel angefertigt zu haben. Ich habe mich anderwärts nicht um einen Doktorgrad beworben und besitze einen entsprechenden Doktorgrad nicht.

Ich erkläre die Kenntnisnahme der dem Verfahren zugrunde liegenden Promotionsordnung der Humboldt-Universität zu Berlin vom 06. Juli 2009.

Inan Edes

Matrikelnummer: 511280

Berlin, 14. März 2016